

بسم الله الرحمن الرحيم



**Electrical and Computer Engineering Department**

**Communication Engineering Program**

**Bachelor Thesis**

**Graduation Project**

**Improvement of the Transmission Capacity by Employing the Wavelet Transformation as a Modulator Using the Multiple Antenna System**

**Project Team**

**Osama Najajri  
Samer Rabah  
Hashem Abu Aram**

**Project Supervisor  
Dr. Gandhi Manasrah**

**Hebron – Palestine  
June, 2012**

جامعة بوليتكنك فلسطين

الخليل – فلسطين

كلية الهندسة والتكنولوجيا

دائرة الهندسة الكهربائية والحاسوب

اسم المشروع :

## Improvement of the Transmission Capacity by Employing the Wavelet Transformation as a Modulator Using the Multiple Antenna System

أسماء الطلاب :

سامر رباح

هاشم ابو عرام

اسامه نجايره

بناءً على نظام كلية الهندسة والتكنولوجيا وإشراف ومتابعة المشرف المباشر على المشروع ومتابعة أعضاء اللجنة الممتحنة تم تقديم هذا المشروع إلى دائرة الهندسة الكهربائية والحاسوب وذلك استكمالاً لمتطلبات درجة البكالوريوس في تخصص هندسة الاتصالات والإلكترونيات

توقيع المشرف

.....

توقيع اللجنة الممتحنة

.....

.....

.....

توقيع رئيس الدائرة

.....

## *Acknowledgements*

Over five years of university life many people have helped us. Without their help it would have been very difficult to get to where we are now, and we are immensely grateful.

Firstly all praise our lord the god almighty (Allah) the ultimate guide and the cherisher who gave us the courage and the power to complete this study with satisfying degree of perfection.

We are so grateful to our Fathers for lending us money and always being available if we need help. Our thanks are due to our mothers for worrying about us and their cares of us. Thanks to our brothers and sisters for their supports and also thanks to good friends and extended family back home who wish us the best.

Every message or comment we receive from home makes us stronger and even surer about what we are doing. Thanks to everyone who has gone to the effort.

We would like to thank those amazing people we have met along the way who have helped us in small or major ways...

Our appreciations to the light that gave us the enough to pass the way, the respected who gave us his attention and encouragement, our awesome teacher our supervisor Dr.Gandhi Manasrah , the father of telecommunication engineering in our university.

Also thanks for all lecturers and particularly communication staff who spend their expensive time and life to join them in their trip of human lights and experts.

## ***Abstract***

The communication systems that use the wireless channel are facing many challenges such as how to improve transmission capacity and quality, reduce bit error rate and efficient utilization of the available bandwidth. There are techniques to overcome these challenges such as orthogonal frequency division multiplexing (OFDM) technique, multiple input multiple output (MIMO) antenna technology and the MIMO-OFDM combination. OFDM is emerged to combat inter symbol interference (ISI), channel distortion and improve the spectral efficiency. ISI is eliminated in OFDM by added a cyclic prefix to the OFDM signal. But this can decrease the bandwidth efficiency greatly. In order to get more improvement of transmission through wireless channel and to keep up with the rapid increase in demand of the wireless technologies such as Wi-Fi and the mobile communications, Discrete Wavelet Transform (DWT) have been considered as alternative platform of conventional OFDM in which there is no need for cyclic prefix overhead due to the overlapping nature of DWT. In this project, we will use the DWT as multicarrier modulator instead of Discrete Fourier Transform (DFT) which under the scenario of having multiple antenna system allow increasing the transmission capacity and reducing bit error rate. Simulation based analysis will be used to the two multicarrier systems, DWT with Haar mother based multicarrier and the conventional OFDM, with BPSK and QAM as two digital modulation techniques in additive white Gaussian noise channel. Based on the bit error rate performance and the transmission capacity, the DWT based multicarrier system was found to be superior the conventional OFDM system.

## المخلص

أنظمة الاتصالات التي تستخدم الوسط اللاسلكي تعاني كثيرا من التحديات مثل كيفية تحسين معدل نقل المعلومات ، تقليل معدل الأخطاء والاستغلال الامثل لحزمة الترددات المتوفرة. هنالك طرق للتغلب على هذه التحديات مثل التقسيم المتعامد للتردد (OFDM)، استخدام أكثر من لاقط (antenna) على المرسل و أكثر من لاقط على المستقبل (MIMO) و كذلك الدمج بين هاتين التقنيتين. التقسيم المتعامد للتردد استطاع أن يتغلب على التشويش بين الإشارات التابعة لنفس المصدر (ISI)و كذلك تغلب على تأثير القناة اللاسلكية على الإشارة وأيضا أعطى كفاءة في استغلال الترددات المتوفرة. التشويش بين الإشارات يمكن إزالته في نظام التقسيم المتعامد للتردد عن طريق إضافة بادئ (cyclic prefix) على الإشارة المرسلة . لكن هذه الإضافة تقلل من كفاءة استغلال الترددات. حتى نحصل على تحسين أفضل للنقل خلال الوسط اللاسلكي وتماشيا مع الطلب المتسارع على تكنولوجيا اللاسلكية مثل الواي فاي وانظمة الاتصالات النقالة، تحويلة ويفلت المنفصلة(DWT) تم اقتراحها كبديل لنظام التقسيم المتعامد للتردد بحيث أنه لا يحتاج إلى إضافة بادئة على الإشارة المرسلة وذلك يعود للطبيعة المتداخله لهذا التحويل. في هذا المشروع، تحويلة ويفلت المنفصلة سوف تستخدم كمعدل متعدد الترددات بدل تحويلة فوربيرر المنفصلة (DFT) مع استخدام نظام متعدد الأنتنا وهذا يسمح بزيادة معدل النقل وتقليل معدل الخطأ. سوف يتم عمل محاكاة للنظامين باستخدام التعديل الرقمي ثنائي الطور (BPSK) و التضمين رباعي السعة (QAM).

# Table of Contents

**Acknowledgments**

**Abstract**

**Table of Content**

**List of Abbreviations**

**Table of Figures**

**Table of Tables**

- Chapter One: Introduction ..... (1-10)**
  - 1.1. Overview ..... 2
  - 1.2. Main Idea Of The Project ..... 2
  - 1.3. Objectives ..... 2
  - 1.4. Wireless Communication Systems ..... 2
    - 1.4.1. Multipath Propagation ..... 3
      - 1.4.1.1. Delay Spread Time ..... 3
      - 1.4.1.2. Inter Symbol Interference (ISI) ..... 4
    - 1.4.2. Doppler Frequency Shift ..... 5
    - 1.4.3. Transmission Capacity ..... 6
  - 1.5. Parallel Transmission Techniques ..... 6
    - 1.5.1. MIMO Systems ..... 7
    - 1.5.2. Conventional OFDM ..... 8
    - 1.5.3. MIMO-OFDM System ..... 10
  
- Chapter Two: Background and Literature Review ..... (11-20)**
  - 2.1. Overview ..... 12
  - 2.2. Fourier Transform ..... 12
    - 2.2.1. Discrete Fourier Transform ..... 12
    - 2.2.2. Short-Time Fourier Transform ..... 13
  - 2.3. Wavelet Transform ..... 13
  - 2.4. Discrete Wavelet Transform ..... 15

2.5. Haar Transform .....	17
2.6. Previous Studies .....	18
<b>Chapter Three: Space Time Block Coding Under MIMO System.....</b>	<b>(21-33)</b>
3.1. Overview .....	22
3.2. Channel Model .....	22
3.2.1. AWGN Channel .....	22
3.2.2 Fading Channel .....	22
3.3. MIMO Channel .....	23
3.4. Channel Capacity .....	24
3.5. Space-Time Block Coding .....	25
3.5.1. Alamouti Coding .....	25
3.5.2. The Alamouti Coding With Multiple Receiving Antennas .....	28
3.5.3. Orthogonal Space-Time Block Coding (OSTBC) .....	29
3.5.3.1. Real OSTBC Design .....	30
3.5.3.1. Complex OSTBC Design .....	31
3.5.4. Orthogonal space-time block coding with multiple transmit antenna.....	31
<b>Chapter Four: Multicarrier Modulation Using Discrete Wavelet Transform .....</b>	<b>(34-48)</b>
4.1. Introduction .....	35
4.2. Motivations For Using Wavelet In Wireless Communication .....	36
4.3. Sub-Band Coding.....	37
4.3.1. Two Channel Filter Bank .....	38
4.3.2. Perfect Reconstruction Condition .....	39
4.4. DWT/IDWT Using Filter Bank Theory .....	40
4.5. Wavelet Orthogonality .....	42
4.6. Multicarrier Modulation Based DWT System Design .....	43
4.6.1. Transmitter Design.....	44
4.6.2. The Channel .....	45
4.6.3. Receiver Design.....	45
4.7. MIMO-DWT System Design .....	46
4.8. The System Performance And Simulation Parameters .....	48

**Chapter Five: Simulation Results ..... (49-73)**

- 5.1. Flow Charts ..... 50
  - 5.1.1. DWT based multicarrier flow chart (SISO case) ..... 50
  - 5.1.2. Flow chart for MIMO-DWT system model..... 51
- 5.2. Simulation Results ..... 53
  - 5.2.1. BER of DWT based multicarrier and OFDM systems ..... 54
  - 5.2.2. MIMO under complex OSTBC ..... 58
    - 5.2.2.1. MIMO Simulation Results with BPSK ..... 58
    - 5.2.2.2. MIMO Simulation Results with QAM..... 62
  - 5.2.3. MIMO- Multicarrier Modulation simulation results..... 64
    - 5.2.3.1. Results of MIMO- MCM using BPSK ..... 64
    - 5.2.3.2. Results of MIMO- MCM using QAM ..... 69
  - 5.2.4. BPSK versus QAM in MIMO- MCM ..... 71
  - 5.2.5. MIMO versus MIMO- MCM ..... 72
  - 5.2.6. OFDM system without guard..... 73

**Chapter Six: Conclusion and Future Works ..... (74-76)**

- 6.1. Overview ..... 75
- 6.2. Conclusions ..... 75
- 6.3. Future Works ..... 76

**References ..... (77)**

**Appendices ..... (80-102)**

- Appendix (A): MATLAB codes ..... 81
- Appendix (B): Orthogonal Matrix Design ..... 98

## List of abbreviations

ADC	Analog To Digital Converter
ADSL	Asynchronous digital Subscriber line
AWGN	Additive White Gaussian Noise
BER	Bit Error Rate
BPSK	Binary Phase Shift Keying
CWT	Continuous Wavelet transform
DFT	Discrete Fourier Transform
DMT	Discrete Multi-Tone Modulation
DVB-T	Digital Video Broadcasting-terrestrial
DWT	Discrete Wavelet Transform
FDM	Frequency Division Multiplexing
FFT	Fast Fourier Transform
ICI	Inter Channel Interference
IDFT	Inverse Discrete Fourier Transform
IDWT	Inverse Discrete Wavelet Transform
IFFT	Inverse Fast Fourier Transform
ISI	Inter Symbol Interference
MCM	Multi-Carrier Modulation
MIMO	Multiple Input Multiple Output
MISO	Multiple Input Single Output
MMSE	Minimum Mean Squared Error
MRC	Maximal Ratio Combining
OFDM	Orthogonal Frequency Division Multiplexing
OSTBC	Orthogonal STBC
PR	Perfect Reconstruction
QMF	Quadrature Mirror Filter
QoS	Quality of Service
RF	Radio Frequency
SFBC	Space-Frequency Block Codes
SIMO	Single Input Multiple Output
SISO	Single Input Single Output
SNR	Signal To Noise Ratio
STBC	Space-Time Block Coding
STFT	Short-Time Fourier Transform
TDM	Time Division Multiplexing
UWB	Ultra Wide Band
V-BLAST	Vertical Bell Laboratories Layered Space Time
WT	Wavelet transform
ZF	Zero forcing
QAM	Quadrature Amplitude Modulation

## Table of Figures

Figure name	Figure description	Page No.
Figure 1.1	Multipath propagation.	3
Figure 1.2	Multipath spread time.	4
Figure 1.3	Inter-Symbol Interference.	5
Figure 1.4	Multiple antenna techniques.	7
Figure 1.5	OFDM spectrum.	8
Figure 1.6	The conventional OFDM transceiver.	9
Figure 1.7	OFDM symbol with cyclic prefix.	9
Figure 2.1.a	Fourier Transform.	15
Figure 2.1.b	STFT.	15
Figure 2.1.c	Wavelet Transform.	15
Figure 2.2.a	Scaling Haar function.	17
Figure 2.2.b	Wavelet Haar function.	17
Figure 2.3	Four different basis functions of Haar wavelet.	18
Figure 3.1	AWGN channel model.	22
Figure 3.2	Fading channel model.	22
Figure 3.3	MIMO channel model.	23
Figure 3.4	2×1 Alamouti coding scheme.	26
Figure 3.5	Alamouti scheme with two receiver.	28
Figure 3.6	OSTBC design OSTBC design with three transmit antenna and one receive.	32
Figure 4.1	Analysis stage of filter bank.	37
Figure 4.2	Synthesis stage of filter bank.	37
Figure 4.3	One level two channel sub-band filter bank.	38
Figure 4.4	Dyadic two channel subband structure.	40
Figure 4.5	Implementation of DWT using decimation process.	40
Figure 4.6	Implementation of IDWT using interpolation process.	41
Figure 4.7	Wavelet based multicarrier modulation structure.	43
Figure 4.8	IDWT modulator with four subcarriers (or subchannels).	44
Figure 4.9	Time-frequency plane of $S_n^m$ .	45
Figure 4.10	MIMO-DWT system model.	46
Figure 4.11	Alamouti coded DWT system.	47
Figure 5.1	Flow chart for DWT based multicarrier system model.	50
Figure 5.2	Flow chart for MIMO-DWT system model	52
Figure 5.3	BER of DWT and OFDM using a) BPSK b) QAM	54
Figure 5.4	BER of DWT and OFDM (with guard) using a) BPSK	56

	b) QAM	
Figure 5.5	SISO multicarrier BPSK vs. QAM	57
Figure 5.6	Different MIMO configurations under OSTBC using BPSK over Rayleigh channel.	59
Figure 5.7	MIMO-STBC $nTx \times 4$	60
Figure 5.8	$M \times M$ MIMO configurations using BPSK.	61
Figure 5.9	Different MIMO configurations under OSTBC using QAM over Rayleigh channel.	62
Figure 5.10	BER performance of $3 \times 6$ vs. $6 \times 3$	63
Figure 5.11	$M \times M$ MIMO using QAM.	63
Figure 5.12	Multicarrier modulation in AWGN with MIMO OSTBC.	64
Figure 5.13	Multicarrier with SIMO under MRC, a) DWT , b) OFDM	65
Figure 5.14	Multicarrier with $2 \times nRx$ MIMO under Alamouti scheme, a) DWT , b) OFDM	65
Figure 5.15	Multicarrier with $3 \times nRx$ MIMO under complex OSTBC, a) DWT , b) OFDM	66
Figure 5.16	BER performance of $3 \times 8$ vs. $8 \times 3$ , a) DWT , b) OFDM	68
Figure 5.17	$M \times M$ MIMO with multicarrier using BPSK, a) DWT, b) OFDM	68
Figure 5.18	MIMO- MCM using QAM under OSTBC, a) DWT, b) OFDM	69
Figure 5.19	The BER of QAM under different MIMO configurations with two multicarrier modulations, a) DWT, b) OFDM	70
Figure 5.20	BPSK vs. QAM with MIMO-DWT	71
Figure 5.21	Extracted Portion of figure 5.20.	71
Figure 5.22	MIMO vs. MIMO-DWT, a) $2 \times 3$ Alamouti, b) $4 \times 2$ OSTBC	72
Figure 5.23	MIMO-OFDM with and without guard using a) BPSK, b) QAM	73

## Table of Tables

Table name	Table description	Page No.
Table 3.1	2×1 Alamouti coding scheme	26
Table 3.2	STBC for three transmit antennas using real signals constellations.	32
Table 4.1	Simulation parameters	48
Table 5.1	MATLAB built in functions for multicarrier generation.	53
Table 5.2	Comparison between DWT and OFDM systems.	58
Table 5.3	Required $E_b/N_o$ at $10^{-4}$ BER for $4 \times nRx$ and $nTx \times 4$ .	61
Table 5.4	Required $E_b/N_o$ in dB at $10^{-4}$ probability of error for MIMO-DWT and MIMO-OFDM using BPSK.	67
Table 5.5	Required $E_b/N_o$ in dB at $10^{-4}$ probability of error for ( $5 \times nRX$ ) MIMO-DWT and MIMO-OFDM using QAM.	70
Table B.1	values of $\rho(N)$	99

# **Chapter 1**

## **Introduction**

## **1.1. Overview**

We will introduce in this chapter a general idea about the project, as well as the aims of the project. Then we will discuss the principle of wireless communication system and the challenges that affect on the transmission through the wireless channel. The techniques that are used to overcome these challenges will be discussed.

## **1.2. Main idea of the project**

The main point of this project is to introduce the Discrete Wavelet Transform (DWT) as a multicarrier modulation (MCM) technique instead of the conventional orthogonal frequency division multiplexing (OFDM) which is based on the Discrete Fourier Transform (DFT). The idea behind this work is how to increase the data rate with limited available bandwidth when the DWT is used as MCM since it does not need cyclic prefix overhead to deal with channel effects such as inter symbol interference (ISI) and inter channel interference (ICI) as in OFDM. In our research we will study the advantages of the MIMO-DWT system as replacement of MIMO-OFDM and we will use the MATLAB program for simulate this system.

## **1.3. Objectives**

- 1) To understand the principle of Discrete Wavelet Transform as a new technique to perform parallel data transmission instead of OFDM.
- 2) Making a simulation for DWT system where BPSK and QAM as two modulation techniques are used and compare the result with OFDM system.
- 3) Making a simulation for MIMO-DWT system where BPSK and QAM as two modulation techniques are used and compare the result with MIMO-OFDM system.
- 4) Knowing the effect of using DWT instead of DFT over transmission capacity and Bit Error Rate (BER).

## **1.4. Wireless communication systems**

The systems that use the free-space (unguided medium) for communicates with each other are called wireless communication systems. When the electromagnetic signals propagate in free-space it will face many propagation obstacles mechanisms due to the surrounding environment such as reflection, diffraction, scattering. The impact of propagation mechanisms on wireless system lead to many challenges that affect on the transmission through wireless channel.

### 1.4.1. Multipath propagation

Phenomenon in which versions of the signal reach the receiver from different paths due to the propagation mechanisms, so at the receiver antenna there is a collection of direct and other multipath copies (components of the transmitted signal) and each component has different delay, phase and power. The combination of these copies may be added constructively or destructively, this lead to rapid change in the amplitude of the received signal which is called fading.

Figure 1.1 shows the principle of multipath propagation, there are four copies of the transmitted signal from four paths as follow : copy ( A ) from direct path ( line of sight ), copy ( B ) from reflected path, copy ( C ) from diffracted path, copy ( D ) from scattered path.

The effect of multipath propagation causes two main problems in wireless system, delay spread and Inter-Symbol Interference.

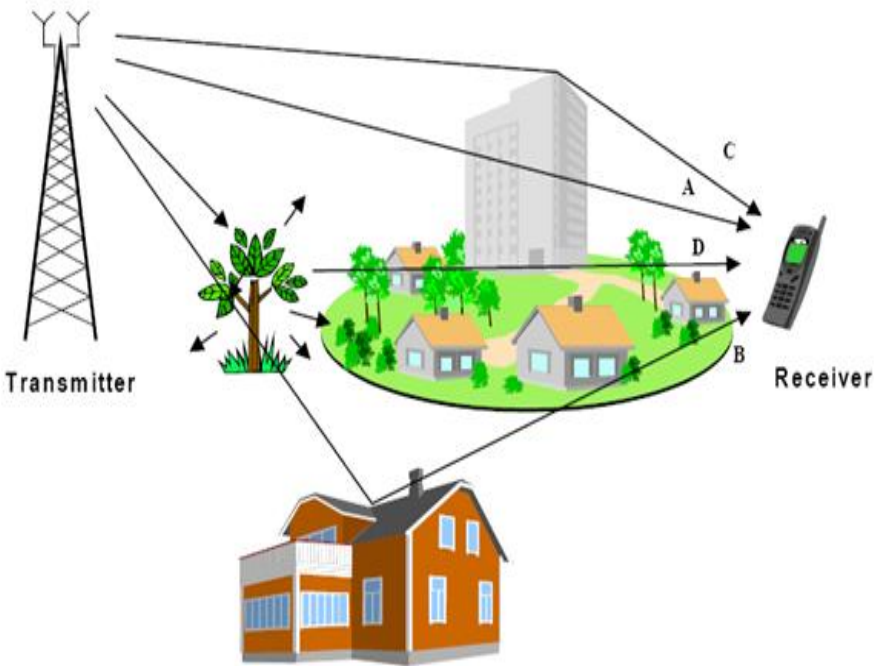


Figure 1.1: Multipath propagation

#### 1.4.1.1. Delay Spread Time

The time between the first arrival component and the last arrival component of the transmitted signal at the receiver due to the different propagation delays for each component is called spread time delay.

The analogous parameter of delay spread in frequency domain is the coherence bandwidth of the channel which defined as the range of frequencies that are strongly correlated when they pass through the channel. Figure 1.2 shows how the received copies have different delay that spread the received signal time.

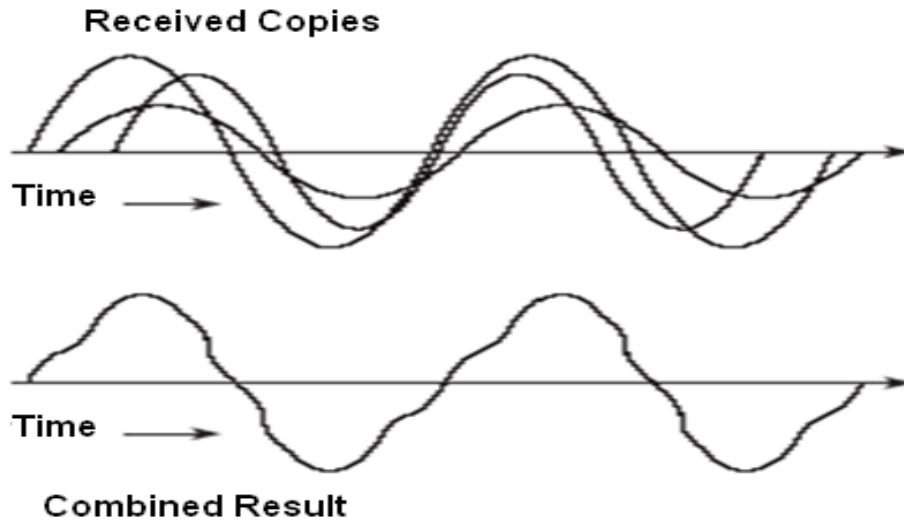


Figure 1.2: multipath spread time

#### 1.4.1.2. Inter Symbol Interference (ISI)

When the maximum delay spread ( $T_m$ ) is greater than symbol time ( $T_s$ ) the components from different signal will overlap and interfere with each other which is called inter-symbol interference (ISI). At the receiver, the combination of the overlapped components will be added constructively or destructively due to the relative phase shift between multipath signal components which causes rapid fluctuation in the received signal power. However, if  $T_m$  is less than  $T_s$  then no significant ISI is encountered. So that the solution to mitigate ISI is reduce the data rate of transmission which is unwanted. The multicarrier modulations and the MIMO systems are appear as powerful techniques that overcome the ISI effect.

Figure 1.3 shows how the symbol overlaps due to ISI. Assuming there are two copies for each transmitted symbol. The second component of the first arrival signal is overlap with the first component of the second arrival signal.

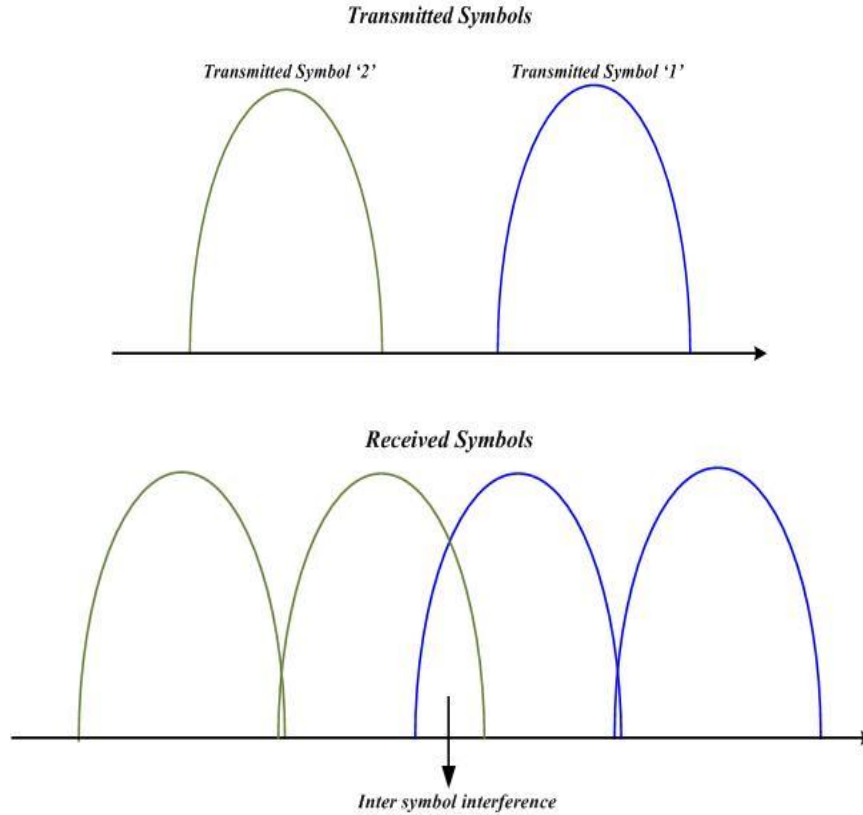


Figure 1.3: Inter-Symbol Interference.

### 1.4.2. Doppler frequency shift

Doppler is the apparent change in wavelength (or frequency) of the transmitted signal when there is relative movement between the transmitter and the receiver [1].

When the transmitter and or the receiver are moving toward each other the frequency of the received signal is higher than the transmitted signal, and when they are moving away from each other the frequency of the received signal is less than the transmitted signal. The amount of the frequency changes due to the Doppler Effect which is called the Doppler frequency shift depends on the relative motion between the transmitter and receiver and on the speed of propagation of the wave according to the following expression:

$$f_d = \frac{2 v f}{c} \cos\theta \quad (1.1)$$

Where:

$f_d$ : The change in frequency of the source seen at the receiver.

$f$ : The frequency of the transmitter.

$v$ : The speed of the target.

$c$ : The speed of light.

$\theta$ : The elevation differences angle.

Doppler shift can cause significant problems if the transmission technique is sensitive to carrier frequency offsets or the relative speed is higher [1]. The analogous to the Doppler frequency in time domain is called coherence time which is characterized the time varying nature of the dispersive channel.

### **1.4.3. Transmission capacity**

The process of improvement the transmission capacity is one of the challenges that face the wireless system; the challenge comes from bandwidth and power limitations due to the regulations. The following equation which is called Shannon Capacity Theorem shows the relationship between the bandwidth of the channel with signal to noise ratio (SNR) and the capacity of system in additive Gaussian noise channel.

$$C = \beta \log_2( 1 + SNR ) \quad (1.2)$$

Where  $C$  is the Shannon capacity in bits per second and  $B$  is the channel bandwidth in Hz.

Increasing the transmission capacity can be achieved by efficient utilization the available bandwidth and improvement SNR parameter.

Diversity techniques are used to improve SNR by supplying the receiver with multiple independent replicas of the same signal by using different frequencies or different time points or using multiple antenna system. MIMO and OFDM systems are techniques that utilize the bandwidth efficiently by mitigation the effect of ISI.

## **1.5. Parallel Transmission Techniques**

This section will discuss the principle of simultaneous transmission techniques of signals which are used to overcome ISI and to achieve high transmission data rate, either by using signal processing or antenna solutions.

### 1.5.1. MIMO system

Using multiple antennas at the transmitter and multiple antennas at the receiver instead of using Single Input Single Output (SISO) is a way to mitigate ISI and increase the data rate.

The multiple antennas can be used to increase data rates through multiplexing or to improve performance through diversity [2]. In MIMO systems the transmitter and receiver antennas can both be used for diversity gain. The multiplexing gain of MIMO system results from the fact that MIMO channel decomposed into number of parallel independent channels, by multiplexing independent data over these independent channels we get increasing in the data rate compared to the SISO system [2].

There are two additional kinds of multiple antenna system which are called Single Input Multiple Output (SIMO) and Multiple Input Single Output (MISO) systems are used for diversity gain. SIMO refers to use one antenna at the transmitter and multiple antennas at the receiver. On other hand, MISO refers to use multiple antennas at the transmitter and one antenna at the receiver. Figure 1.4 shows the four categories of multiple antenna system techniques.

It is also obvious that in MIMO systems channel capacity increases with increase the number of antennas at both sides because each antenna transmits different data stream simultaneously which is known as spatial multiplexing, thus increase the range of transmission and reliability of received system to get this signals, without any consumption of additional bandwidth, leading to improves the spectral efficiency.

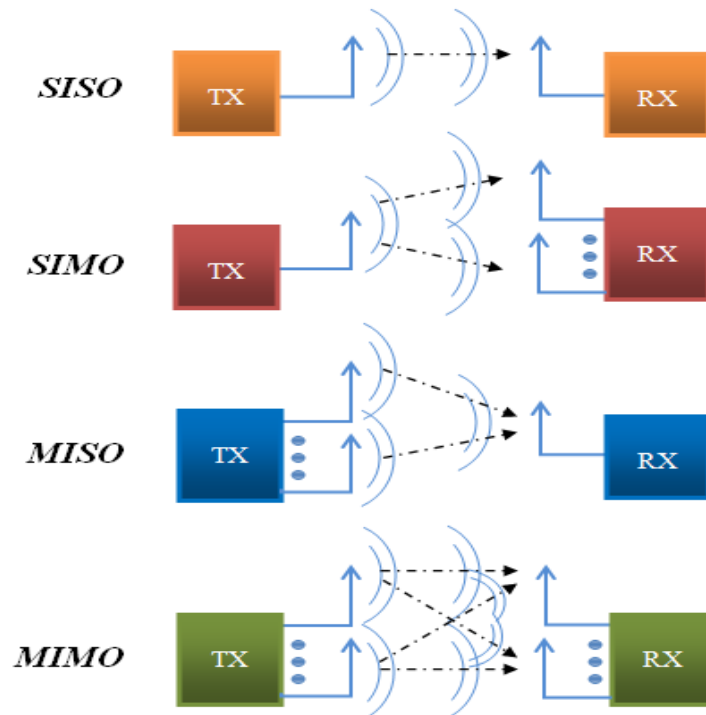


Figure 1.4: Multiple antenna techniques

### 1.5.2. Conventional OFDM

The demand for high data rate is increased, Inter symbol interference would be faced, and that originated from the passive situation of multipath propagation and due to the delay spread stick on it.

Orthogonal frequency division multiplexing is a multicarrier technique that converts the sequential high data rate stream into multiple parallel low data rate streams, these parallel streams are used to modulate different orthogonal subcarriers and they simultaneously transmitted by single antenna, so the data rate is increased and the available bandwidth is efficiently used. Figure 1.5 shows the spectrum of an OFDM signal, the minimum space frequency between two successive subcarriers that used to apply orthogonality condition can be given as:

$$\Delta f = \frac{1}{T_s} \quad (1.3)$$

Where  $T_s$  is the OFDM symbol time.

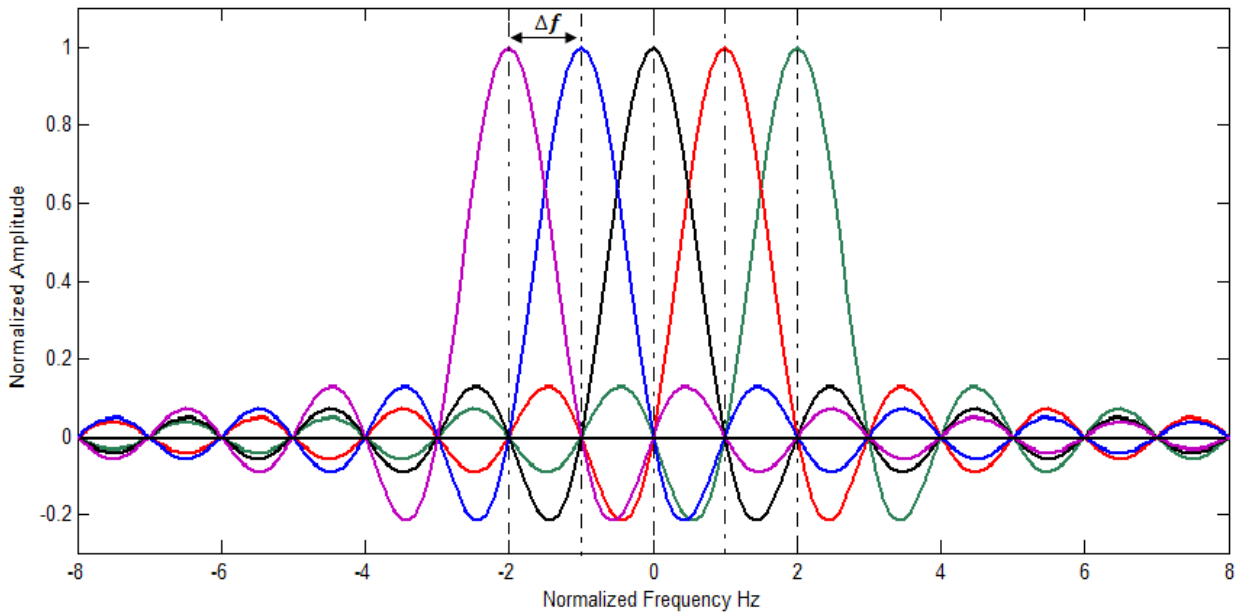


Figure 1.5: OFDM spectrum

Implementation of OFDM system needs a modulator for each subcarrier, which is become difficult and more expensive for hardware implementation when the number of subcarriers increases. Digital signal processing solves this problem by using the Fast Fourier Transform algorithms. Figure 1.6 shows the general block diagram of the conventional OFDM transceiver in which the Inverse Fast Fourier Transform (IFFT) is applied at the transmitter side and the Fast Fourier Transform (FFT) is applied at the receiver side.

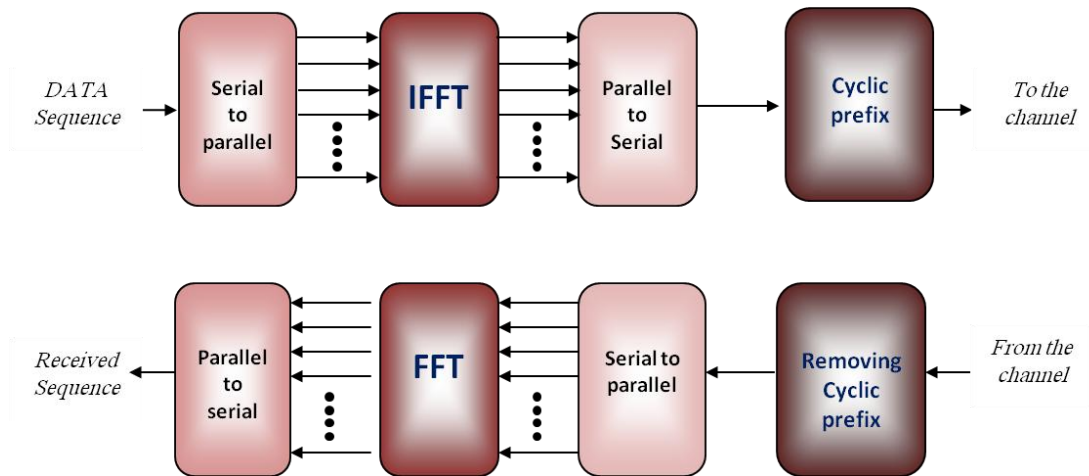


Figure 1.6: the conventional OFDM transceiver

In multipath environment the conventional modulation technique are more sensitive to inter symbol interference due to the high rate of source symbol and less delay spread of channel, so where the data rate is sufficiently high; several adjacent symbol may be completely distorted over frequency selective fading .

With OFDM as modulation scheme this problem would be almost solvable in high efficiency, because of set of signals that used to build blocks of OFDM transmitted symbols, OFDM basic idea is to use large number of parallel narrow band sub-carrier instead of a single wide-band carrier to transport information, with inter carrier guard bands, but the overlapping of bands is controlled to achieve orthogonal state in order to get maximum spectral efficiency.

Relative to symbol time the reduction of symbol rate lead to proportional reduction of the relative delay spread, although that OFDM is reduce the inter guard bands in the transmitter side, the ISI is still a problem faced in the receiver side so to completely eliminate the ISI that result a guard time is introduced for each OFDM symbol which is called cyclic prefix, Figure 1.7 shows how the cyclic prefix is added at the begging of OFDM symbols.

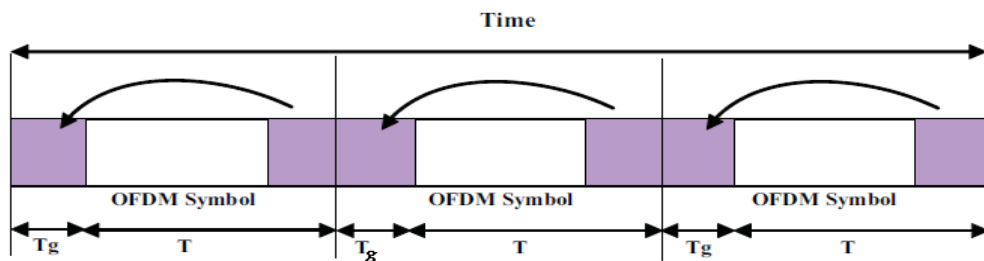


Figure 1.7: OFDM symbol with cyclic prefix

The cyclic prefix is used to overcome ISI and inter carrier interference ICI, but it also adds an overhead that reduces the bandwidth efficiency, so the upcoming challenge is to remove this overhead lead to get a system with high transmission capacity which is our aim in this project.

In addition to the cyclic prefix problem, the conventional OFDM system has other drawbacks. Peak-to-average ratio is one of the most serious problems in the OFDM transmission that the signal component can added up in phase and produce a large output and in some cases they cancel each other producing zero output, result to extreme amplitude excursions of the transmitted signal, also the problem could increases in the transmitter side due to the Power Amplifier Linearity limitation that the practical power amplifiers have an input power range over which they have a linear transfer curve [3,4]. In order to avoid clipping of the transmitted waveform, the power-amplifier at the transmitter must have a wide linear range to include the peaks in the transmitted waveform. Building power amplifiers with such wide linear ranges is a costly affair. Further, this also results in high power consumption [4].

Another important issue in OFDM transmission is sensitivity to imperfect frequency Synchronization which is common for mobile applications. The orthogonality of an OFDM system is only preserved when the receiver and transmitter use the same frequency [3]. Thus receiver has to estimate and correct for the carrier frequency offset of the received signal. Furthermore, the phase information must be recovered if coherent demodulation is employed and the receiver has to estimate the symbol boundaries and the optimal timing instants that minimize the effects of inter-carrier interference (ICI) and inter-symbol interference (ISI) [4].

There are three synchronization problems related to OFDM systems: symbol, carrier frequency and sampling frequency synchronization [3].

### **1.5.3. MIMO-OFDM system**

The combination of MIMO system with OFDM system is very natural and beneficial mechanism. Implementing this combination system need multiple OFDM modulators and multiple radio equipments and this is regarded as a promising solution for enhancing the data rates of next generation wireless communication systems operating in frequency selective fading environments.

## **Chapter 2**

# **Background and Literature Review**

## 2.1. Overview

In this chapter we will discuss the Fourier Transform, DFT and STFT. Then we will give background about the Wavelet Transform, the Discrete Wavelet Transform (DWT), and the theory of wavelet multi-resolution will be presented. Haar Mother Wavelet will be discussed as an example of wavelet mother functions family. After that we will talk about some previous studies that correspond to the OFDM and DWT multicarrier systems.

## 2.2. Fourier Transform

The Fourier Transform is one of the several mathematical tools that is useful for the analysis and processing of signals by representing these signals in frequency domain rather than time-amplitude representation. The Fourier Transform which based on decomposing the signals into sinusoids gives the frequency components (harmonics) of the signal and the power corresponding to each component.

The Fourier Transform is a powerful tool or operation for signals analysis when the frequency contents of these signals are not change with time which is called stationary signals. There are other classifications of the Fourier Transform such as Fourier series, Discrete Fourier Transform (DFT). These classifications depend whether the signal is periodic or aperiodic, continuous or discrete.

### 2.2.1. Discrete Fourier Transform

Is one version of the Fourier Transform that widely used in digital signal processing. The DFT is the discrete-time equivalent to the continuous-time Fourier Transform, in which  $X(k)$  represent the frequency content of time samples  $x(n)$ , the sequence  $x(n)$  can be recovered from  $X(k)$  by the Inverse-DFT (IDFT). The DFT and its inverse can be done according to the following equations:

$$X(k) = \sum_{n=0}^{N-1} x(n)e^{-j2\pi nk/N} \quad 0 \leq k \leq N - 1 \quad (2.1)$$

$$x(n) = \sum_{k=0}^{N-1} X(k)e^{j2\pi nk/N} \quad 0 \leq n \leq N - 1 \quad (2.2)$$

Where: N represents the number of samples.

The DFT is used for implementation the modulation and demodulation process in OFDM system by generate N- orthogonal subcarrier frequencies in which every subcarrier is used to carry one symbol data source, so that there is no need N- hardware modulator and demodulator for implementation of OFDM system.

### 2.2.2. Short-Time Fourier Transform (STFT)

The classical Fourier analysis decomposes a signal into frequency (spectral) components and determines the corresponding power for each component but it does not provide information regarding where in time those spectral components appear [5].

The modified version of the Fourier Transform is the STFT which uses a fixed-duration window that slides over the time signal, i.e., divide the total time duration of the signal into shorter time intervals, and then the FFT will apply for each interval [5]. The main difference between the standard Fourier Transform and the STFT is the use of the window function rather than using kernel function ( $e^{j2\pi t}$ ) which is extended along total time, so that no time resolution in Fourier Transform [5].

STFT use window function  $g(t)$  at some point  $\tau$  which is zero outside a certain time interval then uses the Fourier Transform to find the spectra of the signal according to the following equation:

$$X(f, \tau) = \int_{-\infty}^{\infty} x(t)g^*(t - \tau)e^{-j2\pi ft} dt \quad (2.3)$$

The process of STFT is suitable with non-stationary signals because their frequency contents change with time. The idea behind STFT is considering some portion of a non-stationary signal is stationary, so using many time intervals will give good time resolution but this includes using short time window interval which means poor frequency resolution. On other hand, wide time window interval means better frequency resolution and poor time resolution. So that could not achieve simultaneous frequency and time resolution because the size of the window is fixed with respect to frequency. This problem with STFT is related to Heisenberg Uncertainty in quantum physics which states that one cannot know the exact position and exact momentum simultaneously [5].

### 2.3. Wavelet Transform

Wavelet Transform (WT) is a mathematical function that is emerged as a new tool for multi-resolution decomposition of continuous time signal at different times and different frequencies (or scales) [5].

Wavelet Transform have more than one classification such as Continuous Wavelet Transform (CWT) and Discrete Wavelet Transform (DWT), CWT was developed to alternate the short time Fourier transform so that disposing the resolution problem, that higher frequencies are better resolved in time, and lower frequencies are better resolved in frequency. "Variable resolution" as a certain high frequency component can be located better in time "with less relative error" than a low frequency component and the low frequency component can be located better in frequency compared to high frequency component [6].

In the sense that the signal is multiplied with an orthogonal wavelet function similar to the window function in the STFT, and the transform is computed separately for different segments of the time domain signal [6]. The wavelet transform can be defined as:

$$CWT_x^\psi(\tau, s) = \Psi_x^\psi(\tau, s) = \frac{1}{\sqrt{|s|}} \int_{-\infty}^{\infty} x(t) \psi^*\left(\frac{t-\tau}{s}\right) dt \quad (2.4)$$

Where:

$CWT_x^\psi$ : Continuous wavelet transform of the signal  $x(t)$  using the analysis wavelet  $\psi(t)$ .

$\psi^*\left(\frac{t-\tau}{s}\right)$ : Mother wavelet. All kernels are obtained by translating (shifting) and/or scaling the mother wavelet.

$\tau$ : Translation parameter corresponds to the time information in the signal.

$s$ : Scale parameter, corresponds to the frequency information in the signal, Scale = 1/frequency.

Figure 2.1 shows the difference between three different transforms which are Fourier Transform, STFT and Wavelet Transform in terms of time-frequency tile allocation. From the figure we can see that the Fourier Transform has infinite window and the window in STFT is fixed that slides along the time axis but in Wavelet it is variable in scale and in width.

The Haar orthogonal mother wavelet is the first relates to the wavelet transform. It was proposed by the mathematician Alfred Haar in 1909. Although that the concept of the wavelet did not exist at that time. Until 1981 the geophysicist Jean Morlet was the first who proposed the concept [7].

Afterward, Morlet and the physicist Alex Grossman invented the term wavelet in 1984. The mathematician Yves Meyer constructed the second orthogonal wavelet called Meyer mother wavelet in 1985. The first international conference was held in France in 1987. In 1988, Stephane Mallat and Meyer proposed the concept of multi-resolution. In the same year, Ingrid Daubechies found a systematical method to construct the orthogonal wavelet. In 1989, Mallat proposed the fast wavelet transform [7].

The wavelet transform had numerous applications in the signal and image processing, for example, the wavelet transform is useful for the digital image files compression; that improves memory storage and for faster more reliable transmitting.

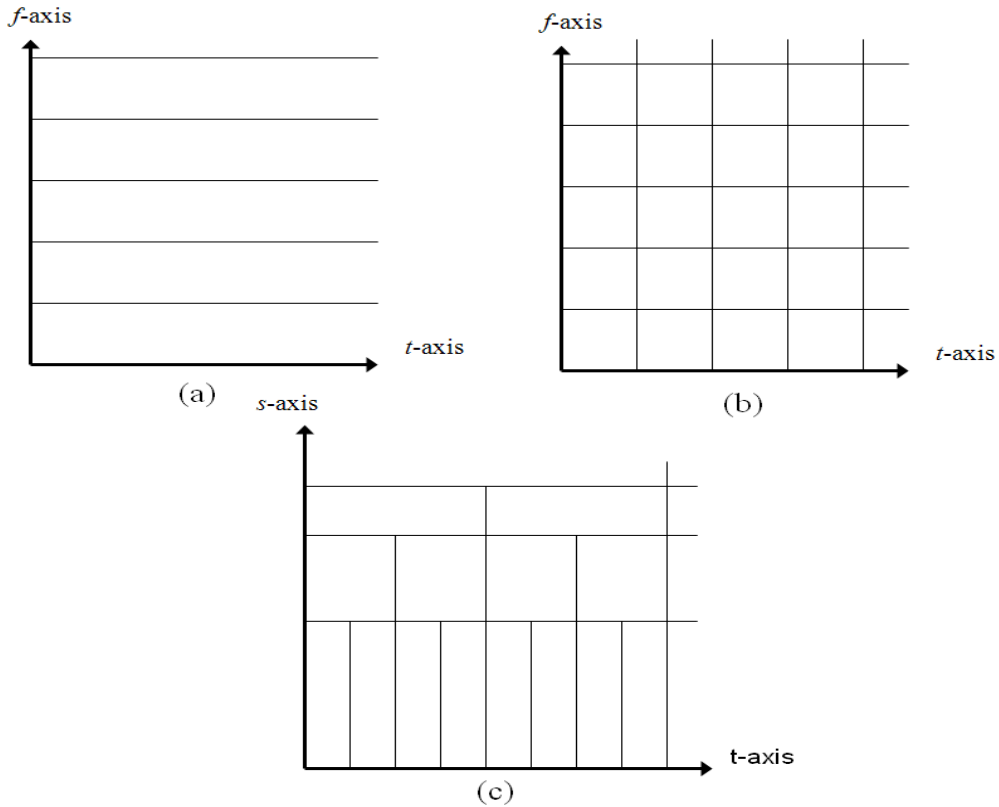


Figure 2.1: (a) Fourier Transform, (b) STFT and (c) Wavelet Transform

## 2.4. Discrete Wavelet Transform

Redundancy and impracticality those are the main drawbacks of CWT to be implemented easily, which is firstly obvious from the nature of CWT, and secondly the continuity status of the parameters of CWT equation [5]. So that the sampling solution had taken effect to the parameter  $(s, \tau)$  to obtain set of wavelet functions in discrete form under condition of overcoming the redundancy problem [5].

Discretizing the scaling variable  $s$  in a manner of  $s_0^m$  and translation variable  $\tau$  in manner of  $n\tau_0 s_0^m$  so that:

$$\psi_{mn}(t) = s_0^{-m/2} \psi(s_0^{-m} t - n\tau_0) \quad (2.5)$$

This forms the basis of discrete wavelet transform, the DWT coefficients of a continuous-time signal  $s(t)$  with using dyadic scaling  $s_0 = 2$  and  $\tau_0 = 1$  are defined as [8]:

$$\begin{aligned}
d_{m,n} &= \langle s(t), \psi_{m,n}(t) \rangle \\
&= 2^{-m/2} \int s(t) \psi(2^{-m}t - n) dt
\end{aligned} \tag{2.6}$$

The signal  $s(t)$  can be reconstructed from its DWT coefficients via the inverse DWT process as:

$$s(t) = \sum_m \sum_n d_{m,n} \psi_{m,n}(t) \tag{2.7}$$

The representation of the signal  $s(t)$  using L-scales (or resolutions) requires two functions; they are called scaling and wavelet functions [8, 9]. The scaling function families  $\phi_n(t)$  are constructed by time-shifted versions of the so-called parent scaling function  $\phi(t)$  at only one scale. From other hand, the wavelet function families  $\psi_{m,n}(t)$  are defined for all L-scales (or resolutions) [8].

Based on  $\phi_n(t)$  and  $\psi_{m,n}(t)$  the signal  $s(t)$  can be represented as:

$$s(t) = \sum_{n=-\infty}^{\infty} c_{L,n} 2^{-L/2} \phi(2^{-L}t - n) + \sum_{m=1}^L \sum_{n=-\infty}^{\infty} d_{m,n} 2^{-m/2} \psi(2^{-m}t - n) \tag{2.8}$$

Where  $c_{L,n}$  and  $d_{m,n}$  are called scaling (averaging) coefficients and wavelet coefficients, respectively. These coefficients are obtained by projection the signal  $s(t)$  onto the scaling and wavelet functions according to the following equations [8, 9]:

$$c_{L,n} = \langle s(t), \phi_{L,n}(t) \rangle = \int s(t) 2^{-L/2} \phi(2^{-L}t - n) dt \tag{2.9.a}$$

$$d_{m,n} = \langle s(t), \psi_{m,n}(t) \rangle = \int s(t) 2^{-m/2} \psi(2^{-m}t - n) dt \tag{2.9.b}$$

The scaling function  $\phi(t)$  is only orthogonal to its translations, whereas the wavelet function  $\psi(t)$  is orthogonal to its scaling and to the translation of its scaling [9].

For orthogonal wavelet system, the scaling functions and the wavelet functions are orthogonal to each other [9], therefore:

$$\int \phi_{m,k}(t) \psi_{m,k}(t) dt = 0 \tag{2.10}$$

The scaled function  $\phi(2t)$  can be used to represent the parent scaling function  $\phi(t)$  and the mother wavelet function  $\psi(t)$  as follows:

$$\phi(t) = \sqrt{2} \sum_n h_n \phi(2t - n) \quad (2.11. a)$$

$$\psi(t) = \sqrt{2} \sum_n g_n \phi(2t - n) \quad (2.11. b)$$

Where  $h_n$  and  $g_n$  are called scalar function coefficients and wavelet function coefficients, respectively. These coefficients are related to each other as follows:

$$g_n = (-1)^n h_{(1-n)} \quad (2.12)$$

The scaling function and the wavelet function are used to extract the low frequency and high frequency components in the signal  $s(t)$ , respectively, this will be shown in chapter 4.

## 2.5. Haar Wavelet

Most standard wavelets are based on one mother wavelet, which is a function with some special properties. The Haar wavelet is the simplest, oldest type of mother wavelet functions, developed by Alfred Haar [10]. The set of Haar functions is defined as a group of square waves with magnitude  $\pm 1$  at some intervals and zero elsewhere and can be written as:

$$\psi(t) = \begin{cases} 1 & , \quad 0 \leq t \leq 0.5 \\ -1 & , \quad 0.5 \leq t \leq 1 \\ 0 & , \quad elsewhere \end{cases} \quad (2.13)$$

The constant function is annihilated by the Haar wavelet, and haar wavelet families are orthogonal. The scaling function corresponding to the Haar wavelet has the value 1 for  $0 < t < 1$  , and 0 for all other values of  $t$  [10]. Figure 2.2 shows the Haar scaling and wavelet functions.

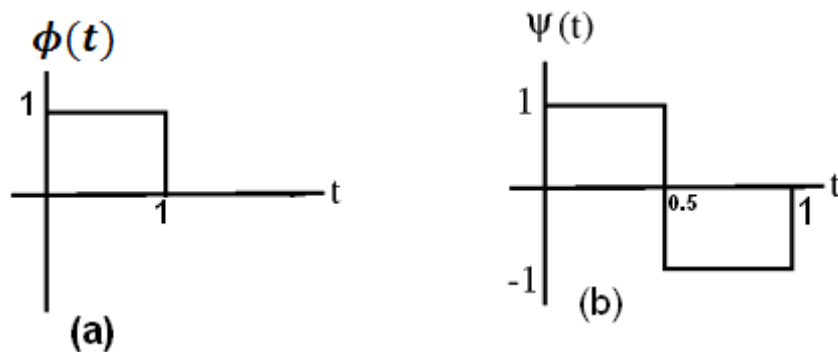


Figure 2.2: (a) scaling Haar function, (b) wavelet Haar function

Figure 2.3 shows four orthogonal basis functions of the Haar wavelet function. The basis functions are *scaled and translated* versions of a mother wavelet  $\psi(t)$ .

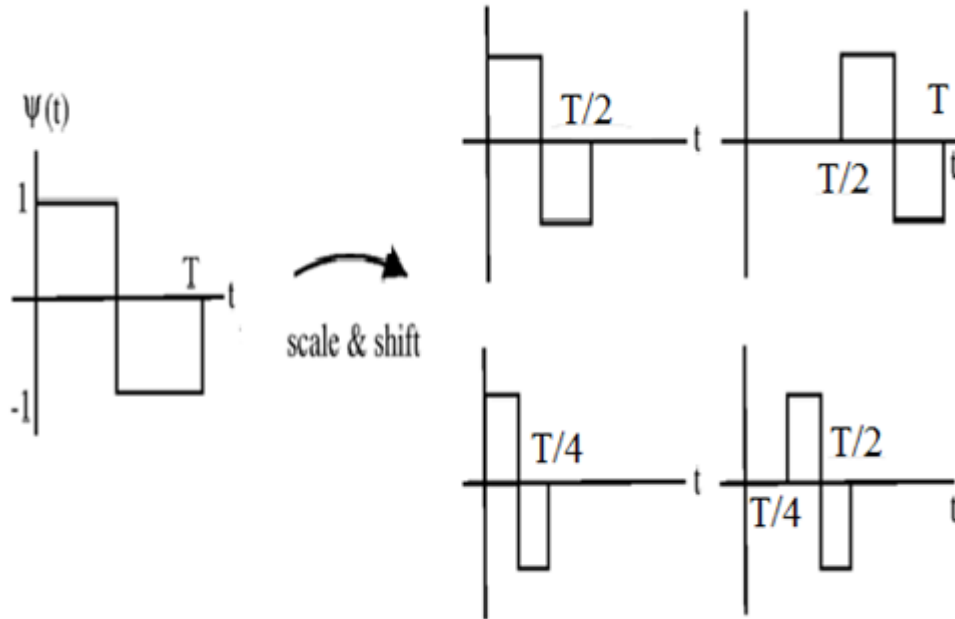


Figure 2.3: Four different basis functions of Haar wavelet.

## 2.6. Previous studies

Multi-carrier modulation is increasingly popular as a transmission technique; especially in high speed wide band communications over wireless channels. Also that the field of Discrete Wavelet Transforms (DWTs) is an amazingly recent one signal processing. The basic principles of wavelet theory were put forth in a paper by Gabor in 1945. Tim Edwards (1991) published a paper discusses the DWT and demonstrates one way in which it can be implemented as a real-time signal processing system [11].

Seong Taek Chung and Andrea Goldsmith [12] proposed an adaptive multicarrier modulation technique, where transmit rate and power are adapted in both time and frequency. They derived an optimal adaptation strategy and determined its performance.

Kok-Wui Cheong & John M. Cioffi (1998) described a form of PR filter banks, the cosine-modulated FIR filter banks, to be used for multi-carrier modulation. After that ANSI for Asymmetric Digital

Subscriber Line (ADSL) suggested that discrete wavelet transform (DWT) in the form of perfect reconstruction (PR) filter banks be used in place of DFT as modulation functions. The advantage of such replacement is better spectral containment in PR filter banks than in DFT [13].

In 2001, Negash and Hikookar [14] present a paper that proposes the Wavelet OFDM as an alternative for conventional Fourier OFDM in order to reduce the level of ISI and ICI interference powers. Simulation results have demonstrated that comparing with the conventional OFDM, in the Wavelet OFDM transmission the IC1 power is significantly and the IS1 power is slightly reduced.

Gao Xingxin, Lu Mingquan and Feng Zhenming (2002) have replaced the conventional FFT based multicarrier modulation with orthogonal wavelet packet in order to get a more flexible and robust performance [15].

Orthogonal frequency division multiplexing (OFDM) is a special form of multi carrier transmission which has found its application in a number of wireless and wired systems. OFDM based on a very simple modulation scheme that uses IFFT and FFT where large number of orthogonal, overlapping, narrow band sub-channels or subcarriers, transmitted in parallel, divide the available transmission bandwidth.

The bit error rate (BER) performance of conventional discrete Fourier transform (DFT) - OFDM system is compared with discrete wavelet transform (DWT)-OFDM system and discrete cosine transform (DCT)-OFDM system in an AWGN environment. Several wavelets such as Haar, Daubechie and Symlet are considered. Deepak Gupta, Torry Harris and Kamal K. Garg,(2008) gived the performance with two modulation format such as BPSK and QPSK. The simulation results that Haar wavelet based scheme yields the lowest average bit error probability and the performance of DFT-OFDM and DWT (Haar)-OFDM with QPSK is better than BPSK modulation format [16].

Khaizuran Abdullah and Zahir M. Hussain, presents a comparative study on Fourier-based OFDM (FFT- OFDM) and Wavelet-based OFDM (DWT- OFDM) in digital video broadcasting-terrestrial (DVB- T) system. They found that the DWT-OFDM outperforms FFT-OFDM in additive white Gaussian noise (AWGN) and Rayleigh fading channels under multipath flat-fading and frequency-selective fading [17].

Prema.G and Amrutha.Ea, found that with MIMO scheme the Wavelet based OFDM outperforms the conventional FFT- OFDM in term of reducing PAPR and BER. They used a framework for 4×4 MIMO- OFDM preprocessing system using pilot symbol assisted rate less codes and wavelet OFDM (WOFDM) proposed to mitigate fading and reducing peak-to-average power ratio (PAPR) [18].

Muhammad Yasir, M. J. Mughal, N.D and Gohar, S. A. Moiz discussed performance and simulation of Wavelet based OFDM V-BLAST MIMO system, (V-BLAST stands for Vertical Bell Laboratories Layered Space Time), over two-ray MIMO wireless channel. BER of this system has been observed

with three different V-BLAST detection algorithms which are Zero Forcing (ZF), Minimum Mean Squared Error (MMSE) and QR-decomposition based V-BLAST detection algorithms. Simulation results shows that (WOFDM) V-BLAST MIMO system using MMSE algorithm has the best performance among the three detection algorithms [19].

Our project will proposes the performance of the MIMO- DWT system using Haar DWT and compared it with MIMO-OFDM in terms of improvement on transmission capacity and reduction of BER in AWGN channel where BPSK as modulation scheme will be used.

## **Chapter 3**

### **Space Time Block Coding under MIMO System**

### 3.1. Overview

The improve of reliability of data transfer in wireless communications can be achieved through the spatial- temporal coding techniques of the data stream such as space- time block coding scheme in which multiple copies of data are transmitted across multiple antenna system at different times thus compensate for fading and thermal noise. In this chapter we will firstly introduce the basic concept of the channel model, and then we will talk about MIMO channel and the channel capacity concept. STBC and orthogonal STBC are explained in detailed in this chapter as coding technique in multiple antenna system.

### 3.2. Channel models

The wireless channel incorporates a number of stochastic effects including thermal noise (or additive noise), fading and interference.

#### 3.2.1. AWGN channel

AWGN channel has flat amplitude, linear phase frequency response for all frequencies, so that modulated signals pass through it without any amplitude less and phase distortion of frequency components [8]. Figure 3.1 shows the general model of the AWGN channel.

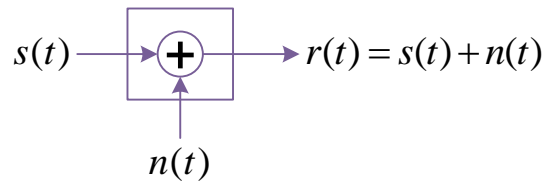


Figure 3.1: AWGN channel model.

#### 3.2.2. Fading channel

The wireless channel suffers from the multi-path problem which causes the fading. The impulse response of the fading channel is random time-varying which generate random changes in the amplitude, delays and phase of multi-path component [8]. Figure 3.2 shows the general model of the fading channel.

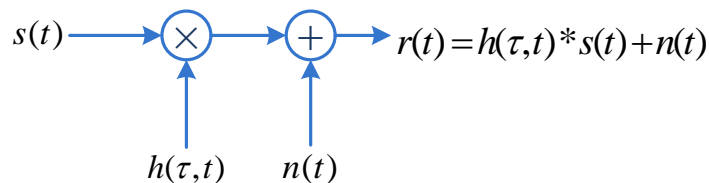


Figure 3.2: Fading channel model.

The standard time-variant channel impulse response is:

$$h(\tau, t) = \sum_{n=1}^{N(t)} a_n(t) e^{-j\varphi_n(t)} \delta(\tau - \tau_n(t)) \quad (3.1)$$

Where:

$N(t)$ : The number of multipath components.

$a_n(t)$ : Multipath component amplitude.

$\varphi_n(t)$ : Multipath component phase shift.

$\tau_n(t)$ : Multipath component delay time.

The parameters,  $N(t)$ ,  $a_n(t)$ ,  $\varphi_n(t)$ , and  $\tau_n(t)$  are time varying and random. To characterize the statistical nature of the channel, fading distributions will be used. Rayleigh fading channel model has proven useful in rich scattering environments to describe the envelope distribution of the received signal. The received signal  $r(t)$  can be expressed as:

$$r(t) = h(\tau, t) * s(t) + n(t) \quad (3.2)$$

Where: \* is the convolution operator.

### 3.3. MIMO channel

MIMO channel can be realized with multi-element array antennas, there is an individual channels between given pairs of transmit and receive antennas as shown in Figure 3.3.

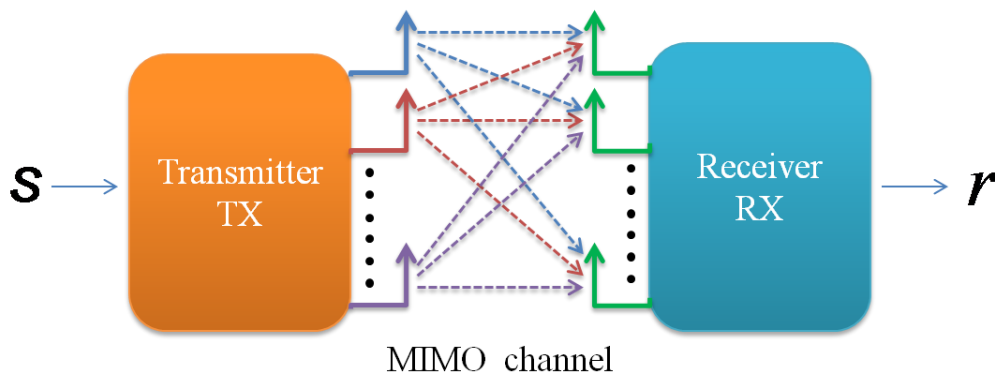


Figure 3.3: MIMO channel model

The received signal vector  $r$  could be written as:

$$r = Hs + n \quad (3.3)$$

Where:

$r$ :  $M_R \times 1$  received signal vector.

$s$ :  $M_T \times 1$  received signal vector.

$n$ :  $M_R \times 1$  additive noise vector.

$H$ : is the MIMO channel matrix described by  $M_R \times M_T$  matrix as:

$$H = \begin{bmatrix} h_{11} & h_{12} & \dots & h_{1M_T} \\ h_{21} & h_{22} & \dots & h_{2M_T} \\ \cdot & \cdot & \dots & \cdot \\ \cdot & \cdot & \dots & \cdot \\ \cdot & \cdot & \dots & \cdot \\ h_{M_R1} & h_{M_R2} & \dots & h_{M_R M_T} \end{bmatrix} \quad (3.4)$$

$h_{ij}$  : Channel gain from transmitter antenna  $j$  to receiver antenna  $i$ .

### 3.4. Channel capacity

The basic measure of performance limits in communication is the capacity of a channel, which represents the maximum data rates that can be transmitted over wireless channels with arbitrarily small error probability can be achieved. In particular, Shannon who was invented the theory of channel capacity defined the channel capacity as the maximum mutual information between the transmitted and the received signals [2, 20]. For the AWGN channel with channel bandwidth  $\beta$  and received signal power  $P$ , the Shanon capacity is given by:

$$C = \beta \log_2 \left( 1 + \frac{P}{\beta N_0} \right) \quad (3.5)$$

Where:  $C$  is the capacity (bits/s) and  $N_0$  is the noise power.

Wireless channels typically exhibit flat or frequency-selective fading. Unlike the AWGN case, the capacity of a flat fading channel is not given by a single formula because capacity depends on what is known about the time-varying channel at the transmitter and/or receiver [2].

The capacity of a MIMO channel is an extension of the mutual information formula for a SISO channel to a matrix channel and it increases at least linearly with the minimum number of transmit or receive antennas [2, 20].

### 3.5. Space-time block coding

Space-time coding is a spatial and temporal coding technique designed for multiple antenna transmission when the channel information at the transmitter unknown, the space-time coding introduce a correlation between the transmitted signals from different antenna at different time periods [21]. Space-time block coding (STBC) is one approach of space-time coding technique that support spectral efficiencies and performance gains by exploits the spatial and temporal diversity available in MIMO block fading channels [21].

Selection combining and maximal ratio combining (MRC) are two widely used combining algorithms with receive diversity which places no particular requirements on the transmitter, but requires a receiver that processes and combines the N received streams [22]. However, STBC is a transmit diversity technique in which the transmitted streams are pre-processed before transmitted.

#### 3.5.1. Alamouti coding

Alamouti coding is the first and simplest orthogonal STBC, which uses two antennas for transmitting two symbols simultaneously in two successive time slots.

In Alamouti scheme, the symbols  $s_0$  and  $s_1$  are transmitted simultaneously from antenna one and antenna two, respectively during the first time slot. In the second time slot  $-s_1^*$  and  $s_0^*$  are transmitted simultaneously from antenna one and antenna two, respectively, Where  $*$  is the complex conjugate operator. This process is repeated for all transmission sequence ( $s_0 s_1 s_2 \dots s_n$ ). Table 3.1 shows the spatial and temporal process of  $2 \times 1$  Alamouti coding scheme. Figure 3.4 shows the Alamouti coding scheme with two transmitter antennas.

The received signals at the receiver antenna over two consecutive symbol periods are:

$$r_0 = r(t) = h_0 s_0 + h_1 s_1 + n_0 \quad (3.6. a)$$

$$r_1 = r(t + T) = -h_0 s_1^* + h_1 s_0^* + n_1 \quad (3.6. b)$$

Where:

$n_0, n_1$ : represent the AWGN samples at time t and t +T respectively.

$r_0, r_1$ : The received symbols on the first and second time slot respectively.

$h_0$ : is the channel response from first transmitter antenna to receiver antenna.

$h_1$ : is the channel response from second transmitter antenna to receiver antenna.

The received signals can be written as:

$$\begin{bmatrix} r_0 \\ r_1^* \end{bmatrix} = \begin{bmatrix} h_0 & h_1 \\ h_1^* & -h_0^* \end{bmatrix} \cdot \begin{bmatrix} s_0 \\ s_1 \end{bmatrix} + \begin{bmatrix} n_0 \\ n_1 \end{bmatrix} \quad (3.7)$$

Table 3.1 :  $2 \times 1$  Alamouti coding scheme.

Spatial \ Temporal	Antenna 0	Antenna 1
$t$	$s_0$	$s_1$
$t + T$	$-s_1^*$	$s_0^*$

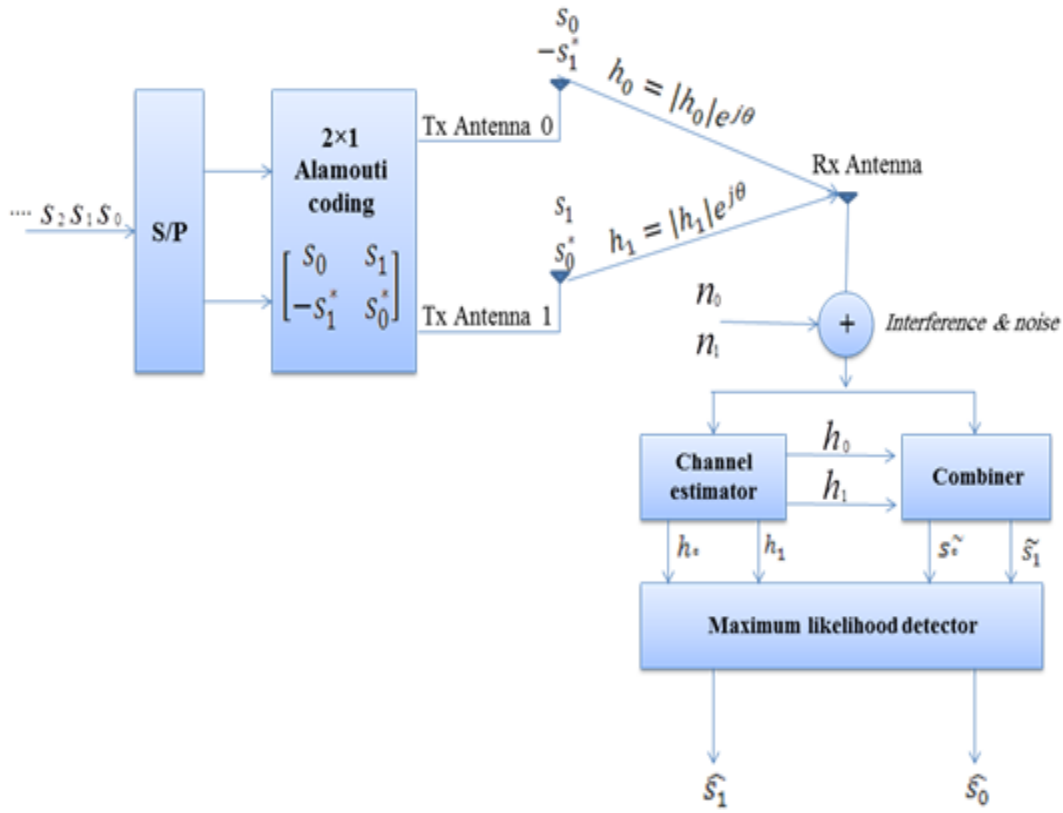


Figure 3.4:  $2 \times 1$  Alamouti coding scheme.

The signal combiner combines the received signal with channel state information which is estimated by channel estimator, the two combined signals  $\tilde{s}_0$  and  $\tilde{s}_1$  are expressed as:

$$\tilde{s}_0 = h_0^* r_0 + h_1 r_1^* \quad (3.8.a)$$

$$\tilde{s}_1 = h_1^* r_0 - h_0 r_1^* \quad (3.8.b)$$

Substituting  $r_0$  and  $r_1$  from equation (3.6):

$$\tilde{s}_0 = (|h_0|^2 + |h_1|^2)s_0 + h_0^*n_0 + h_1n_1^* \quad (3.9.a)$$

$$\tilde{s}_1 = (|h_0|^2 + |h_1|^2)s_1 - h_0n_1^* + h_1^*n_0 \quad (3.9.b)$$

Hence, this very simple decoder that just linearly combines the two received samples  $r(t)$  and  $r(t + T)$  is able to eliminate all the spatial interference. The resulting SNR can be computed as:

$$\gamma_\Sigma = \frac{(\sum_i |h_i|^2)^2 E_s}{\sigma^2 \sum_i |h_i|^2} = \frac{\sum_{i=0}^1 |h_i|^2 E_s}{\sigma^2} \quad (3.10)$$

Where:  $\sigma^2$  is the power spectral density of the AWGN and  $E_s$  is the signal energy.

Each transmit antenna must halve its transmit power so that the total transmit energy per actual data symbol is  $E_s$  in order to keep the transmit power the same as in the MRC case [22]. The  $2 \times 1$  Alamouti code achieves the same diversity order and data rate as a  $1 \times 2$  receive diversity system with MRC, but with a 3 dB penalty due to the redundant transmission required to remove the spatial interference at the receiver [21, 22].

The decision in maximum likelihood decoder is based on the minimum Euclidian distance, therefore the decision rules are expressed as:

$$\hat{s}_0 = \arg \min_{\hat{s}_0 \in S} \{(|h_0|^2 + |h_1|^2 - 1)|\hat{s}_0|^2 + d^2(\tilde{s}_0, \hat{s}_0)\} \quad (3.11.a)$$

$$\hat{s}_1 = \arg \min_{\hat{s}_1 \in S} \{(|h_0|^2 + |h_1|^2 - 1)|\hat{s}_1|^2 + d^2(\tilde{s}_1, \hat{s}_1)\} \quad (3.11.b)$$

Where:  $d^2(x, y)$  is the squared Euclidian distance between the signals and can be calculated as following,  $d^2(x, y) = (x - y)(x^* - y^*)$ .

$S$ : The set of all possible modulated symbol pairs (or set of all transmission sequence symbol pair).

If the signals have equal energy as in PSK system, then  $|\hat{s}_0|^2 = |\hat{s}_1|^2 = E_s$ . Therefore, the decision rules may be simplified to:

$$\hat{s}_0 = \arg \min_{\hat{s}_0 \in S} \{d^2(\tilde{s}_0, \hat{s}_0)\} \quad (3.12.a)$$

$$\hat{s}_1 = \arg \min_{\hat{s}_1 \in S} \{d^2(\tilde{s}_1, \hat{s}_1)\} \quad (3.12.b)$$

### 3.5.2. The Alamouti coding with multiple receiver antennas

The diversity order will be improved when we apply the Alamouti coding scheme with multiple receive antennas system. The encoding and transmission for this configuration is identical to the conventional Alamouti with one receive antenna [21].

Figure 3.5 shows 2×2 communication system, this system has two receive antenna. We will study this system as case of multiple receive antennas with Alamouti coding.

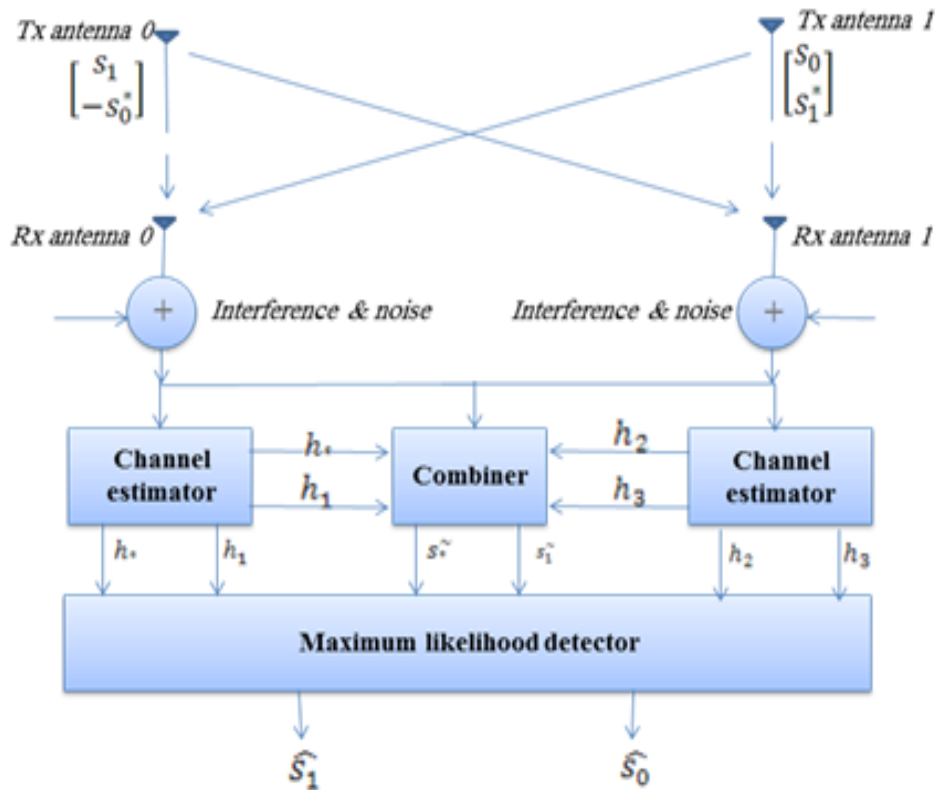


Figure 3.5: Alamouti scheme with two receiver.

If we assume the channel is constant over two consecutive symbols, then the received signals are:

$$\begin{aligned}
 r_0 &= h_0 s_0 + h_1 s_1 + n_0 \\
 r_1 &= h_2 s_0 + h_3 s_1 + n_1 \\
 r_2 &= -h_0 s_1^* + h_1 s_0^* + n_2 \\
 r_3 &= -h_2 s_1^* + h_3 s_0^* + n_3
 \end{aligned} \tag{3.13}$$

Where:  $n_0, n_1, n_2,$  and  $n_3$  are complex random variables representing receiver thermal noise and interference.

As a result of combining scheme the following signals will be produced at the combiner output:

$$\tilde{s}_0 = (|h_0|^2 + |h_1|^2 + |h_2|^2 + |h_3|^2)s_0 + h_0^*n_0 + h_1n_1^* + h_2^*n_2 + h_3n_3^* \quad (3.14. a)$$

$$\tilde{s}_1 = (|h_0|^2 + |h_1|^2 + |h_2|^2 + |h_3|^2)s_1 - h_0n_1^* + h_1^*n_0 - h_2n_3^* + h_3^*n_2 \quad (3.14. b)$$

The resulting SNR can be computed as:

$$\gamma_\Sigma = \frac{(\sum_i |h_i|^2)^2 E_s}{\sigma^2 \sum_i |h_i|^2} \frac{E_s}{2} = \frac{\sum_{i=0}^3 |h_i|^2 E_s}{\sigma^2} \frac{E_s}{2} \quad (3.15)$$

This is like MRC with 4 receive antennas, where again there is a 3dB penalty due to transmitting each symbol twice [22].

### 3.5.3. Orthogonal space-time block coding (OSTBC)

In OSTBC, the orthogonality between the signal sequences enables to achieve the maximum transmit diversity and allows the receiver to detect the transmitted signal from different antennas by simple linear processing operation [21]. The orthogonal matrix  $G_N$  is expressed as:

$$G_N = \sum_{n=1}^N s_n \cdot B_n \quad (3.16)$$

Where:  $N$  represent the number of transmitter antennas and  $B_n$ : Hurwitz-radon family of size  $N$ , where  $B_1 = I_N$  (identity matrix).

In general if there are  $N$  transmit antenna and  $K$ - symbols, then the orthogonal matrix  $G_{K \times N}$  has the following property:

$$G_{K \times N}^H G_{K \times N} = \sum_{k=1}^K |s_k|^2 \cdot I_N \quad (3.17)$$

Where:  $G_{K \times N}^H$  is called Hermitian matrix (or conjugate transpose) of  $G_{K \times N}$ .

The entries of orthogonal matrix may be real or complex based on the signal constellations. The rate of the code is defined as the number of the transmitted symbol,  $K$ , over the number of time periods for transmission of one block of coded symbol  $T$ ,  $R = \frac{K}{T}$ . Appendix (B) shows in details how we can construct and design the orthogonal matrix, real and complex.

### 3.5.3.1. Real OSTBC design

A generalized orthogonal design is  $T \times N$  orthogonal matrix  $G_{T \times N}$  with real entries  $s_0, -s_0, s_1, -s_1 \dots s_K, -s_K$  such that  $G_{T \times N}^H G_{T \times N} = q(s_0^2 + s_1^2 + \dots s_K^2)I_N$ . The code rate in real design is  $R = 1$ .

2×2 design:

$$\begin{aligned} G_2 &= s_0 I_2 + s_1 B_2 \\ &= s_0 \begin{bmatrix} 1 & 0 \\ 0 & 1 \end{bmatrix} + s_1 \begin{bmatrix} 0 & 1 \\ -1 & 0 \end{bmatrix} = \begin{bmatrix} s_0 & s_1 \\ -s_1 & s_0 \end{bmatrix} \end{aligned} \quad (3.18)$$

4×4 design:

$$G_4 = s_0 I_4 + s_1 B_2 + s_2 B_3 + s_3 B_4 \quad (3.19. a)$$

$$\text{Where: } B_2 = \begin{bmatrix} 0 & 1 & 0 & 0 \\ -1 & 0 & 0 & 0 \\ 0 & 0 & 0 & -1 \\ 0 & 0 & 1 & 0 \end{bmatrix} \quad B_3 = \begin{bmatrix} 0 & 0 & 1 & 0 \\ 0 & 0 & 0 & 1 \\ -1 & 0 & 0 & 0 \\ 0 & -1 & 0 & 0 \end{bmatrix} \quad B_4 = \begin{bmatrix} 0 & 0 & 0 & 1 \\ 0 & 0 & -1 & 0 \\ 0 & 1 & 0 & 0 \\ -1 & 0 & 0 & 0 \end{bmatrix}$$

$$G_4 = \begin{bmatrix} s_0 & s_1 & s_2 & s_3 \\ -s_1 & s_0 & -s_3 & s_2 \\ -s_2 & s_3 & s_0 & -s_1 \\ -s_3 & -s_2 & s_1 & s_0 \end{bmatrix} \quad (3.19. b)$$

8×5 design:

$$G_{8 \times 5} = \begin{bmatrix} s_0 & s_1 & s_2 & s_3 & s_4 \\ s_1 & -s_0 & s_3 & -s_2 & s_5 \\ s_2 & -s_3 & -s_0 & s_1 & -s_6 \\ s_3 & s_2 & -s_1 & -s_0 & -s_7 \\ s_4 & -s_5 & s_6 & s_7 & -s_0 \\ s_5 & s_4 & s_7 & -s_6 & -s_1 \\ s_6 & s_7 & -s_4 & s_5 & s_2 \\ s_7 & -s_6 & -s_5 & -s_4 & s_3 \end{bmatrix} \quad (3.20)$$

### 3.5.3.2. Complex OSTBC design

A general complex orthogonal design is an  $T \times N$  orthogonal matrix  $G_{2T \times N}$  with complex entries  $s_0, -s_0, s_1, -s_1 \dots s_K, -s_K$  and their conjugates  $s_0^*, -s_0^*, s_1^*, -s_1^* \dots s_K^*, -s_K^*$ . Such that  $G_{2T \times N}^H G_{2T \times N} = q(|s_0|^2 + |s_1|^2 + \dots + |s_K|^2)I_N$ . The code rate in complex design is  $= \frac{1}{2}$ , except in Alamouti the code rate is 1.

In general, the complex orthogonal matrix  $G_{2T \times N}$  is as follow:

$$G_{2T \times N} = \begin{bmatrix} G \\ G^* \end{bmatrix} \quad (3.21)$$

Where  $G$ : is  $T \times N$  real design orthogonal matrix and  $G^*$  is the complex conjugate of  $G$ .

2x2 design which is Alamouti code with two transmitting antenna.

$$G_{2 \times 2} = \begin{bmatrix} s_0 & s_1 \\ -s_1^* & s_0^* \end{bmatrix} \quad (3.22)$$

8x4 complex design:

$$G_{8 \times 4} = \begin{bmatrix} s_0 & s_1 & s_2 & s_3 \\ -s_1 & s_0 & -s_3 & s_2 \\ -s_2 & s_3 & s_0 & -s_1 \\ -s_3 & -s_2 & s_1 & s_0 \\ s_0^* & s_1^* & s_2^* & s_3^* \\ -s_1^* & s_0^* & -s_3^* & s_2^* \\ -s_2^* & s_3^* & s_0^* & -s_1^* \\ -s_3^* & -s_2^* & s_1^* & s_0^* \end{bmatrix} \quad (3.23)$$

### 3.5.4. Orthogonal space-time block coding with multiple transmit antenna

In Alamouti scheme there are two transmit antenna. If the number of transmit antennas is greater than two the OSTBC design is used. In this section we will show the OSTBC design with three transmit antenna and how the combiner at the receiver combines the receive signals in order to reconstruct the transmitted signals. Figure 3.6 shows the three transmit antenna with one receive antenna.

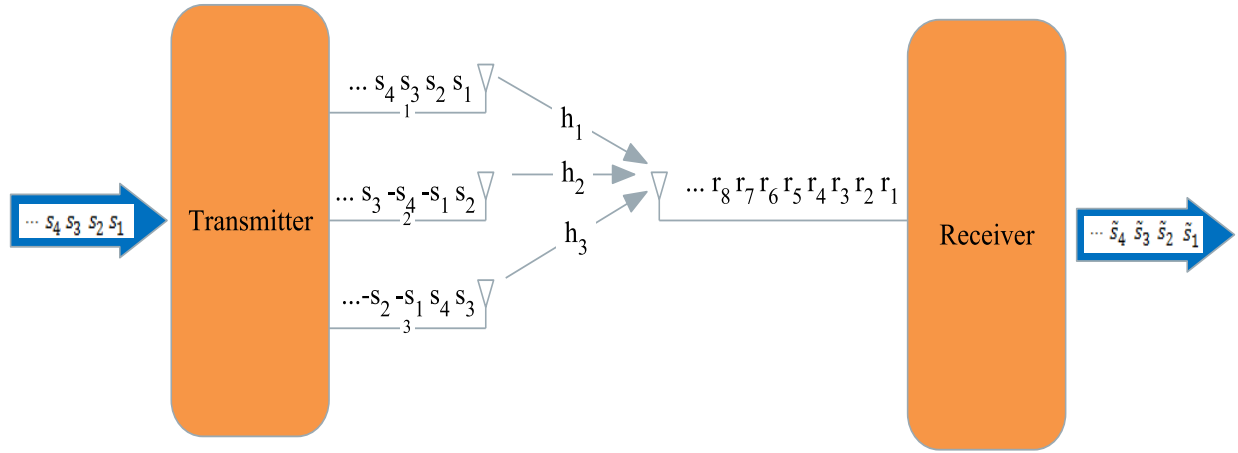


Figure 3.6: OSTBC design OSTBC design with three transmit antenna and one receive.

With  $N = 3$ , the number of time periods for transmission of one block of coded symbol is four with code rate  $R = 1$ . At a given symbol period, three signals out of four are transmitted simultaneously from three transmit antennas. The encoding, mapping and transmission of the STBC can be summarized in the following table 3.2. For complex OSTBC (code rate  $R = \frac{1}{2}$ ), eight symbol intervals are needed to transmit four different symbols using three transmitting antennas.

Table 3.2: STBC for three transmit antennas using real signals constellations.

<b>Spatial</b> \ <b>Temporal</b>	$TX_1$	$TX_2$	$TX_3$
$t$	$s_1$	$s_2$	$s_3$
$t + T$	$s_2$	$-s_1$	$s_4$
$t + 2T$	$s_3$	$-s_4$	$-s_1$
$t + 3T$	$s_4$	$s_3$	$-s_2$

For a three transmit and one receive antenna system, the channel coefficients are modeled by a complex multiplicative distortions,  $h_1$  for the first transmit antenna,  $h_2$  for the second transmit antenna and  $h_3$  for the third transmit antenna. Assuming the fading is constant across four consecutive symbols.

With  $\alpha = \frac{1}{2}$ , the received vector relation is:

$$r = Hs + n$$

$$\begin{bmatrix} r_1 \\ r_2 \\ r_3 \\ r_4 \\ r_5^* \\ r_6^* \\ r_7^* \\ r_8^* \end{bmatrix} = \begin{bmatrix} h_1 & h_2 & h_3 & 0 \\ -h_2 & h_1 & 0 & h_3 \\ -h_3 & 0 & h_1 & -h_2 \\ 0 & -h_3 & h_2 & h_1 \\ h_1^* & h_2^* & h_3^* & 0 \\ -h_2^* & h_1^* & 0 & h_3^* \\ -h_3^* & 0 & h_1^* & -h_2^* \\ 0 & -h_3^* & h_2^* & h_1^* \end{bmatrix} \begin{bmatrix} s_1 \\ s_2 \\ s_3 \\ s_4 \end{bmatrix} + \begin{bmatrix} n_1 \\ n_2 \\ n_3 \\ n_4 \\ n_5^* \\ n_6^* \\ n_7^* \\ n_8^* \end{bmatrix} \quad (3.24)$$

As a result of combining scheme the estimated symbols are:

$$\begin{aligned} \tilde{s}_1 &= 2(|h_1|^2 + |h_2|^2 + |h_3|^2)s_1 + \eta_1 \\ \tilde{s}_2 &= 2(|h_1|^2 + |h_2|^2 + |h_3|^2)s_2 + \eta_2 \\ \tilde{s}_3 &= 2(|h_1|^2 + |h_2|^2 + |h_3|^2)s_3 + \eta_3 \\ \tilde{s}_4 &= 2(|h_1|^2 + |h_2|^2 + |h_3|^2)s_4 + \eta_4 \end{aligned} \quad (3.25)$$

Where the noise terms are obtained from  $\eta = H^H n$ .

In this section we presented the OSTBC analysis for three transmitted antenna, the same approach when we use higher number of transmit antenna is applied. If we have multiple receive antennas, then the previous analysis is applied for each antenna and finally the estimated symbols are resulted from all combiners.

It should be noted that any OFDM-based system, the space-time coding can be implemented as space-frequency block codes (SFBC), where different sub-carriers of OFDM can be used as a replacement for the time dimension of a space-time code. This assumes that adjacent subcarriers have the same amplitude and phase, which is typically approximately true in practice [22, 23]. If space-time coding is used in OFDM, then the STBC is implemented over two OFDM symbols. Since OFDM symbols can be quite long in duration, care must be taken to make sure that the channel is constant over subsequent OFDM symbols [22].

## **Chapter 4**

# **Multicarrier Modulation Using Discrete Wavelet Transform**

## 4.1. Introduction

Multicarrier modulation (MCM) is an effective technique of wireless communication; unlike traditional single carrier systems it divides the bandwidth into independent narrow sub-band channels, and uses it to transmit parallel low data streams which are divided from the original high data stream. The number of subchannels chosen to make the symbol time for each sub-stream much greater than the delay spread of the channel and to make the sub-stream bandwidth less than the channel coherence bandwidth to avoid ISI [24]. Multicarrier modulation can be interpreted as a transmultiplexer that takes time-division multiplexed (TDM) data and transforms it to frequency division multiplexed (FDM) data. With this view, multicarrier modulation provides an efficient means to access and distribute multiple multiplexed data streams. This is potentially very attractive for high speed, broadband networks, which often multiplex multiple data sources during transmission [25].

As mentioned in previous chapters the OFDM is one implementation of multicarrier modulation techniques for wireless system where the sub-channels are orthogonal to each other using Discrete Fourier Transform (DFT) for modulation, other implementation of MCM is Discrete Multitone (DMT) modulation for wire line systems such as ADSL. The question then remains as to how to partition the bandwidth. In OFDM, DFT, in the form of FFT is used to partition the bandwidth. However, a cyclic prefix has to be used and this will reduce the throughput. In particular, we will examine a form of Wavelet transforms which are broadly classified as continuous wavelet (CWT) and discrete wavelet transforms (DWT), DWT has an advantage over DFT which there is no need to use a cyclic prefix and this mean increase the capacity of the system also DWT has flexibility, lower sensitivity to channel distortion, interference mitigation and better utilization of spectrum [26].

Multicarrier modulation is used extensively in wireless communication systems such as in 3G and 4G cellular systems for its advantage of mitigation wireless channels problems such as ISI, also it used in WIMAX system for the ability of increase the system capacity. Multicarrier techniques can be combined with multiantenna transmitters and receivers to provide high performance efficiency and increase the data rate of wireless communication systems.

In this chapter we will introduce an overview about the wavelet features that motivate for using the wavelet transform as modulator in multicarrier system. We define the concept and discuss the subband coding that used to construct the subcarrier in wavelet based multicarrier modulation. Tow channel perfect reconstruction filter banks is discussed in detail including the interpolation and decomposition processes. Also we explain how two channel filter bank is used to implement DWT and IDWT. Then we present the system design for wavelet based multicarrier modulation, then we will discuss the DWT- MIMO system as a parallel transmission technique. Finally, the performance parameters are introduced, such as bit error rate (BER) and the data rate (or system capacity) concepts.

## 4.2. Motivation for Using Wavelets in Wireless Communication

In this section we will introduce a few features of wavelet transform. There are many features that motivate to use wavelet transform in wireless communication, such as:

- 1) Semi-arbitrary division of the signal space and multi-rate systems, Wavelet transform has the ability to create a different symbol length and bandwidth for the subcarriers which means multi-rate system with different transport delays [27, 28].
- 2) Flexibility with time-frequency tiling, wavelets has also ability to arrange the time-frequency tiling in a case of minimizing the channel disturbances. By flexibly aligning the time-frequency tiling, the effect of noise and interference on the signal can be minimized. This can enhance the quality of service (QoS) of wireless systems [27, 28]. With the promise of greater flexibility and improved performance against channel effects, wavelet based basis functions have emerged as strong candidates for MCM in wireless channels [29].
- 3) Waveform diversity, Wavelets give a new dimension to the physical diversities currently exist namely, space, frequency and time-diversity. Wavelet diversity which is similar to spread spectrum systems minimizes inter-cell interference [27, 28].
- 4) Sensitivity to channel effects, the performance of wavelet modulation scheme holds the promise of reducing the sensitivity of the system to harmful channel effects like inter-symbol interference (ISI) and inter-carrier interference (ICI) [27].
- 5) Flexibility with sub-carriers, wavelet transform allows for a configurable transform size and hence a configurable number of carriers. For instance, to reconfigure a transceiver according to a given communication protocol; the transform size could be selected according to the channel impulse response characteristics, computational complexity or link quality [27].
- 6) Power conservation, Wavelet-based algorithms have long been used for data compression. This added significance for mobile wireless devices, which are mostly energy starved, reduced volume of data means the power needed for transmission is also reduced [27].

Wavelets have found beneficial applicability in various aspects of wireless communication systems design including channel characterization, interference mitigation and de-noising, modulation and multiplexing, multiple access communication, Ultra Wideband (UWB) communication, cognitive radio, and networking. The power of the wavelet transform comes from the fact that the basis functions of the wavelet are localized in time (or space) and frequency, and have different resolutions in these two domains [28].

### 4.3. Subband coding

The process of splitting the full-band source signal into different frequency bands and encode each band individually based on their spectrum energies is called sub-band coding technique [5].

The study of subband coding starts from the digital filter bank system, which is a group of filters that has different center frequencies. Digital filter banks find various good applications in communications signal processing. In general, they can be used to obtain very sharp frequency selectivity to isolate different communications frequency channels from each other and from interfering spectral components [30].

Typically, the filter bank design has two stages which are used in signal transmission system. The first stage is called analysis stage, which is located at the transmitter side, and corresponds to the decomposition process in which the signal samples are reduced by M factor. The second stage is called synthesis stage, which is located at the receiver side and corresponds to the interpolation process in which the signal samples are increased by M factor [5].

The analysis stage consists of sub-band filter followed by down sampler as shown in Figure 4.1. The output of this stage can be written in frequency domain as:

$$Y(z) = \frac{1}{M} \sum_{k=0}^{M-1} V(z^{\frac{1}{M}} e^{-j\frac{2\pi}{M}k}) \quad (4.1)$$

Where:  $V(z) = X(z)H(z)$ , and  $z$  corresponds to Z-domain.

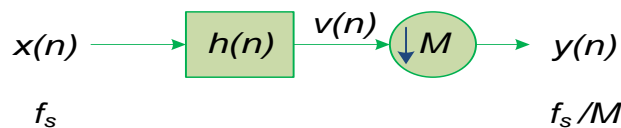


Figure 4.1: Analysis stage of filter bank.

Where:  $f_s$  is the sampling rate and  $h(n)$  is the analysis filter.

The synthesis stage consists of sub-band filter located after up sampler as shown in Figure 4.2. The output of this stage can be written in frequency domain as:

$$X(z) = Y(z^M)G(z) \quad (4.2)$$

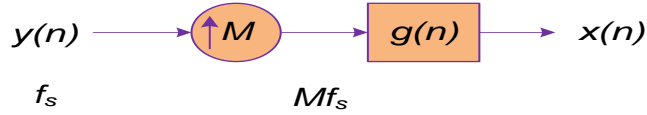


Figure 4.2: Synthesis stage of filter bank.

Where:  $g(n)$  is the synthesis filter.

M-band filter bank system is used to study and analyze the multi-resolution signal processing system. Two channel filter bank is the common and the efficient way to implement the discrete wavelet transform (DWT) [5]. The subband filter class used with the channel filter is Quadrature Mirror Filter (QMF). QMF is a digital filter, which achieve aliasing cancelation, its impulse response defined as:

$$h_1(n) = (-1)^n h_0(n) \quad (4.3)$$

Where:  $h_0(n)$  is low pass filter.

#### 4.3.1. Two channel filter bank

The structure of one level two channel sub-band filter bank is shown in Figure 4.3. After the signal passes the analysis stage, it is separated into two subbands. The synthesis part reconstructs the original signal. Typically the signal passes through more than one level.

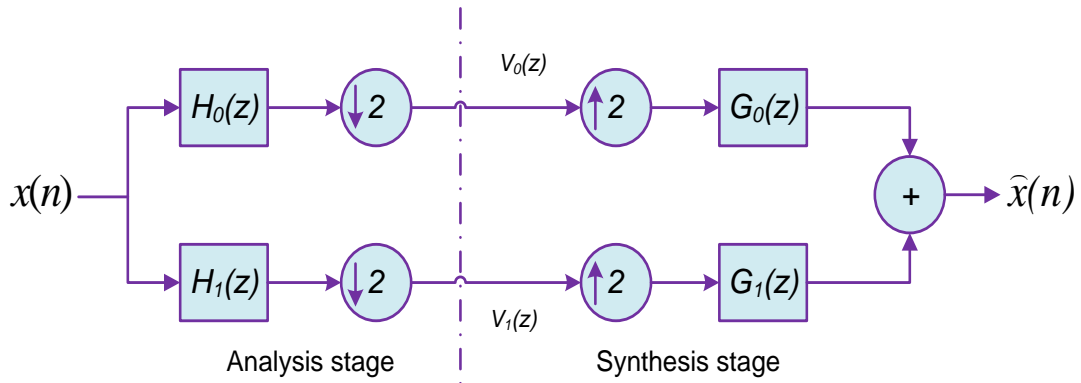


Figure 4.3: One level two channel sub-band filter bank.

By using equation (4.1) we can write the z-transform of the outputs of the analysis stage as:

$$V_0(z) = \frac{1}{2} [H_0(z^{1/2})X(z^{1/2}) + H_0(-z^{1/2})X(-z^{1/2})] \quad (4.4. a)$$

$$V_1(z) = \frac{1}{2} [H_1(-z^{1/2})X(-z^{1/2}) + H_1(-z^{1/2})X(-z^{1/2})] \quad (4.4.b)$$

By using the equation 4.2, the reconstructed signal output of the synthesis stage can be written as:

$$\hat{X}(z) = \frac{1}{2} [G_0(z)H_0(z) + G_1(z)H_1(z)]X(z) + \frac{1}{2} [G_0(z)H_0(-z) + G_1(z)H_1(-z)]X(-z) \quad (4.5)$$

Where  $H_0(z)$  and  $G_0(z)$  are related to the low pass analysis and synthesis filters, respectively, and  $H_1(z)$  and  $G_1(z)$  are related to the high pass analysis and synthesis filters, respectively.

The resulting  $\hat{X}(z)$  could be written as:

$$\hat{X}(z) = T(z)X(z) + S(z)X(-z) \quad (4.6)$$

Where:  $S(z)$  is called the aliasing term corresponding to  $X(-z)$ .

### 4.3.2. Perfect reconstruction conditions

Without using the up and down sampler, the output of the two-channel QMF banks is:

$$Y(z) = \left( \sum_{k=0}^1 G_k(z)H_k(z) \right) X(z) \quad (4.7)$$

When up and down sampler are available, the synthesis stage can be reconstructed the full-band signal  $X(n)$  if the following conditions are achieved:

1. Eliminate the aliasing term in equation 4.8, i.e,  $S(z) = 0, \forall z$ , so that:

$$G_0(z)H_0(z) + G_1(z)H_1(-z) = 0 \quad (4.8)$$

2.  $T(z)$  has unity amplitude & pure delay, so:

$$T(z) = z^{-n_0} = e^{-j\omega n_0}, \quad z = e^{-j\omega} \quad (4.9)$$

If these conditions are satisfied then:

$$\hat{X}(Z) = e^{-j\omega n_0} X(z) \quad (4.10.a)$$

$$\hat{x}(n) = x(n - n_0) \quad (4.10.b)$$

#### 4.4. DWT/IDWT using filter bank theory

The wavelet transform can be regarded as a form of subband coding where the signal to be analyzed is passed through a series of filter banks. The outputs of the different filter levels are represent the wavelet and scaling function transform coefficients [27].

The two channel subband structure that will be used is the dyadic or octave band structure which splits only the lower half of the spectrum into two equal bands at any level of the filter bank, so no further decomposition of the higher band at any level [5], as shown in Figure 4.4.

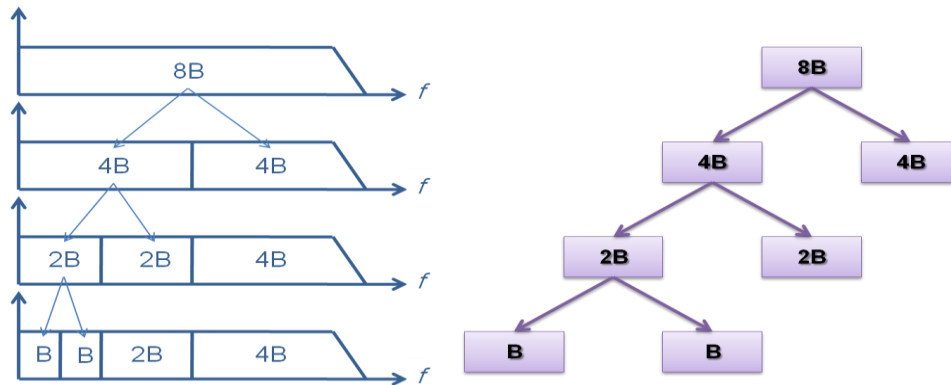


Figure 4.4: Dyadic two channel subband structure.

The multi-level two channels perfect reconstruction filter bank system is used for determining the DWT coefficients [5]. The signal is decimated into sub-bands in the analysis stage. This decimation doubles the frequency resolution since every band is half the previous band due to filtering operation. However the time resolution is halved due to down sampling operation.

The DWT of the full-band source signal is the concatenation of all coefficients starting from the last level of decomposition. Figure 4.5 show the decimation process used for determines the DWT coefficients for a given signal using Mallat-tree decomposition algorithm.

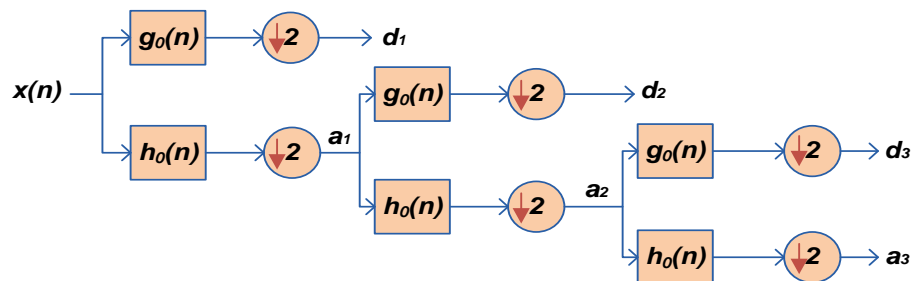


Figure 4.5: Implementation of DWT using decimation process.

Where:

$d_m(n)$  : Detailed or wavelet coefficients.  $m = 1, 2, \dots, L$ , where  $L$ : is the number of filter bank level.

$a_m(n)$ : Approximation coefficients.  $m = 0, 1, 2, \dots, L$ .

$h_0(n)$ : Low pass filter which enables to remove the high frequency information and provides  $a_m(n)$  coefficients of the signal.

$g_0(n)$ : High pass filter which preserve the high frequencies and provides the detail information about the signal, i.e,  $d_m(n)$  coefficients.

The approximation and wavelet coefficients at any scale can be calculated by:

$$a_{m+1}(n) = \sum_k a_m(k)h_0(2n - k) \quad (4.11. a)$$

$$d_{m+1}(n) = \sum_k a_m(k)g_0(2n - k) \quad (4.11. b)$$

Where:  $a_0(n)$  corresponds to the source signal  $x(n)$ , i.e,  $a_0(n) = x(n)$ .

The process of reconstruction the source signal from the DWT coefficients is called the inverse discrete wavelet transform IDWT. Figure 4.6 shows the structure of the synthesis filter bank which are used for interpolated the original signal.

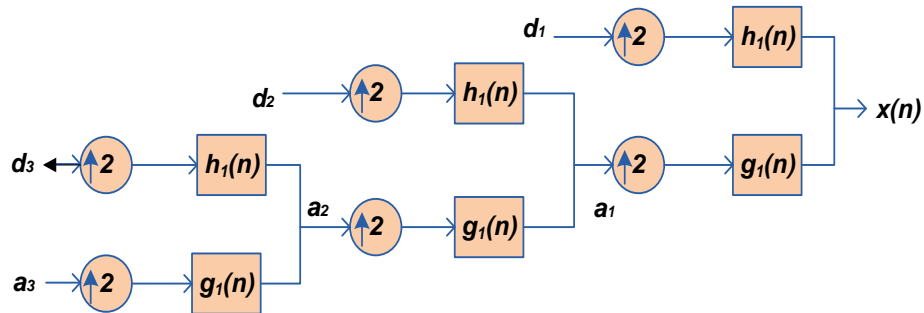


Figure 4.6: Implementation of IDWT using interpolation process.

For every level of reconstruction filter bank the approximation and details coefficients are up sampled and passed through low pass and high pass synthesis filters and then added.

The reconstruction approximation coefficients  $a_m(n)$  can be expressed as:

$$a_m(n) = \sum_k a_{m+1}(k)g_1(n - 2k) + d_{m+1}(k)h_1(n - 2k) \quad (4.12)$$

The full band signal is recovered by using the same number of filter bank levels as in the decomposition process. The Mallat algorithm works equally well if the analysis filters  $g_0(n)$  and  $h_0(n)$  are exchanged with the synthesis filters  $g_1(n)$ ,  $h_1(n)$  for perfectly reconstruction, such that:

$$h_1(n) = h_0(-n) \quad (4.13.a)$$

$$g_1(n) = g_0(-n) \quad (4.13.b)$$

An important feature of the discrete wavelet transform is the relationship between the impulse responses of the high pass (analysis) and low pass (scale) filters [27]. The high pass filter and the low pass filter in each stage (analysis and synthesis) are related to each other according to the following relationship:

$$g(n) = (-1)^n h(L - 1 - n) \quad (4.14)$$

## 4.5. Wavelet orthogonality

The wavelet orthonormal basis is a family of linearly independent functions  $\psi_{m,n}(t)$ , these basis functions are built by scaling and translating the mother wavelet function  $\psi(t)$ . The construction of a wavelet orthonormal basis is designed from a given orthogonal mirror filters,  $h(n)$  and  $g(n)$ . The mirror filters satisfy the following orthogonal condition:

$$\sum_n h(n)h(n - 2k) = \delta(k) = \begin{cases} 0 & k \neq 0 \\ 1 & k = 0 \end{cases} \quad (4.15)$$

This orthogonality property leads to make the wavelets orthogonal to each other, so that:

$$\int_t \psi_{j,k}(t) \psi_{m,n}(t) dt = \begin{cases} 1 & \text{if } j = m \text{ and } k = n \\ 0 & \text{otherwise} \end{cases} \quad (4.16)$$

The orthogonality of the wavelet carriers relies on both their time position and their frequency localization (scale). This makes the wavelet based multicarrier transmission less sensitive to Doppler shift effect that particularly attacks the carriers orthogonality, which is leading to noticeable BER improvements, under certain circumstances [31]. However, for comparison, the OFDM carriers orthogonality relies on their precise positioning on the frequency axis and so that the orthogonality will be affected by Doppler effect. Wavelet basis are more spectrally compact than traditional OFDM basis, they have less out of band energy. In other words, the side lobes of the OFDM spectrum, which is a sinc spectrum, contain an important amount of energy that create inter channel interference [31].

## 4.6. Multicarrier modulation based DWT system design

Multicarrier modulation can be viewed as a general transmultiplexer system, which consists of synthesis part and analysis part. Discrete Wavelet Transform is proposed as high performance digital signal processing technique for use in implementing multicarrier modulation. In DWT the orthogonality between the subcarriers is satisfied by orthogonal wavelet filter banks. The block diagram design of multicarrier transceiver digital system based on DWT is shown in Figure 4.7.

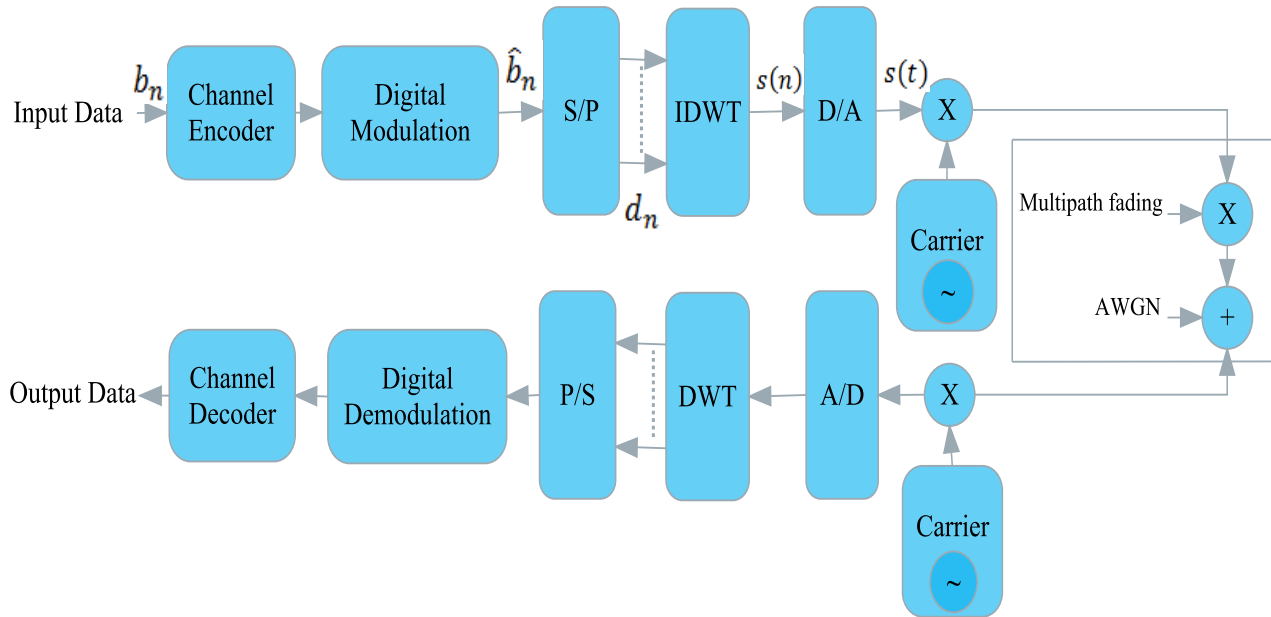


Figure 4.7: Wavelet based multicarrier modulation structure.

The system design comprise of an inverse discrete wavelet transform (IDWT) as modulator at the transmitter and a discrete wavelet transform (DWT) as demodulator at the receiver. The main and the important difference between the conventional OFDM and DWT multicarrier system is there no cyclic prefix blocks in the transmitter or in the receiver parts. Due to the overlapping nature of wavelets, the wavelet based multicarrier has very high spectral containment and therefore does not need a cyclic prefix to deal with the delay spreads of the channel [29]. Wavelet based multicarrier can better combat narrowband interference and more robust against inter channel interference (ICI). By not requiring the cyclic prefix, the available bandwidth would be more efficiently used, and hence high data rate can be achieved.

The transmitter design and receiver design as will as the channel effect will be discussed in detail in the following subsections.

#### 4.6.1. Transmitter design

At the transmitter, the sequence of binary digits from the data source is passed to the channel encoder and then the transmitter uses a digital modulator to modulate the encoded bits stream into symbols stream. This stream is passed through a serial to parallel converter (or demultiplexer), giving  $N$  lower data stream at dyadic sub rate of the source rate. Then the IDWT will be applied to the  $N$ - data stream and generating the sequence  $s(n)$  at the data source rate. The sequence  $s(n)$  is converted to analog signal through the digital to analog converter (DAC) and passed onto the radio frequency (RF) modulation and then to the wireless channel.

IDWT represents the key point of the multicarrier transmitter in which the orthogonal wavelet modulation is performed. IDWT process can be performed via interpolation process in which the signals at every level are upsampled by two and passed through the synthesis filter banks. Figure 4.8 show the structure of IDWT process with 4-subchannel. This Figure show that the rate of the source symbol is reduced in dyadic form and at the end of synthesis process the output signal has the rate of the source symbol.

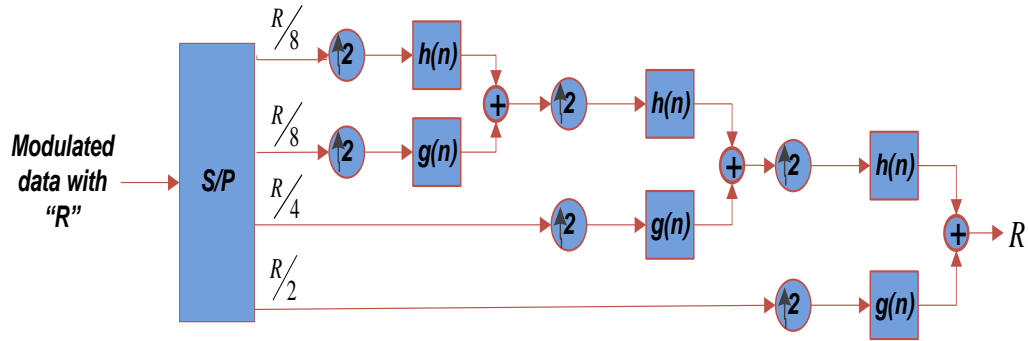


Figure 4.8: IDWT modulator with four subcarriers (or subchannels).

The synthesis filters  $h(n)$  and  $g(n)$  are comprised the orthonormal wavelet bases. Every wavelet basis is seen as a subcarrier and the transmitted symbols are multiplied by these subcarriers. The orthogonality of the individual basis function prevents inter symbol interference (ISI), furthermore, their mutual orthogonality prevents interference across scales [32]. The transmitted signal  $s(t)$  can be expressed as:

$$s(t) = \sum_{m \in M} \sum_n S_n^m \psi_{m,n}(t) \quad (4.17)$$

Where:  $\psi_{m,n}(t)$  is the mother wavelet and represent the basis wavelet functions (subcarriers),  $S_n^m$  is the data that is modulated onto the wavelets subcarriers at different scales, and  $M$  represent the number of frequency bands (or number of subcarriers).

Figure 4.9 show the time-frequency plane (or tiling diagram) which give an indication of the energy concentration of each symbol, and each tile represents a given basis function (or subcarrier).

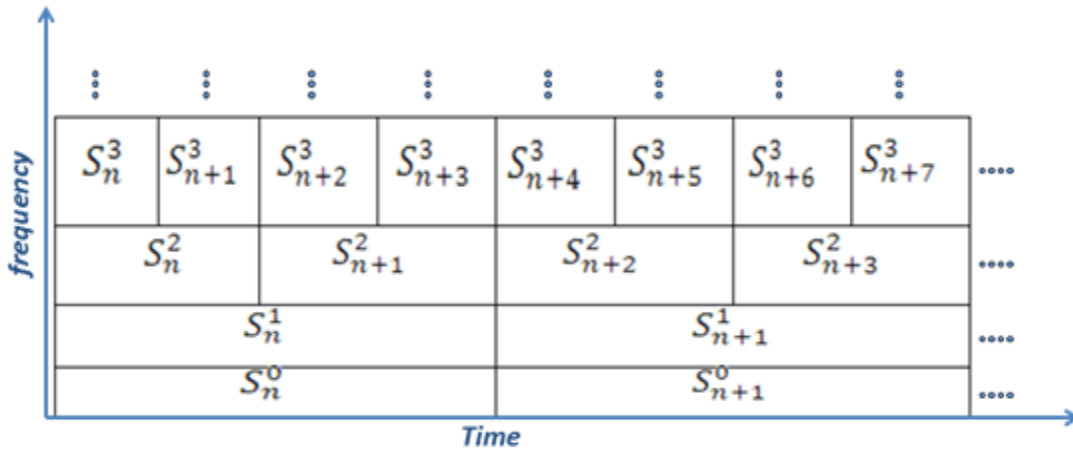


Figure 4.9: Time-frequency plane of  $S_n^m$ .

#### 4.6.2. The channel

The transmitted signal passes through the communication channel such as an additive White Gaussian noise channel (AWGN) or multipath channel. When orthogonality between carriers is lost after the transmitted signal passes through a non-uniform channel, the amount of interference between carriers in wavelet systems is much lower than in Fourier systems since the side lobes contain much less energy therefore the ICI is reduced in wavelet based multicarrier [29].

#### 4.6.3. Receiver design

At the receiver side, the RF demodulation is performed firstly, then the signal  $r(t)$  is digitized through the analog to digital converter (ADC). The DWT process is applied on the sample points of  $r(n)$  and produces the recovered data symbols  $\tilde{d}(n)$ . The sequence  $\tilde{d}(n)$  is multiplexed using parallel to serial converter. De-mapping, decisions and decoding process is performed on the received serial symbols in a similar manner as any other digital communication system.

DWT process can be performed via decimation process in which the signals at every level are passed through the analysis filter banks and downsampled by two. The orthogonality is the key feature that allows subcarrier separation at the receiver. If there is no noise, the received signals are the exactly same as the transmitted data symbols as long as we use the perfect reconstruction filter bank.

## 4.7. MIMO- DWT system design

MIMO technology is becoming very attractive technique in wireless communications because it achieves significant performance improvement in data throughput and spectral utilization of the bandwidth. The MIMO technique is one category of multiple antenna system configurations in which there are more than one antenna at the transmitter and more than one antenna at the receiver. Multiple antenna configurations have another two categories SIMO and MISO. SIMO configuration corresponds to using one antenna at the transmitter and multiple antennas at the receiver. MISO configuration corresponds to using multiple antennas at the transmitter and only one antenna at the receiver. In MIMO technique, both the diversity gain and capacity gain can be achieved. However, only the diversity gain will be achieved by other two multiple antenna system.

The diversity performance in MIMO system can be improved through the space time block coding (STBC) technique. Space time block coding can achieve transmit diversity and power gain without sacrificing the bandwidth [21].

The combination between the multicarrier modulation and the MIMO configuration in one system combines the advantages of these two technologies in broadband communications. MIMO-OFDM has been considered in many researches, these researches show the improvement in performance due to the advantages of combination. The performance will be more improved if we combine the DWT as multicarrier modulation with MIMO technology rather than MIMO-OFDM combination. MIMO-DWT system will be discussed in this section including the blocks diagram design that explains the structure of this system.

In general, the MIMO-DWT system is composed of  $M_T$  transmitting antennas,  $M_R$  receiving antennas, and  $N$  discrete wavelet transform (DWT) subcarriers as indicated in Figure 4.10. IDWT acts as multicarrier modulator for each transmitting antenna and DWT as demodulator for each receiving antenna.

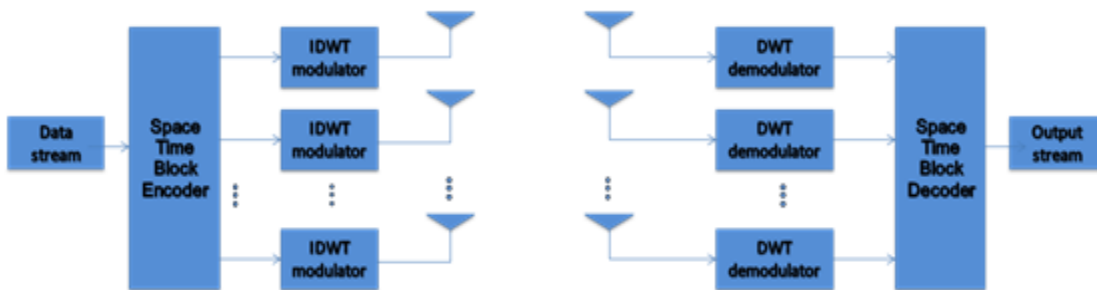


Figure 4.10: MIMO-DWT system model.

At the transmitter part of MIMO-DWT system, the incoming symbols stream is encoded by the STBC encoder which produces  $M_T$  code words. At each branch (or antenna) every  $N$  code words uses one IDWT modulator. The coded transmitted data symbols can be defined as:

$$s_k = [s_k^0 \quad s_k^1 \quad s_k^2 \quad \dots \quad s_k^{(N-1)}] \quad (4.18)$$

Where:  $s_k^i$  is the coded (or the output of STBC encoder) transmitted data symbol from antenna  $k$  on the  $i$  subcarrier,  $0 \leq k \leq M_T - 1$ .

All of the symbols output from  $M_T$  IDWT modulator is transmitted at the same time from different transmit antennas. These symbols are transferred through the MIMO channel. The receiver side receives these symbols using  $M_R$  receiving antennas. After that, the receiving symbols are passed through the DWT demodulator and then to the STBC decoder. The original data can be recovered through the traditional receiver stages of the digital communication system.

The MIMO-DWT system model with two antennas at the transmitter and one antenna at the receiver using Alamouti coding scheme is shown in Figure 4.11. With two transmitting antenna, the index  $k$  in equation (4.18) takes two values, i.e,  $k = [0 \quad 1]$ . The Alamouti encoder and decoder in MIMO-DWT do the same process that was discussed in chapter 3.

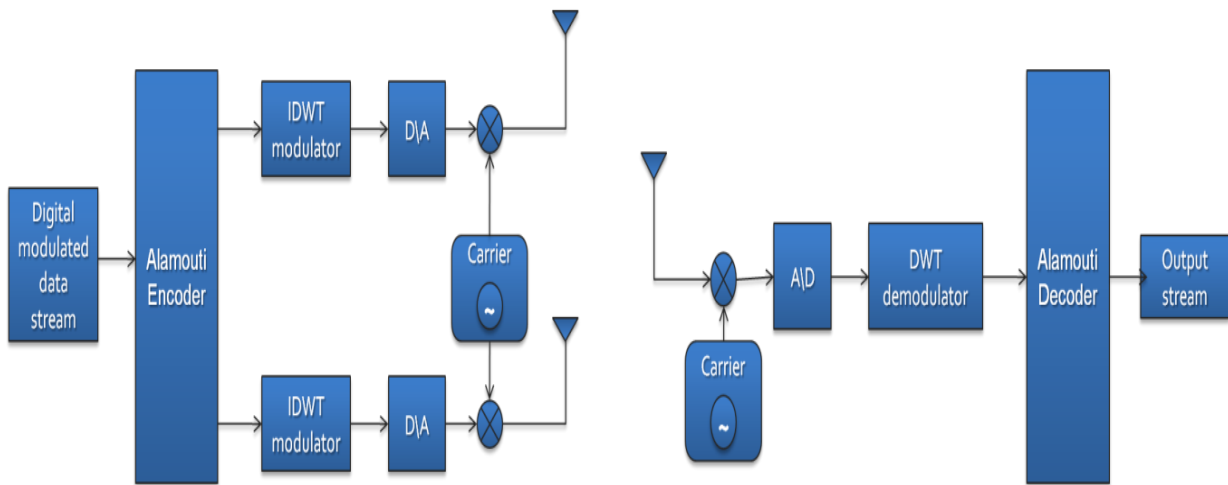


Figure 4.11: Alamouti coded DWT system.

## 4.8. The system performance and simulation parameters

The performance of any communication system must be considered. The bit error rate (BER) and the capacity (or data rate) are two parameters for measure the performance of our system model. **The bit error rate (BER)** is the number of bit errors divided by the total number of transferred bits during time interval. The bit error rate (BER) of BPSK and QAM in AWGN channel can be calculated by these equations, respectively:

$$P_b = Q\left(\sqrt{\frac{2E_b}{N_0}}\right) \quad (4.19)$$

$$P_b = Q\left(\sqrt{\frac{E_b}{N_0}}\right) \quad (4.20)$$

Where:  $P_b$  is the probability of error, and  $\frac{E_b}{N_0}$  is the SNR value.

In simulation part the bit error rate (BER) can be measured by this function in MATLAB [number, ratio] = biterr(x, y) compares the elements in x and y. Where x is transmitted data and y is received data.

**The Capacity** represents the number of bit that can be transferred per unit time. The capacity is a measure of the rate of the system at which data can be sent through the channel, specified in bits per second (bps).

**Simulation Parameters** are shown in Table 4.1. In DWT we will use Haar mother wavelet.

Table 4.1: Simulation parameters.

Parameter	Specification
Number Of Data Subcarriers(N)	64
Modulation Type	BPSK, QAM
SNR	0-15 dB
Space time block coding	Alamouti scheme Higher order OSTBC
MIMO configuration	Different configuration
Channel	AWGN channel
	Rayleigh for MIMO

# **Chapter 5**

## **Simulation Results**

The simulation results of our project will be shown in this chapter, but at the beginning we will present the flow charts for DWT based multicarrier system and for MIMO-DWT.

## 5.1. Flow Charts

Two main flow charts are presented:

### 5.1.1. DWT based multicarrier flow chart (SISO case)

Figure 5.1 show the flow chart for multicarrier modulation using discrete Wavelet transform system model.

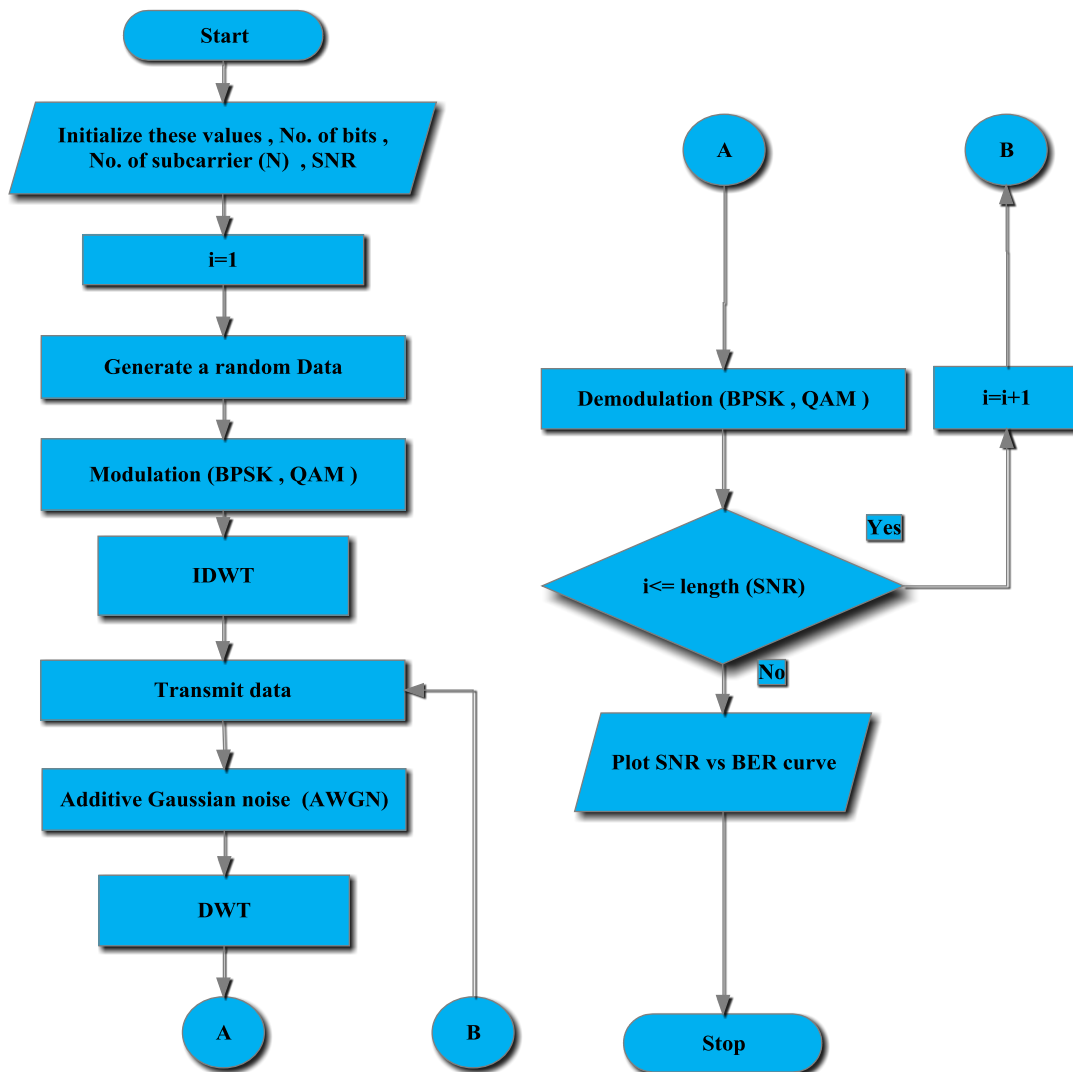
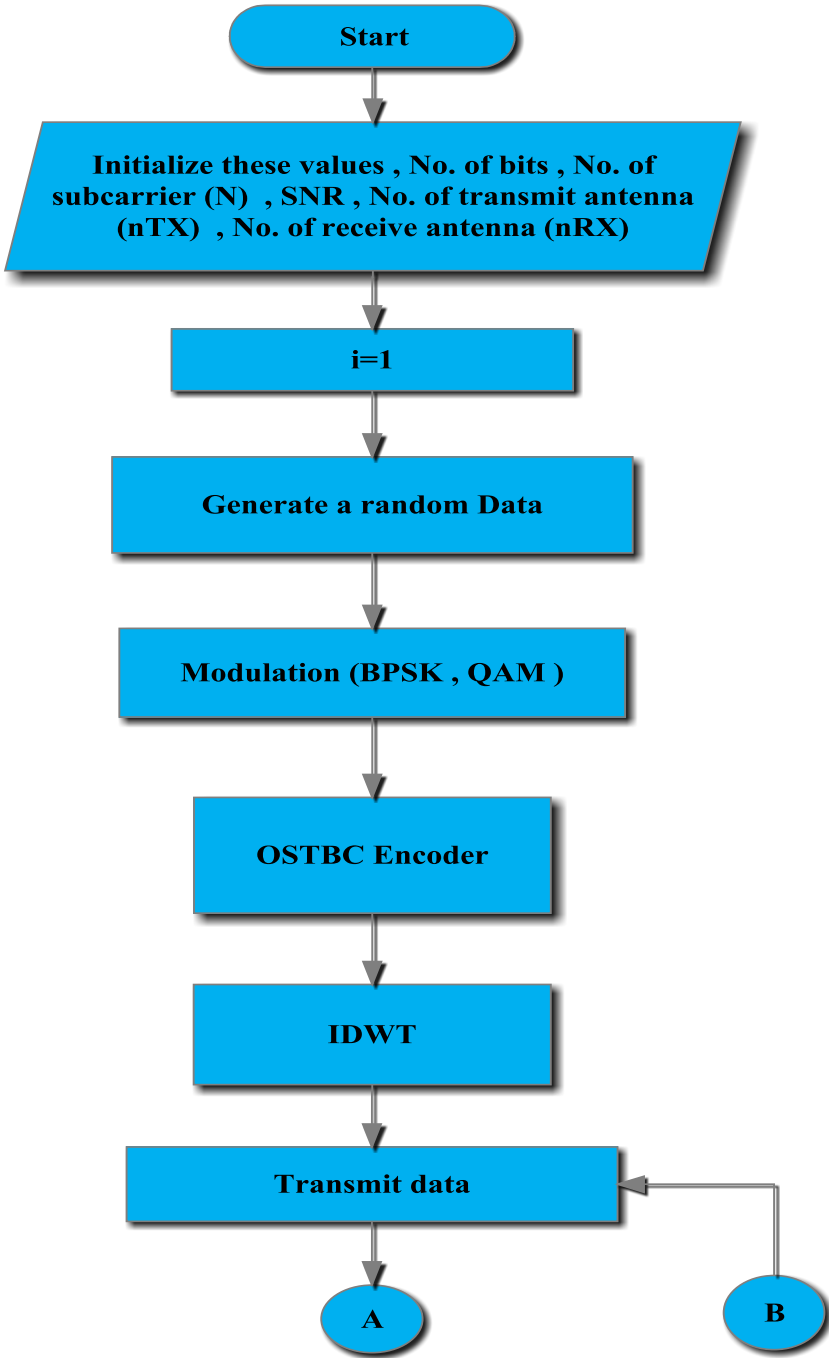


Figure 5.1: flow chart for DWT based multicarrier system model.

**5.1.2. Flow chart for MIMO-DWT system model**

Figure 5.2 show the flow chart for DWT based multicarrier using multiple antennas system model. All the steps in this flow chart are discussed in the previous chapters in detailed.



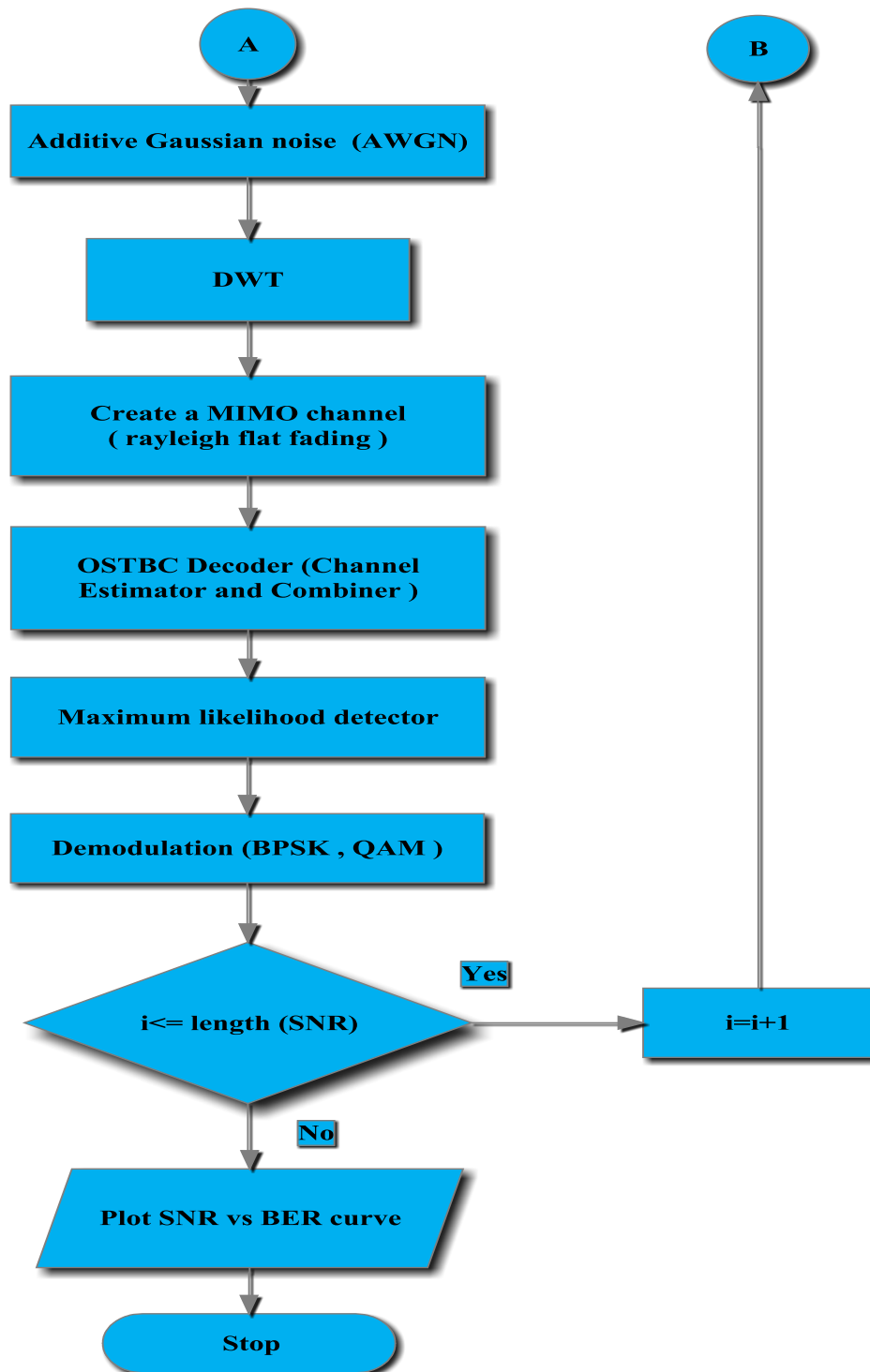


Figure 5.2: flow chart for MIMO-DWT system model

## 5.2. Simulation Results

The performance of our system is measured in terms of bit error rate (BER) and capacity. In the simulation results we show the BER curves for DWT based multicarrier system and conventional OFDM system and we make a comparison between them based on BER and capacity. The capacity is measured by two points of view; how many times is needed to transmit one multicarrier symbol or how many data bits transmitted with one multicarrier symbol.

The generation of multicarrier modulation for two systems in MATLAB simulation is performed using built in functions, table 5.1 summarize these functions with their operation:

Table 5.1: MATLAB built in functions for multicarrier generation.

Function	Operation
<code>idwt(AC, DC, 'haar')</code>	Inverse discrete Wavelet Transform with Haar mother wavelet. AC and DC represent the approximation and detailed coefficients, respectively.
<code>dwt(s, 'haar')</code>	Discrete Wavelet Transform with Haar mother wavelet.
<code>ifft(s)</code>	Inverse Discrete Fourier Transform of $s$ .
<code>fft(x)</code>	Discrete Fourier Transform of $x$ .

Two modulation schemes are studied in comparison, BPSK and QAM, and with different antenna configurations. The simulation results divide into three cases:

- 1) BER of DWT based multicarrier and OFDM systems with SISO system.
- 2) BER of MIMO with higher order complex OSTBC (code rate  $\frac{1}{2}$ ). Alamouti scheme (code rate 1) will be used with  $2 \times M_R$  system.
- 3) BER of MIMO with two multicarrier systems, MIMO-DWT and MIMO-OFDM.

In SISO OFDM we consider two cases, OFDM symbol with guard band (null subcarriers) and without. The difference between these two cases will be shown.

### 5.2.1. BER of DWT based multicarrier and OFDM systems

In this part we will study the following two cases:

- 1) BER for DWT Multicarrier and OFDM systems using BPSK/QAM modulation in AWGN channel.

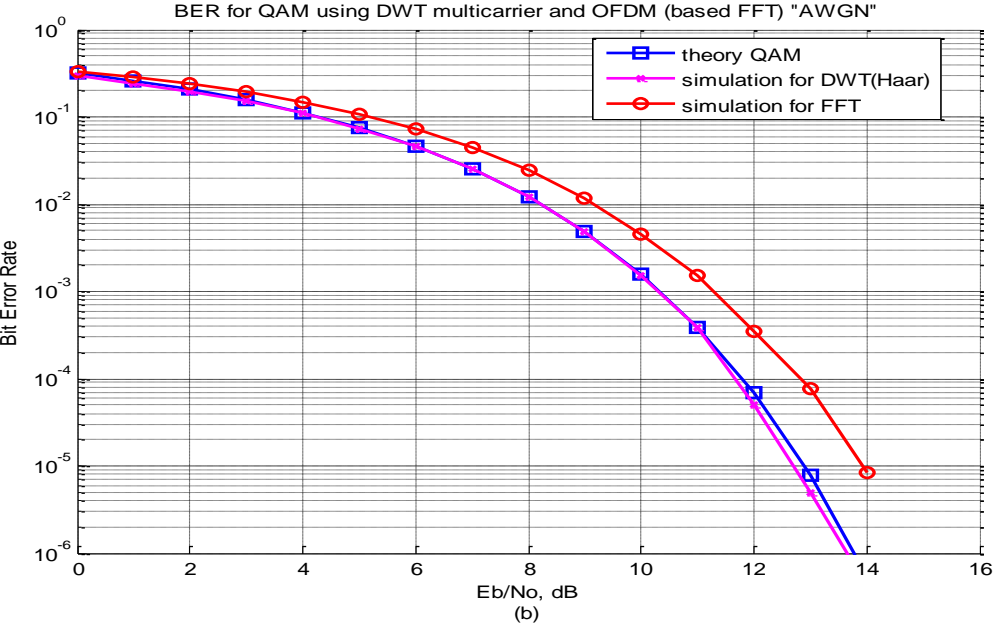
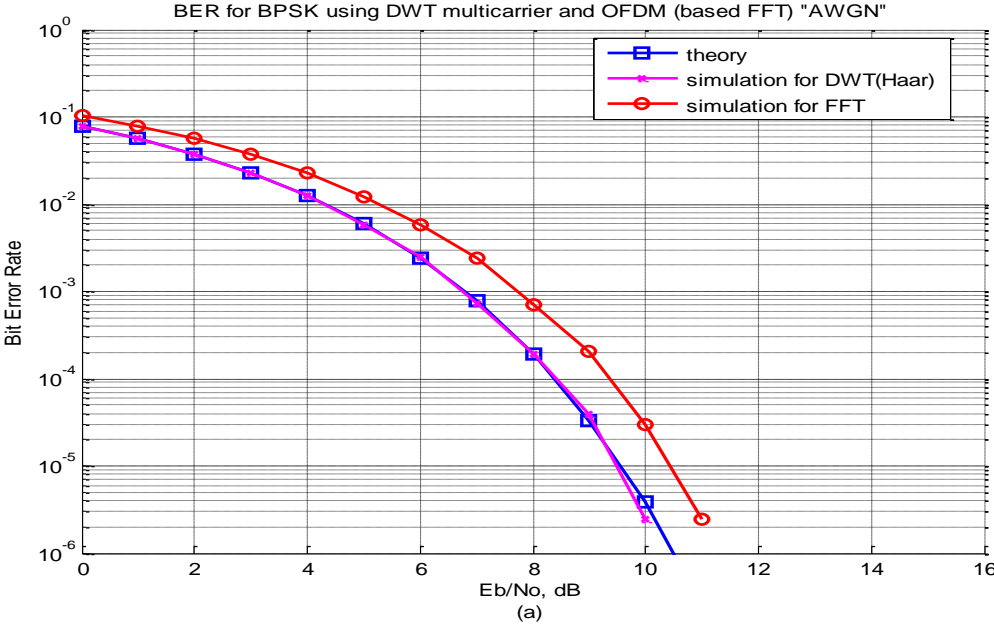


Figure 5.3: BER of DWT and OFDM using a) BPSK b) QAM

Figure 5.3 shows the bit error rate versus signal to noise ratio for DWT based multicarrier system, conventional OFDM system and for system with single carrier using BPSK modulation as shown in (a), and QAM as shown in (b) in AWGN channel. From this Figure we can notice that the probability of error for DWT based multicarrier system is less than the probability of error of the conventional OFDM over all values of signal to noise ratio (SNR). Also we can see that the BER for DWT based multicarrier is approximately the same as the theoretical BER that yields from single carrier with both modulation scheme (BPSK and QAM).

The transmission capacity (bit per sec) that can be achieved with multicarrier modulation is better than with single carrier modulation. We can notice that in QAM we transmit more bits per subcarrier but with higher BER.

In addition to the better performance in BER of DWT based multicarrier compared with conventional OFDM based multicarrier, the transmission capacity and the bandwidth utilization with DWT outperforms the OFDM due to the cyclic prefix extension with OFDM symbol. Every DWT symbol contains 64 subcarriers each one carry one bit data in BPSK scheme and two bit in QAM scheme without any other overhead. In contrast, the length of OFDM symbol accommodate for 80 subcarriers. Only 64 of them are used for transmit data and the remaining are for cyclic prefix interval. In other word, the transmission time for one OFDM symbol is large than for one DWT symbol. As a result the capacity in DWT is better than in OFDM.

The difference between bit error rate of two multicarrier systems (DWT and OFDM) is not large, this is due to the assumption that we use which state that the channel impulse response is flat, i.e,  $h(t) = \delta(t)$ , and only what we see is the effect of the additive white Gaussian noise channel.

In addition of cyclic prefix, many wireless communication systems that use the conventional OFDM as multicarrier such as Wi-Fi technology (802.11) add guard band (null subcarriers) to limit the multipath interference (ISI interference) from one symbol to the next. For every OFDM symbol, there are 12 null subcarriers from 64 subcarriers and they act as guard band for the channel. We took the addition of guard into account in our work and we will use it over all part of simulation results.

In the following figure we will show the performance of conventional OFDM system with guard band compared with DWT multicarrier system.

2) BER for DWT Multicarrier and OFDM (with guard band interval) systems using BPSK/QAM modulation in AWGN channel.

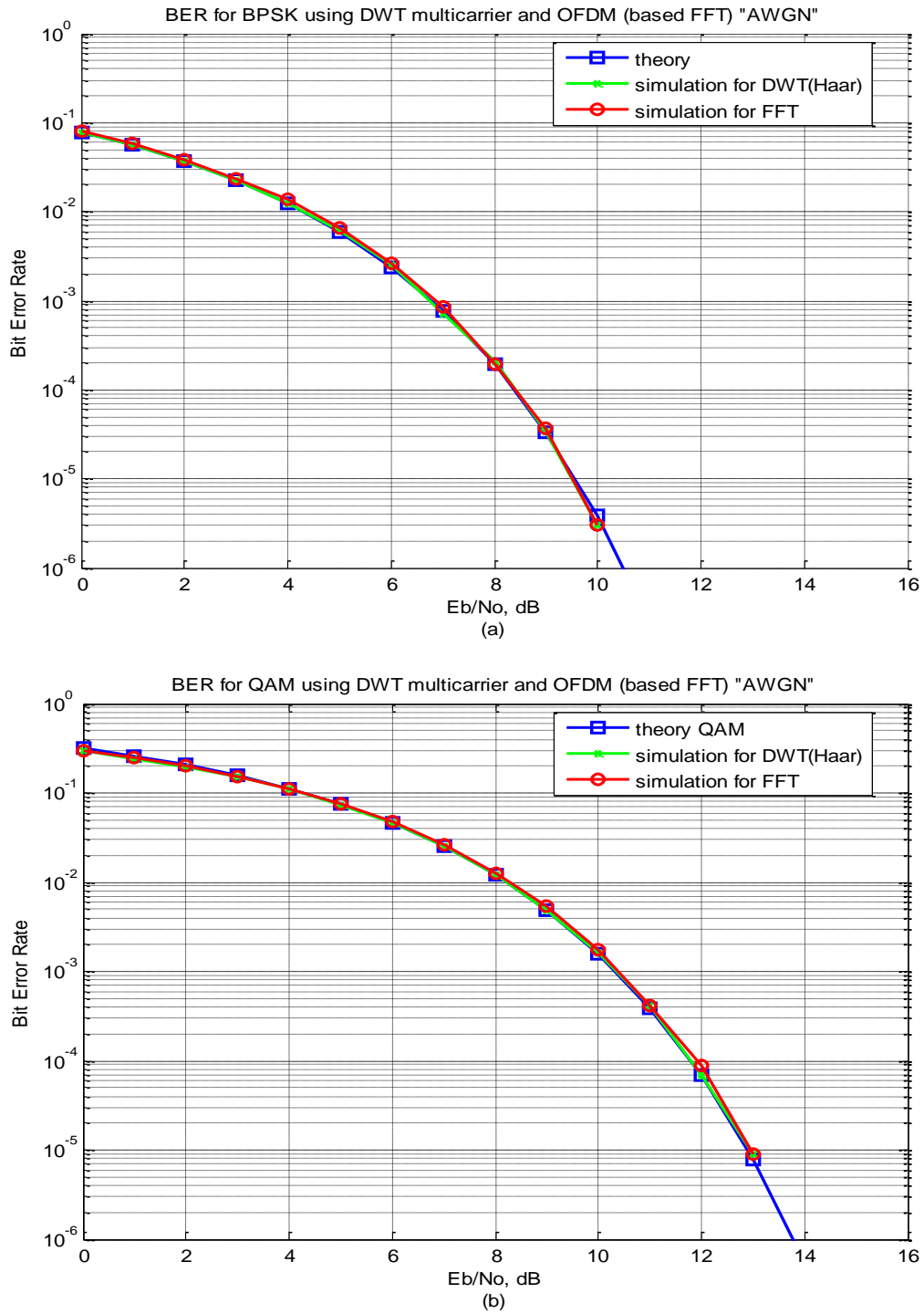


Figure 5.4: BER of DWT and OFDM (with guard) using a) BPSK b) QAM

Figure 5.4 show the relationship between signal to noise ratio and bit error rate for DWT based multicarrier system, conventional OFDM system, and for system with single carrier using BPSK modulation as shown in (a), and QAM as shown in (b) in AWGN channel. From this Figure we can notice that the probability of error for DWT based multicarrier system and conventional OFDM are approximately the same as the theoretical BER that yields from single carrier over all values of signal to noise ratio (SNR) in the two modulation scheme. However, the transmission capacity (bits per sec) that can be achieved in DWT and OFDM is better than the capacity of single carrier system due to the advantages of multicarrier modulation.

Although the BER for DWT and OFDM are the same in AWGN channel, the transmission capacity (bits per sec) with DWT system is superior the capacity in OFDM system. Every DWT symbol contains 64 subcarriers each one carry one bit data in BPSK scheme and two bit in QAM scheme without any other overhead. In contrast, every OFDM symbol has only 52 subcarrier out of 64 subcarrier carry data, 12 subcarrier as guard band to mitigate the effect of inter symbol interference (ISI) and a length of 16 subcarrier cyclic prefix to overcome the effect of the channel (inter channel interference). So that the available bandwidth is utilized when the DWT is used as multicarrier modulation.

In the following figure we will show the difference between the two modulation scheme (BPSK and QAM) in single carrier and multicarrier modulation.

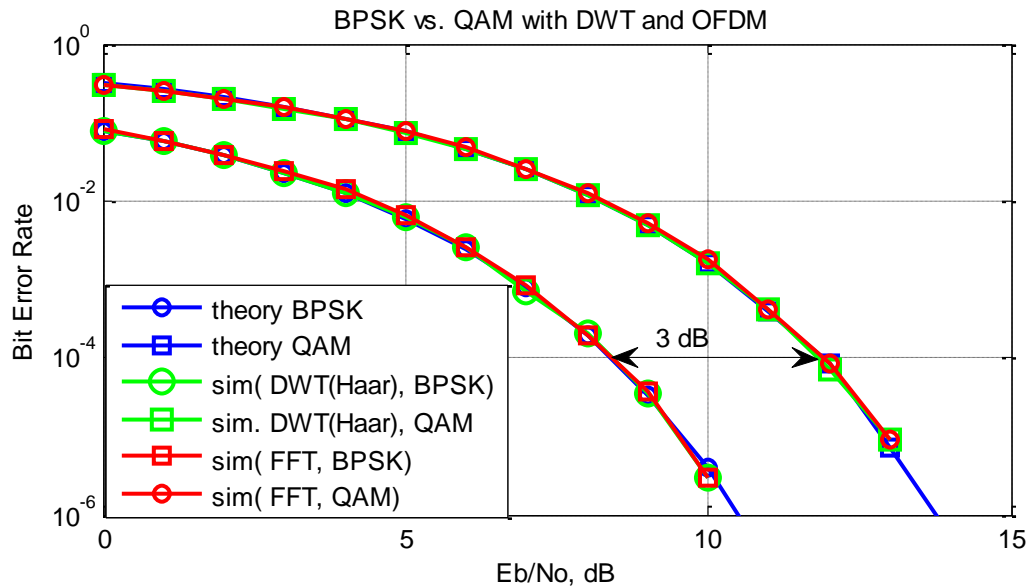


Figure 5.5: SISO multicarrier BPSK vs. QAM

In QAM modulation every subcarrier carry two data bits, so that the transmission capacity that can be achieved in QAM scheme is twice the transmission capacity with BPSK scheme whether with single carrier or multicarrier but the probability of error increased and we need twice the transmission power to achieve the same BER as in BPSK as shown in Figure 5.5.

Table 5.2 show the comparison of DWT based multicarrier and OFDM based multicarrier in terms of capacity (the transmitted data measured bits per one multicarrier symbol) and the bandwidth utilization efficiency (the ratio between the length of subcarrier that carry data over the total multicarrier symbol length). This comparison between two multicarrier system in the present and absent of guard band.

Table 5.2: comparison between DWT and OFDM systems.

	OFDM		DWT based multicarrier
	Without guard	With guard	
Bandwidth utilization efficiency ( $\eta$ )	64 subcarriers for data.	52 subcarriers for data.	64 subcarriers for data.
Capacity (bits/ symbol)	$\eta = \frac{64}{80}$	$\eta = \frac{52}{80}$	$\eta = \frac{64}{64} = 1$
BPSK	64-bit / symbol	52 -bit / symbol	64- bit /symbol
QAM	128 bit/symbol	104 -bit /symbol	128- bit/symbol

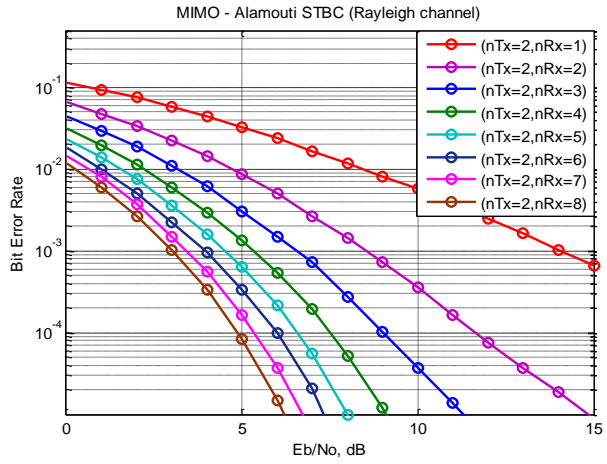
Table 5.2 shows that the achievable capacity when using DWT as multicarrier is superior the conventional OFDM whether the guard (null subcarrier) are present or not. The capacity is better when the QAM scheme is used.

### 5.2.2. MIMO under complex OSTBC

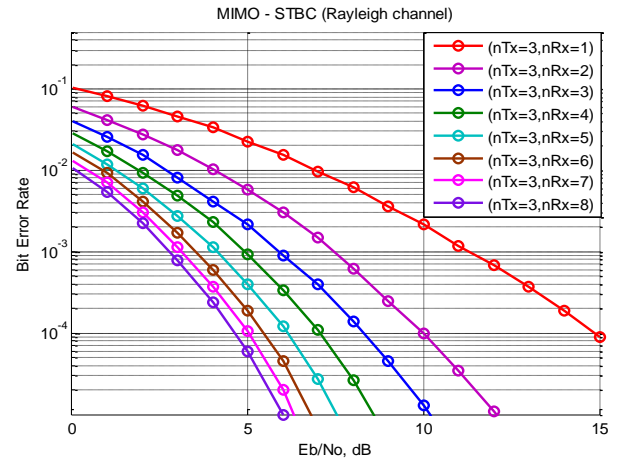
In this part we will show the performance in terms of bit error rate of Multiple Input Multiple Output system (MIMO) with the complex Orthogonal Space Time Block Coding (OSTBC), code rate  $R = \frac{1}{2}$ , using two different modulation schemes, BPSK and QAM, over Raleigh fading channel. In  $2 \times nRx$  system we use the Alamouti STBC ( $R = 1$ ).

#### 5.2.2.1. MIMO Simulation Results with BPSK

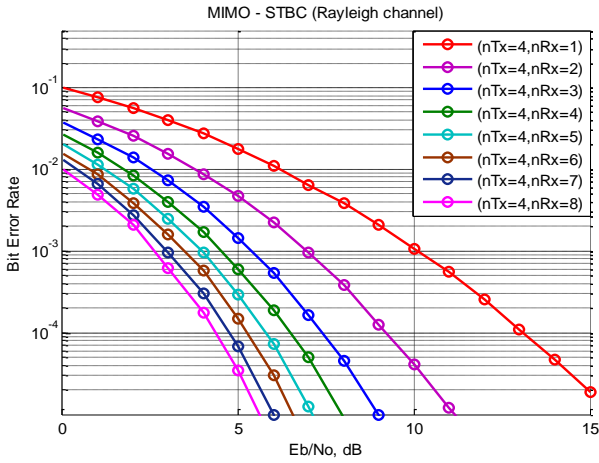
The comparison will start by varying the number of receive antennas, and show the improvement on the performance curves in the following figures. Each graph in Figure 5.6 represent the bit error rate (BER) of MIMO system with multiple receives antennas at fixed number of transmits antennas ( $nTx = 2,3,4,5,6$  and 8).



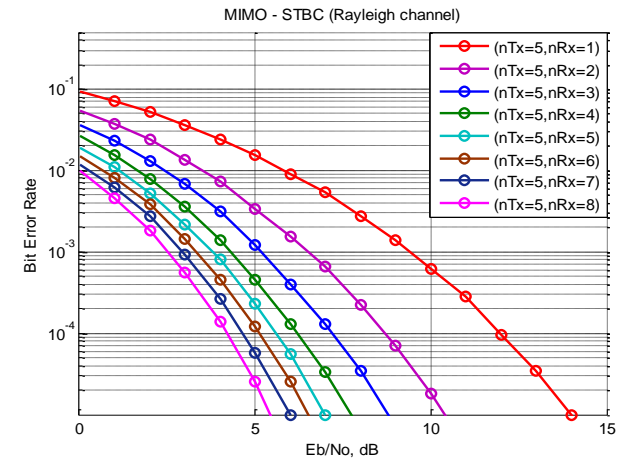
(a):  $2 \times nRx$



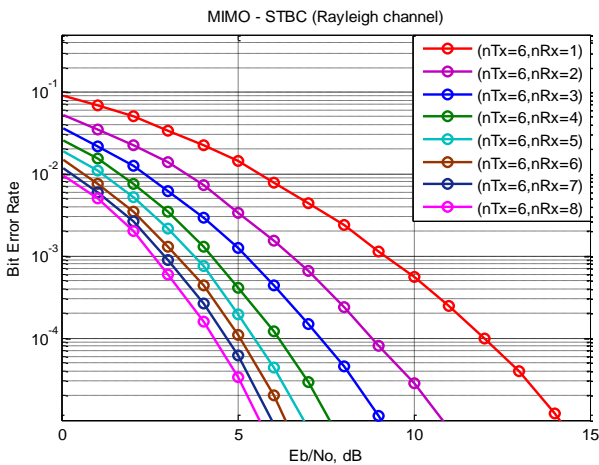
(b):  $3 \times nRx$



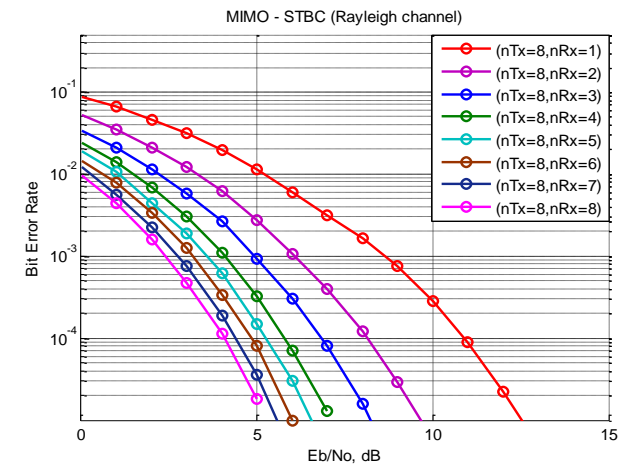
(c):  $4 \times nRx$



(d):  $5 \times nRx$



(e):  $6 \times nRx$



(f):  $8 \times nRx$

Figure 5.6: different MIMO configurations under OSTBC using BPSK over Rayleigh channel.

It is noticeable that at any given transmit antenna, the bit error rate decreases with increase the number of receive antenna over all values of signal to noise ratio (SNR) which is logically because when we receive the same signal more than once, and combine them at the receiver output, this causes to improve the SNR of the received signal. This improvement in SNR is due to increase in diversity order and to the array gain in which more receive antennas means receive more power.

With number of receive antenna increase the decrease in BER becomes slowly, in other words, the improvement in BER is diminishing with increasing in the number in receive antennas. For example, if we take  $2 \times nRx$  and at a given SNR we find that the BER of  $2 \times 2$  is less than  $2 \times 1$ ,  $2 \times 3$  is less than  $2 \times 2$  and so on but the difference of BER between  $2 \times 3$  and  $2 \times 2$  is less than between  $2 \times 2$  and  $2 \times 1$ .

If we look at specific receive antenna and we move from figure (5.6.a) to figure (5.6.f), i.e, increase the number of transmit antenna, then we can notice that the bit error rate is decrease with increase the number of transmit antenna over all values of SNR. Figure 5.7 clarifies  $nTx \times 4$  as an example of multiple number of transmit antenna at fixed number of receive antenna. As the number of transmitting antennas increases, the performance continues to improve, but each time to a lesser degree since the more antennas are installed, the more interference is presented. It is clear that the improvement in the bit error rate due to the increase in the number of transmit antenna is less than the improvement in BER due to increase in the number of receive antenna.

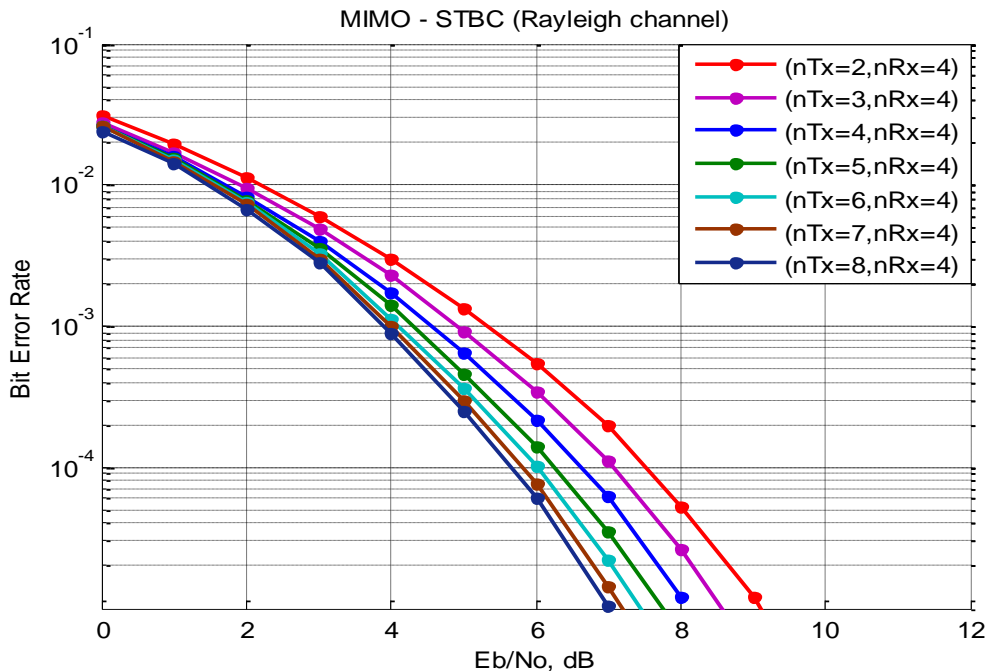


Figure 5.7: MIMO-STBC  $nTx \times 4$

Table 5.3 summarizes the comparison between  $4 \times nRx$  (Figure 5.6.c) and  $nTx \times 4$  (Figure 5.7) in terms of required signal to noise ratio for each of the schemes to achieve a probability of error (BER)  $10^{-4}$ .

Table 5.3: required  $E_b/N_o$  at  $10^{-4}$  BER for  $4 \times nRx$  and  $nTx \times 4$  .

No. of $nRx$ , $nTx$		2	3	4	5	6	7	8
Required	$4 \times nRx$	9.18	7.38	6.5	5.78	5.25	4.78	4.42
$E_b/N_o$ in dB	$nTx \times 4$	7.55	7.08	6.63	6.26	6	5.81	5.66

From table 5.3 we can conclude that we have better performance when the number of receive antenna is greater than number of transmit antenna. Also it is clear when the number of receive antenna increase the required SNR is decreased more quickly compared with transmit antenna.

Figure 5.8 shows simulation results in terms of BER for equal number of transmit and receive antennas. From this figure we can notice that less power will be needed for transmission if we move from  $2 \times 2$  to  $8 \times 8$ . For example, if we look at BER  $10^{-4}$  then the required SNR is decreased by 7.8 dB when ascending from the  $2 \times 2$  to the  $8 \times 8$  configurations.

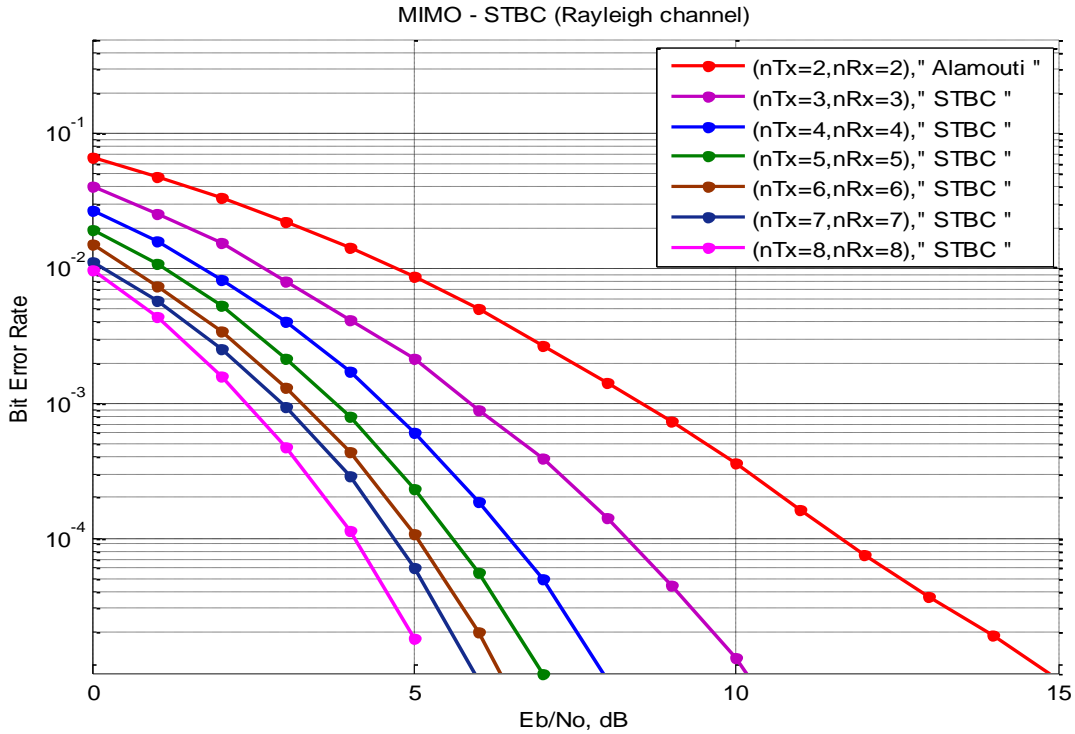


Figure 5.8:  $M \times M$  MIMO configurations using BPSK.

### 5.2.2.2. MIMO Simulation Results with QAM

In this section we will show the simulation results for MIMO system under OSTBC over Rayleigh flat fading channel using QAM as modulation scheme. We select some MIMO configurations results, and then we make a comparison between selected results with BPSK case.

Figure 5.9 clarifies the bit error rate performance versus signal to noise ratio of MIMO system with QAM in Rayleigh flat fading channel. Figure 5.9.a show the performance of MIMO with Alamouti STBC scheme and Figure 5.9.b show the performance with complex OSTBC.

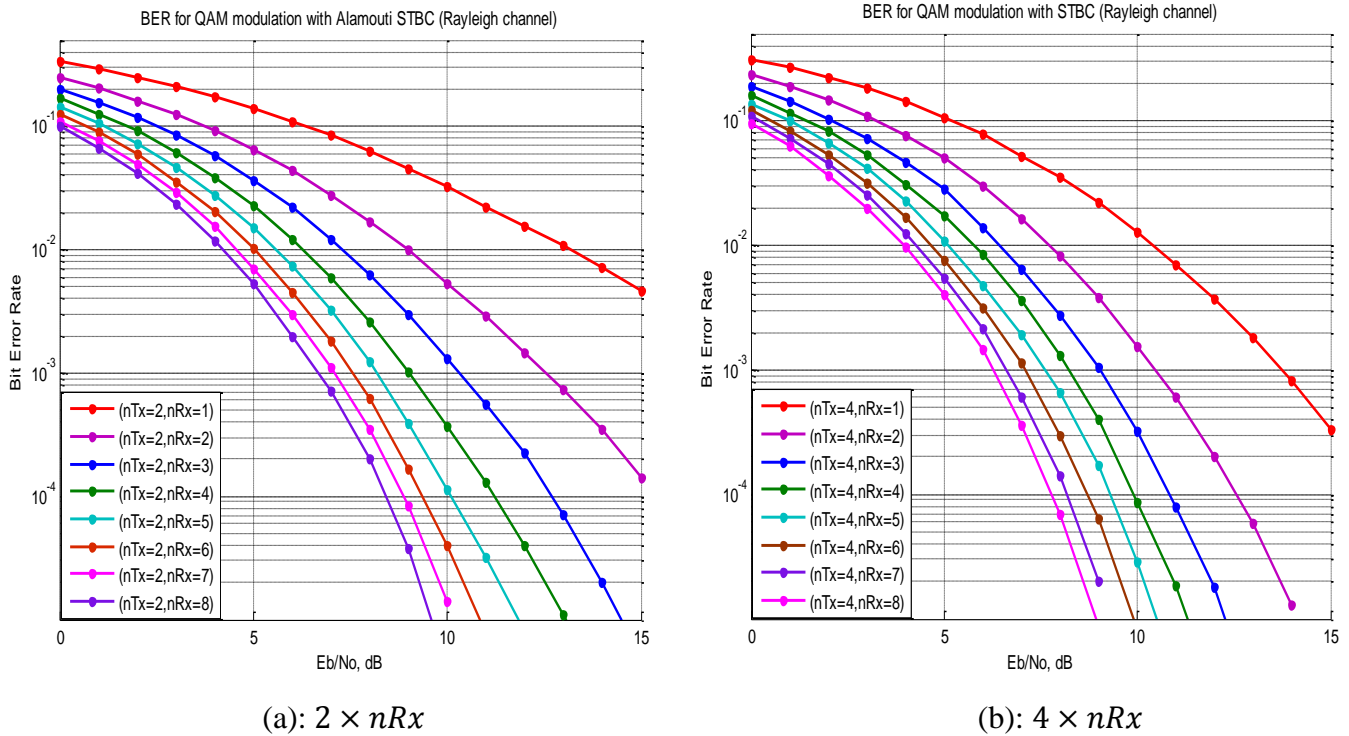


Figure 5.9: different MIMO configurations under OSTBC using QAM over Rayleigh channel.

From these two figures we can notice that the bit error rate of  $4 \times nR_x$  is better than  $2 \times nR_x$  over all values of  $nR_x$  and SNR. With the number of receive antenna increase the bit error rate decrease.

Figure 5.10 show the difference between  $3 \times 6$  and  $6 \times 3$  MIMO system with QAM modulation, we can notice that the performance of  $3 \times 6$  is better than  $6 \times 3$ , so that the increase in the number of receive antenna is preferable than increase in the number of transmit antenna in terms of bit error rate. For comparison between them, when  $E_b/N_0 = 8dB$ , the probability of error in  $3 \times 6$  is 0.00032 and it is 0.00159 in  $6 \times 3$ , there are  $1.27 \times 10^{-3}$  difference in BER between them.

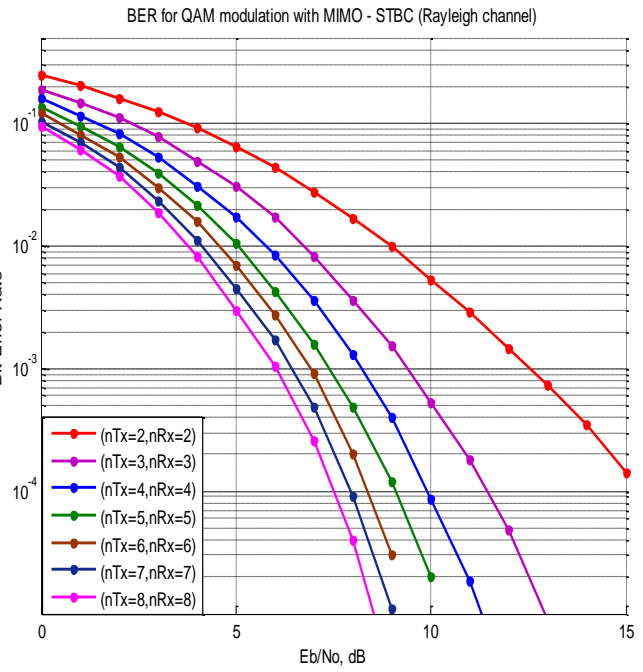
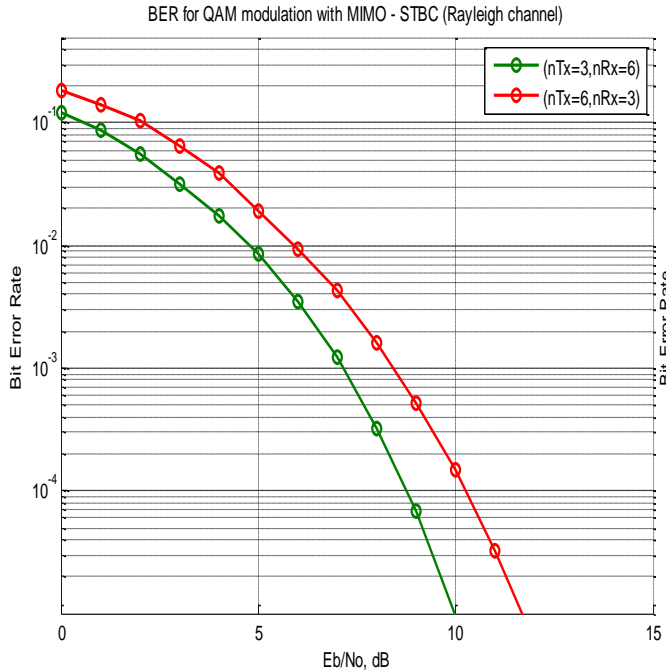


Figure 5.10: BER performance of  $3 \times 6$  vs.  $6 \times 3$       Figure 5.11:  $M \times M$  MIMO using QAM.

Figure 5.11 shows simulation results in terms of BER for equal number of transmit and receive antennas. From this figure we can notice that less power will be needed for transmission if we move from  $2 \times 2$  to  $8 \times 8$ . For example, if we look at BER  $10^{-3}$  then the required SNR is decreased by 6.5 dB when ascending from the  $2 \times 2$  to the  $8 \times 8$  configurations.

In BPSK modulation scheme we need less signal power at specific probability of error than in QAM. However, in QAM scheme the available bandwidth is better utilized than in BPSK scheme since we transmit two bit per symbol.

It is clear that the MIMO system enhances system performance in the multi-path environment without requiring additional bandwidth. The simulation result with two modulation scheme shows that the bit error rate performance improve as the transmit or receive antenna increase but the increase of receive antenna is better. However, the increases in transmit antenna increase the array gain (multiplexing gain) and as a result increase the transmission capacity.

### 5.2.3. MIMO- Multicarrier Modulation simulation results

The simulation results for MIMO-DWT and MIMO-OFDM will be shown in this section. Two modulation schemes will be used. We study the performance of the two multicarrier schemes in AWGN channel. As we mentioned before, MIMO operate in Rayleigh flat fading channel. The block diagram in Figure 5.12 explain how we build our program to deal with two channels in which we examine the effect of the AWGN on multicarrier modulation only.

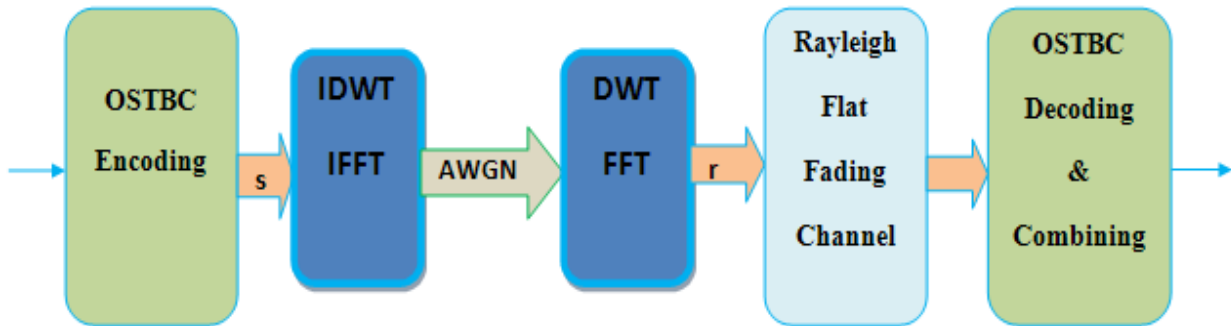
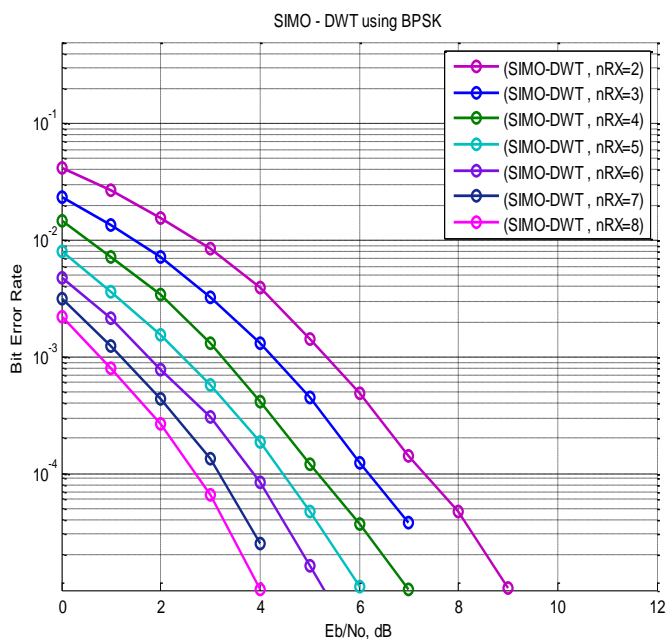


Figure 5.12: multicarrier modulation in AWGN with MIMO OSTBC.

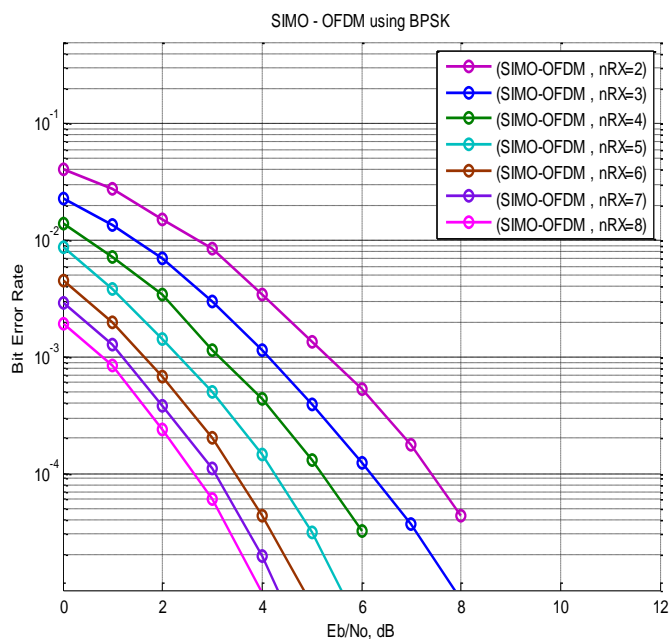
In this section we will compare between the simulation results for MIMO-DWT system and MIMO-OFDM system in terms of BER and capacity with BPSK and QAM as modulation techniques. OSTBC with complex design is used as block coding for MIMO as transmit diversity. Number of transmit and receive antenna is varied in the range of one to eight antennas. In OFDM system we concentrate on the case where the guard band (12 null subcarriers) is presented but we show a comparison with OFDM without guard in the final results.

#### 5.2.3.1. Results of MIMO- MCM using BPSK

In the beginning we will show a simulation results of MIMO- MCM using BPSK under three MIMO scenarios; SIMO (single transmitter and multiple receiver) case in which we use at the receiver the maximal ratio combiner (MRC),  $2 \times nRx$  MIMO system (two transmit and multiple receive) in which we use the Alamouti space time block coding scheme as transmit diversity and MIMO with higher than two transmit antenna where the complex OSTBC is used as transmit diversity.

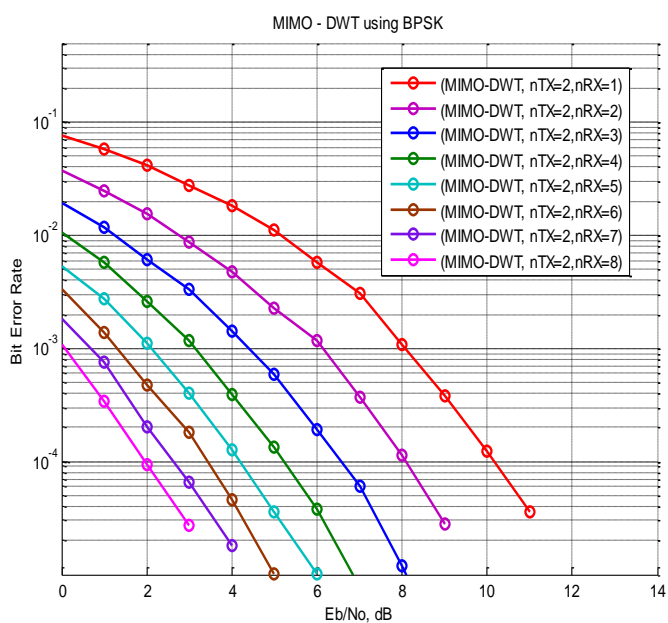


(a)

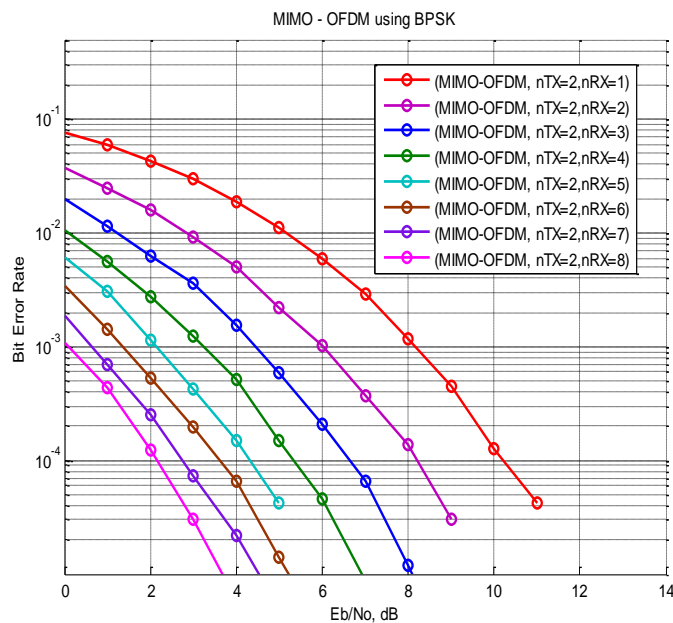


(b)

Figure 5.13: Multicarrier with SIMO under MRC, a) DWT , b) OFDM



(a)



(b)

Figure 5.14: Multicarrier with  $2 \times nRx$  MIMO under Alamouti scheme, a) DWT , b) OFDM

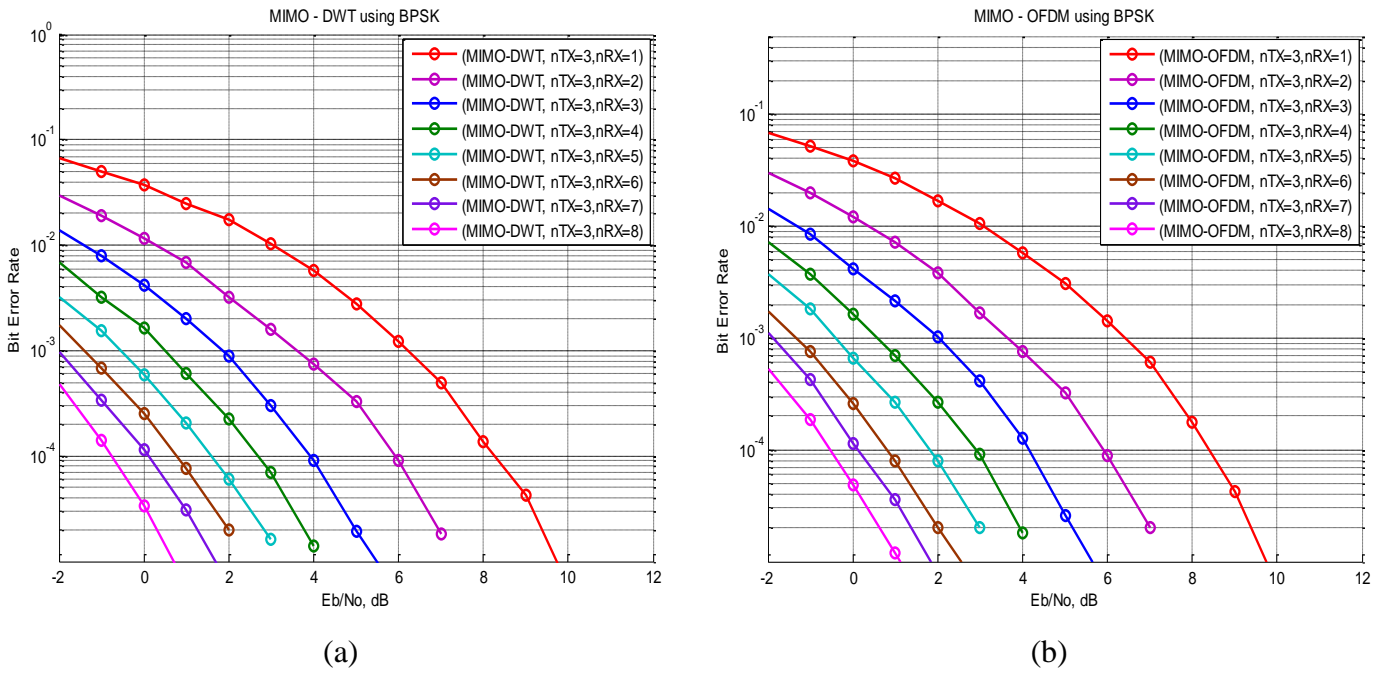


Figure 5.15: Multicarrier with  $3 \times nRx$  MIMO under complex OSTBC, a) DWT, b) OFDM

The previous three figures (5.13, 5.14, and 5.15) are referring to the three cases mentioned before, SIMO, Alamouti and complex OSTBC, respectively. These figures display the bit error rate versus signal to noise ratio for the two multicarrier systems in which (a) represent MIMO-DWT and (b) represent MIMO-OFDM where the BPSK as modulation technique is considered.

From these figures we can notice that the bit error rate of DWT based multicarrier system under all cases of MIMO scheme is *approximately* the same as the bit error rate of the conventional MIMO-OFDM system where we consider the guard (12-null subcarriers) is presented with each OFDM symbol. The transmission capacity in MIMO-DWT is superior the MIMO-OFDM since every DWT symbol carry 64 bit data whereas the OFDM symbol carry 52 bit data. As the transmit antenna increase the higher capacity is achieved.

We can notice that the BER decreases when the number of receive antenna increases. For example, the performance of  $1 \times 3$  is better than  $1 \times 2$  and  $2 \times 4$  is better than  $2 \times 3$  and so on. Also it is obvious that when the antenna increases at the receiver the SNR is needed to achieve specific probability of error decreases and so that we transmit the signal with lower power. With OSTBC including Alamouti, as the transmit antenna increase the performance in terms of BER of the two systems is becomes better.

We can see that the performance of SIMO  $1 \times 2$  and  $1 \times 3$  is better than  $2 \times 1$  Alamouti and  $3 \times 1$  OSTBC respectively, because in SIMO we use the maximal ratio combiner (MRC) where there is no redundant transmission of data as in STBC scenario.

Table 5.4 gives the required SNR in dB for achieve  $10^{-4}$  probability of error with the three cases in the two multicarrier systems (DWT and OFDM).

Table 5.4: required  $E_b/N_o$  in dB at  $10^{-4}$  probability of error for MIMO-DWT and MIMO-OFDM using BPSK.

Cases No. of receiver	MIMO-DWT system			MIMO-OFDM system		
	SIMO	Alamouti	OSTBC with 3-transmit antenna	SIMO	Alamouti	OSTBC with 3-transmit antenna
1	*	<b>10.16</b>	<b>8.21</b>	*	<b>10.16</b>	<b>8.34</b>
2	<b>7.27</b>	<b>8.13</b>	<b>5.93</b>	<b>7.43</b>	<b>8.3</b>	<b>5.92</b>
3	<b>6.16</b>	<b>6.52</b>	<b>3.91</b>	<b>6.16</b>	<b>6.64</b>	<b>4.16</b>
4	<b>5.15</b>	<b>5.27</b>	<b>2.84</b>	<b>5.17</b>	<b>5.3</b>	<b>2.92</b>
5	<b>4.48</b>	<b>4.2</b>	<b>1.62</b>	<b>4.26</b>	<b>4.34</b>	<b>1.84</b>
6	<b>3.89</b>	<b>3.51</b>	<b>0.78</b>	<b>3.51</b>	<b>3.65</b>	<b>0.8</b>
7	<b>3.21</b>	<b>2.5</b>	<b>0.11</b>	<b>3.07</b>	<b>2.76</b>	<b>0.09</b>
8	<b>2.73</b>	<b>1.94</b>	<b>-0.75</b>	<b>2.59</b>	<b>2.14</b>	<b>-0.5</b>

\* represent the SISO case that we studied it before in AWGN only.

From the values of  $E_b/N_o$  in the table we can notice that as the receive antenna increase the required SNR is decreased. If we take the difference between the required SNR of the  $1 \times 2$  SIMO- MRC and  $2 \times 1$  Alamouti, we can find it approximately equal 3 dB. The values of SNR in the table for MIMO-DWT often small less than the MIMO-OFDM which gives us that the performance of DWT system is better till the guard is presented with OFDM system in terms of BER. In all circumstances the achievable transmission capacity with DWT based multicarrier system is better than in OFDM.

Figure 5.16 shows the difference between  $3 \times 8$  and  $8 \times 3$  MIMO- multicarrier system with Discrete Wavelet Transform (DWT) based multicarrier as in (a) and the conventional OFDM as in (b) using BPSK modulation, we can notice that the performance of  $3 \times 8$  is better than  $8 \times 3$  in the two multicarrier system, so that the increase in the number of receive antenna is preferable than increase in the number of transmit antenna in terms of bit error rate. For example, when the  $E_b/N_o = 2$  dB, the probability of error of the  $3 \times 8$  is  $3.019 \times 10^{-6}$  and  $8.413 \times 10^{-5}$  in  $8 \times 3$  with the two multicarrier systems approximately, there are  $8.11 \times 10^{-5}$  difference in BER between  $3 \times 8$  and  $8 \times 3$ .

Figure 5.17 shows simulation results in terms of BER for MIMO- multicarrier where the number of transmit and receive antennas are equal with DWT based multicarrier as in (a) and the conventional OFDM as in (b) using BPSK modulation. From this figure we can notice that less power will be needed for transmission if we move from  $2 \times 2$  to  $6 \times 6$  in the two multicarrier systems.

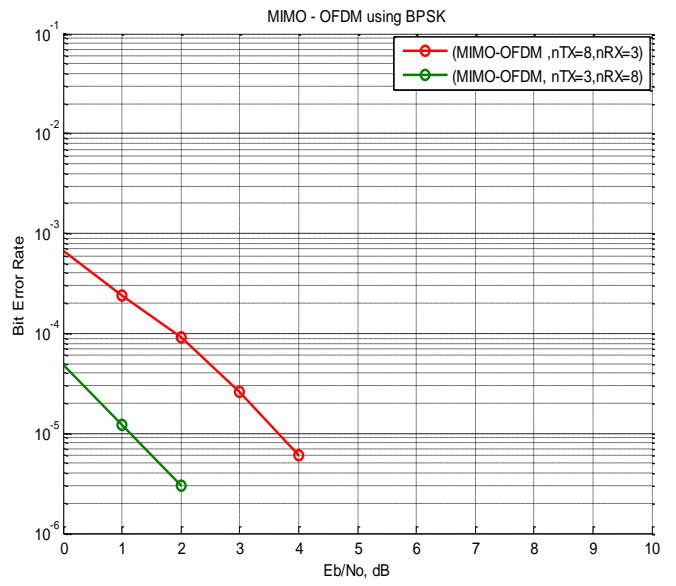
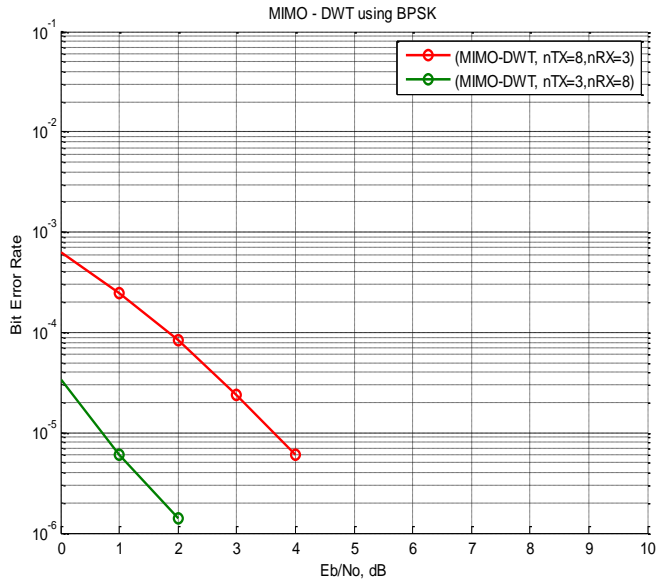


Figure 5.16: BER performance of  $3 \times 8$  vs.  $8 \times 3$ , a) DWT, b) OFDM

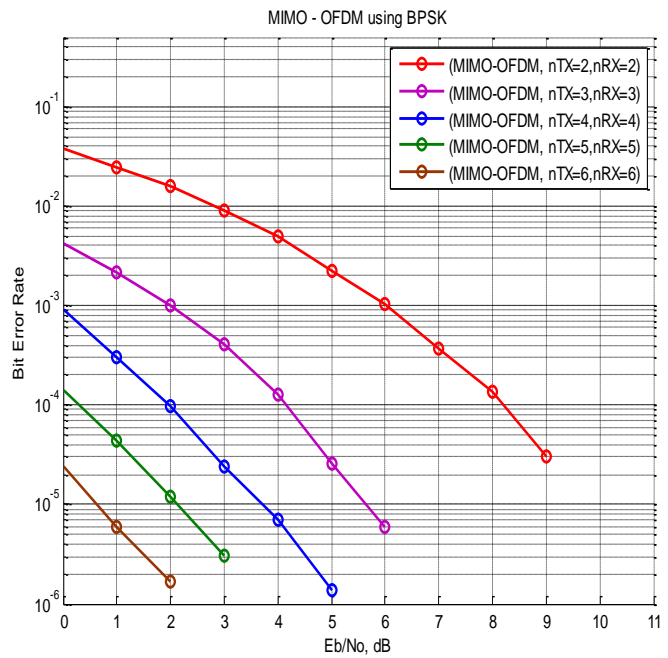
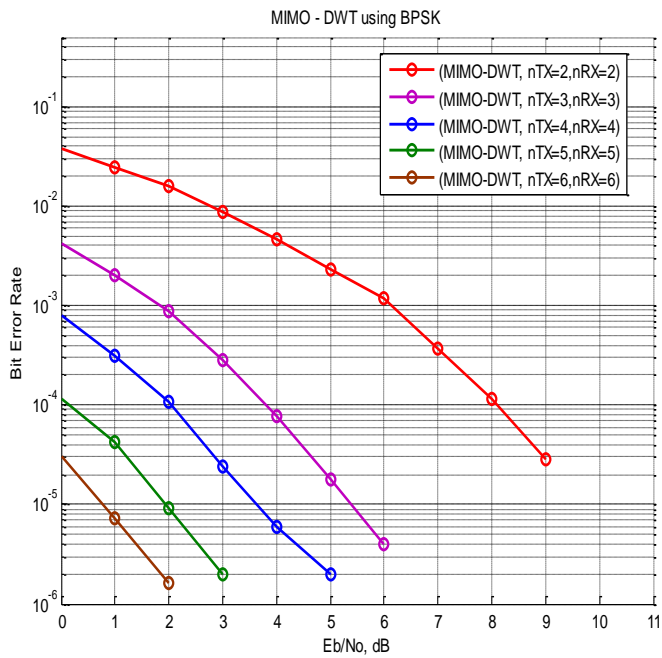


Figure 5.17:  $M \times M$  MIMO with multicarrier using BPSK, a) DWT, b) OFDM

### 5.2.3.2. Results of MIMO- MCM using QAM

Applying QAM instead of BPSK with MIMO- MCM system, has led to some important results, and has emphasized what we already know about the BER performance of both modulation techniques. As we mentioned before, compared with BPSK system, QAM as digital modulation technique in communication systems increase the data rate in which the available bandwidth is better utilized but with higher probability of error.

Figure 5.18 show the bit error rate versus signal to noise ratio for  $(5 \times nRx)$  MIMO- MCM systems in which (a) represent MIMO-DWT system and (b) represent MIMO-OFDM system using QAM as modulation technique under complex orthogonal space time block coding (OSTBC) case.

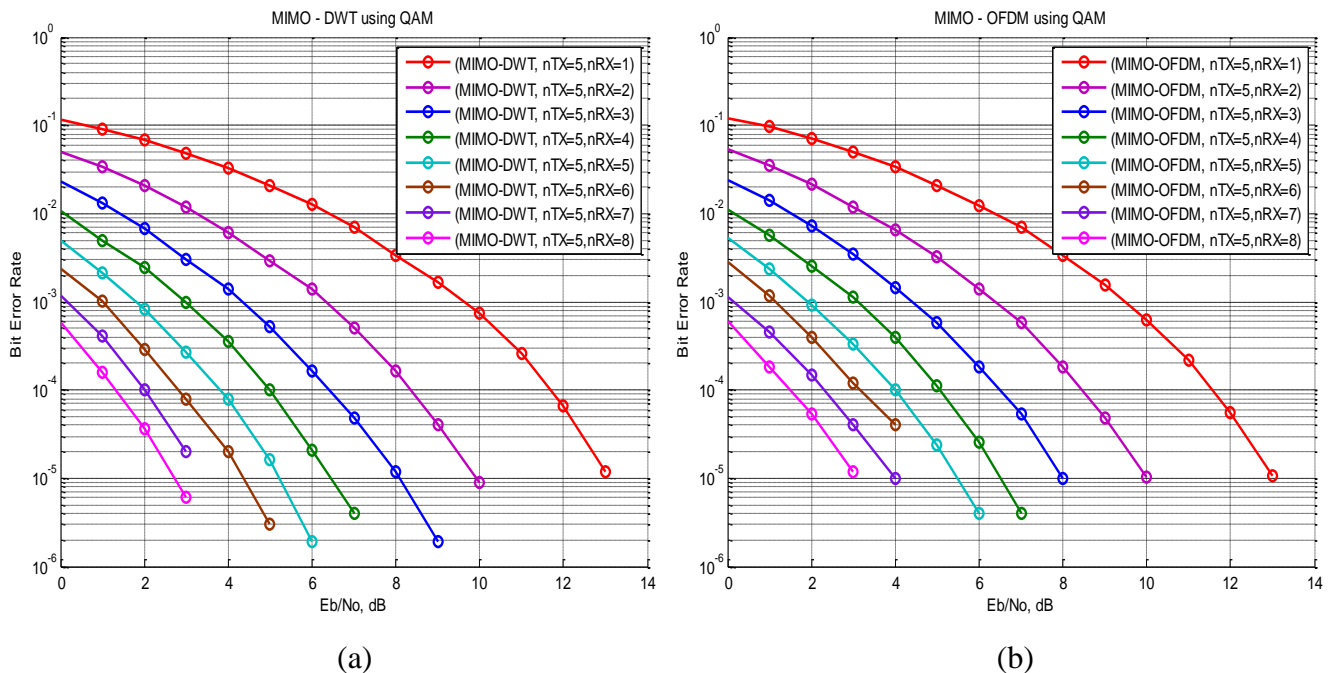


Figure 5.18: MIMO- MCM using QAM under OSTBC, a) DWT, b) OFDM

From this figure we can notice that the bit error rate curves is decreasing with the increasing in the number of receive antenna. The BER performance of the two multicarrier schemes is approximately the same and this is clear from the two graphs (a) and (b) in Figure 5.18.

Table 5.5 show the required SNR in dB to achieve  $10^{-4}$  probability of error for  $(5 \times nRx)$  MIMO with the two multicarrier modulation schemes.

	nRx	1	2	3	4	5	6	7	8
Required $E_b/N_o$ in dB	MIMO-DWT system	<b>11.73</b>	<b>8.39</b>	<b>6.41</b>	<b>5</b>	<b>3.82</b>	<b>2.78</b>	<b>2</b>	<b>1.33</b>
	MIMO-OFDM system	<b>11.62</b>	<b>8.44</b>	<b>6.47</b>	<b>5.08</b>	<b>4</b>	<b>3.15</b>	<b>2.28</b>	<b>1.47</b>

Table 5.5: required  $E_b/N_o$  in dB at  $10^{-4}$  probability of error for  $(5 \times nRx)$  MIMO-DWT and MIMO-OFDM using QAM.

It is clear from this table how the required SNR is decreased with the number of receiving antenna increase in two multicarrier systems. We can notice that in MIMO-DWT often the required SNR is small less than for MIMO-OFDM at specific BER. As mentioned before, the transmission capacity in DWT system is better than OFDM system and the capacity in QAM is twice the capacity in BPSK.

Figure 5.19 shows the difference in BER performance between  $2 \times 1$  Alamouti and  $1 \times 2$  SIMO-MRC,  $5 \times 3$  and  $3 \times 5$  with the two multicarrier systems. It is clear that the BER of  $1 \times 2$  is better than  $2 \times 1$  due to the redundant transmission in  $2 \times 1$  Alamouti, and the BER of  $3 \times 5$  is better than  $5 \times 3$  since more receive antennas means receive more power.

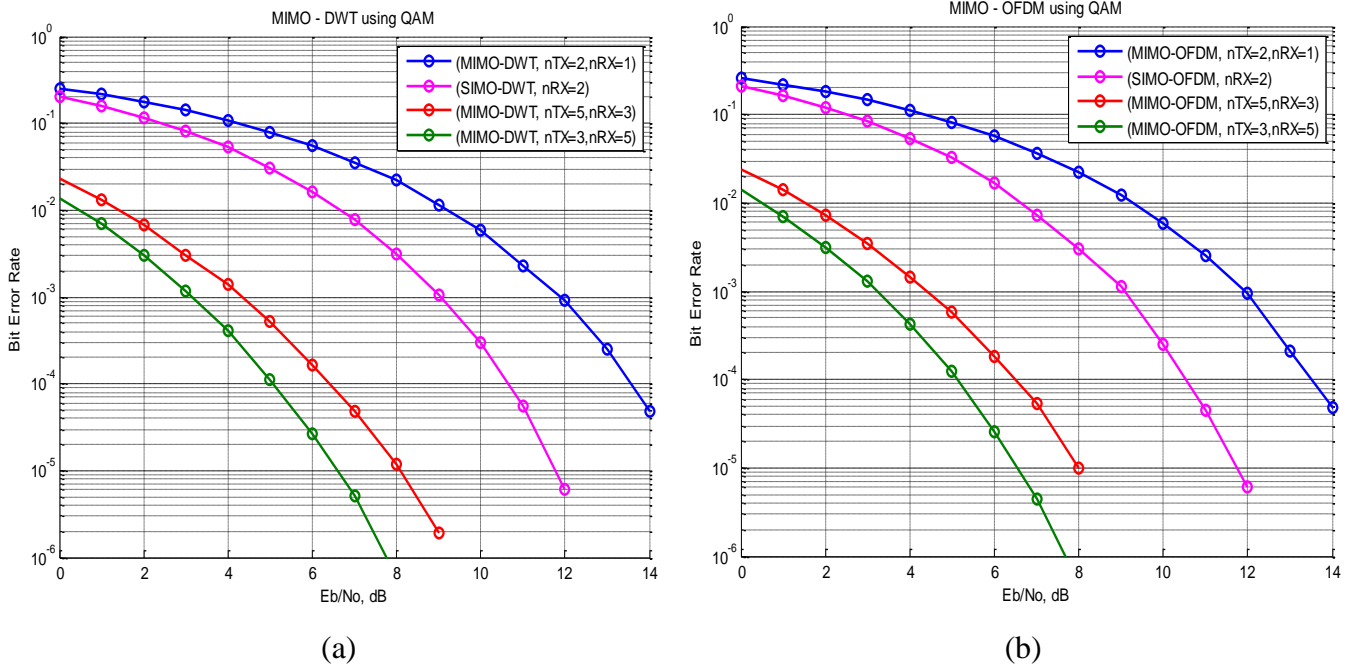


Figure 5.19: the BER of QAM under different MIMO configurations with two multicarrier modulations, a) DWT, b) OFDM

### 5.2.4. BPSK versus QAM in MIMO- MCM

In this section we will show the difference between two modulation schemes that we used in our simulation of the two multicarrier systems, BPSK and QAM. 4-QAM modulation has constellation diagram as Quadrature Phase Shift Keying, QPSK.

Figure 5.20 show the BER performance of  $4 \times 5$  MIMO with DWT multicarrier system using two modulation schemes, BPSK and QAM. It is clear that the probability of error of MIMO-DWT using BPSK is better than using QAM.

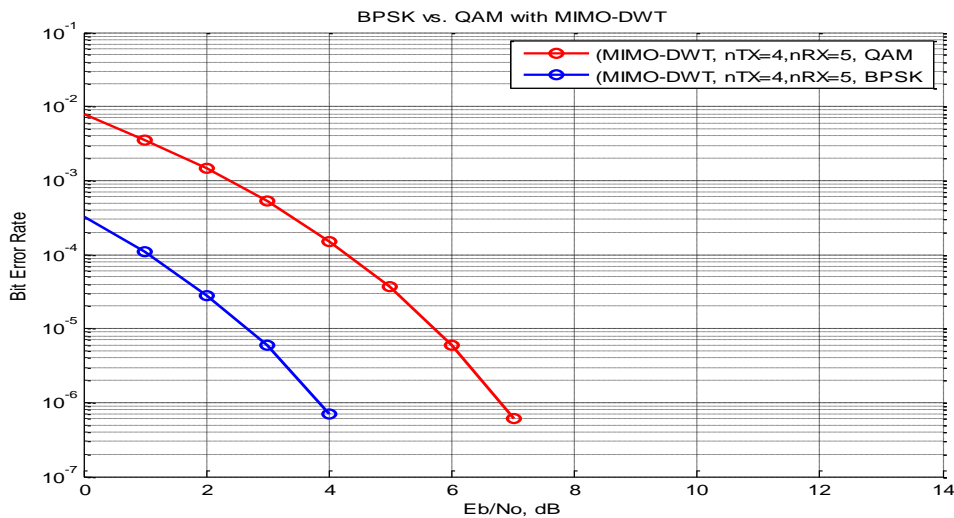


Figure 5.20: BPSK vs. QAM with MIMO-DWT

Figure 5.21 is Extracted Portion for Figure 5.20 to show the difference between the required signal to noise ratio at specific BER in BPSK and QAM. We can notice that the difference is 3 dB between them at any BER approximately.

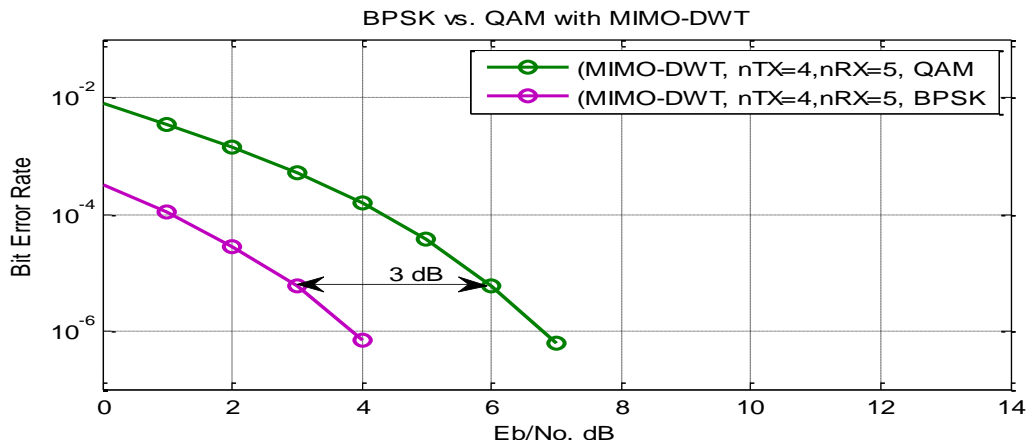


Figure 5.21: Extracted Portion of figure 5.20.

It is shown in all the MIMO, MIMO-OFDM and MIMO-DWT systems that the BPSK has an advantage in BER performance over the QAM because the Euclidian distance in QAM between the points on constellation diagram is smaller than in BPSK. However, the data rate that achieved with QAM is better than BPSK since QAM can encode two bits per symbol.

### 5.2.5. MIMO versus MIMO- MCM

The comparison between MIMO and MIMO-DWT is shown in Figure 5.22. We show two cases, BER of  $2 \times 3$  Alamouti as in graph (a) and BER of  $4 \times 2$  OSTBC as in graph (b).

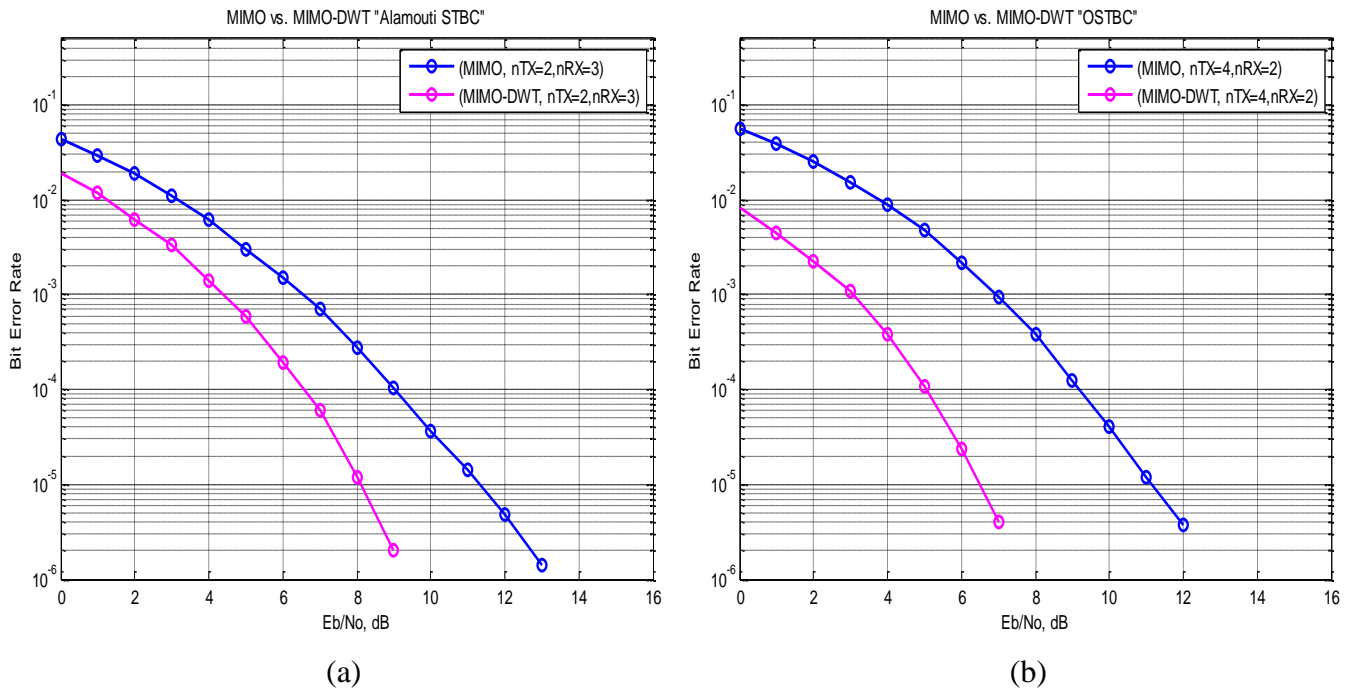


Figure 5.22: MIMO vs. MIMO-DWT, a)  $2 \times 3$  Alamouti, b)  $4 \times 2$  OSTBC

It is worth to point the improvement in the system when multicarrier modulation is applied whether DWT based multicarrier or OFDM. In the above figures, at a certain signal-to-noise ratio, there is a noticeable drop in the bit-error-rate. For example, looking at the point 6 dB in Figure 5.22.a, the BER of MIMO is  $1.492 \times 10^{-3}$  and  $1.923 \times 10^{-4}$  in MIMO-DWT, so the difference between the BER between MIMO and MIMO-DWT is  $1.2997 \times 10^{-3}$ , i.e, there is drop in BER by  $1.2997 \times 10^{-3}$  as a result of MIMO-DWT combination. This improvement in BER is better in Figure 5.22.b in which the BER drop by  $2.176 \times 10^{-3}$ .

### 5.2.6. OFDM system without guard

In this section we will show the effect of remove the guard (12 null subcarriers) from OFDM symbol. In this case the OFDM symbol contains 64 data subcarriers. Figure 5.23 clarifies the BER performance of the conventional OFDM with and without guard under different MIMO configurations.

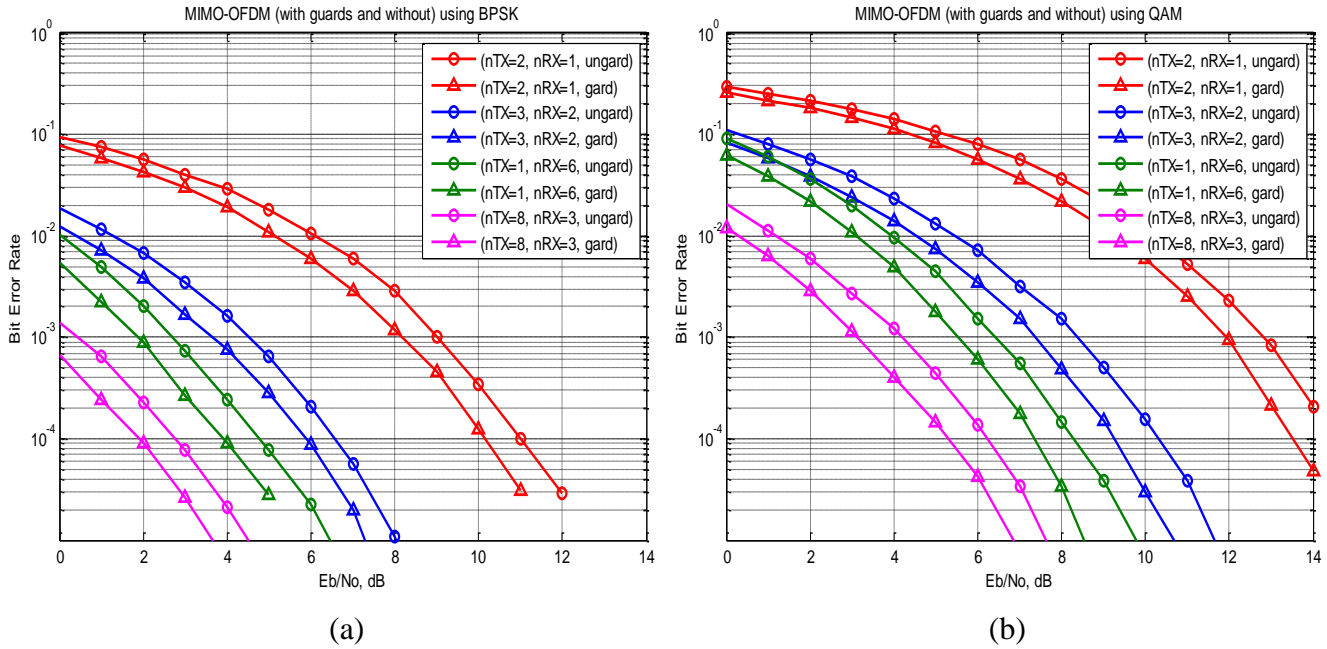


Figure 5.23: MIMO-OFDM with and without guard using a) BPSK, b) QAM

It is clear that from this figure the bit error rate performance of MIMO-OFDM with guard is better than without with two modulation schemes. For comparison, if we take  $3 \times 2$  MIMO configuration and looking at the point 5 dB in Figure 5.23.a, the BER of MIMO-OFDM with guard is  $2.845 \times 10^{-4}$  whereas the BER of MIMO-OFDM without guard is  $6.543 \times 10^{-4}$ , so there is drop in BER by  $3.698 \times 10^{-4}$  due to the use of guard. The drop in BER in Figure 5.23.b is by  $5.646 \times 10^{-3}$  with  $3 \times 2$  MIMO configuration and at 5 dB.

The transmission capacity without guard is better than with guard since the 12-null subcarriers are used for carry data bits. But when we need reliable communication system we need less bit error rate, so that there is trade off in the conventional OFDM system. In DWT based multicarrier system we do not add 12-null subcarriers and it is still superior the conventional OFDM in terms of capacity and BER.

# Chapter 6

## Conclusion and Future Works

## 6.1. Overview

In this chapter we summarize and present conclusions based on the MATLAB simulation results in Chapter 5. The objectives of this research, which was mentioned in chapter 1, are achieved as expected. Then we suggest some future research areas for Discrete Wavelet Transform (DWT) based multicarrier systems.

## 6.2. Conclusions

Over all the performance results of DWT based multicarrier and MIMO-DWT systems compared with the conventional OFDM and MIMO-OFDM systems, we conclude that:

- 1) All the simulation results that we studied whether in SISO or in MIMO- MCM, we found that the performance of the discrete Wavelet transform with Haar mother (Haar- DWT) based multicarrier modulation is superior to the performance of conventional orthogonal frequency division multiplexing (OFDM) in terms of bit error rate and transmission capacity.
- 2) Using the DWT as multicarrier modulator in wireless systems rather than using the conventional OFDM ( based on FFT) does not need a cyclic prefix extension which represent an overhead, i.e, reduce the transmission capacity. In other words, in DWT the available bandwidth is wisely utilized and we achieve higher data rate.
- 3) If we insert a guard band (null subcarriers) in conventional OFDM, then the BER performance OFDM and DWT is approximately the same. However, this improvement in BER in OFDM will reduce the data rate since there are subcarrier does not carry data.
- 4) MIMO technology improves the data rate in broadband wireless communication. The combination between MIMO and multicarrier modulation schemes improve the BER performance of wireless communications systems. Of course, MIMO with DWT as multicarrier is a very attractive technique for most of modern telecommunication systems that looking for achieve high data rate with small BER.
- 5) Employing more antennas at the receiver side is the key factor, since it was noticed that the performance in BER increases linearly with the number of receive antennas due to increase in diversity order and to the array gain in which more receive antennas means receive more power. On the other hand, after a certain level of increase of the transmit antennas, there is no large improvement.
- 6) The BER performance of communication systems with binary phase shift keying (BPSK) is better than with Quadrature amplitude modulation (QAM). However, the data rate with QAM is superior BPSK.

### 6.3. Future Works

In order to develop this research, we propose the ideas that lead to adoption of this current work in several areas. We suggest number of ideas:

- 1) Replacement the OFDM based technology such as Wi-Fi, WIMAX, cognitive radio and 4G mobile communication, by DWT based multicarrier.
- 2) In our simulation work, we examine the effect of additive white Gaussian noise (AWGN) channel on the multicarrier (DWT and OFDM) systems as explained in Figure 5.9. So we propose to study the effect of fading channel, flat and frequency selective fading, with different distribution such as Rayleigh, Rician and Nakagami distributions.
- 3) In this research we use the Haar mother wavelet for MCM. There are different mother wavelets such as Daubechies, Morlet, Shannon and Gaussian mother wavelets. We suggest studying the performance of these wavelet functions and comparing it with Haar mother wavelet under multiple antenna system.
- 4) Change the code rate of the OSTBC design.
- 5) Using other digital modulation techniques such as M- QAM, M- PSK
- 6) In our simulation, we consider the number of subcarriers is 64 subcarriers. We suggest exploring the performance of DWT based multicarrier and MIMO-DWT with 128 subcarriers.

## References

- [1] Mohamed Ahmed Mohamedian , Iman Abuel Maaly A/Elrahman and Izz Eldin Mohamed Osman, *performance of orthogonal frequency division multiplexing (OFDM) under the effect of wireless transmission system drawbacks*, Sudan Engineering Society journal, Vol. 52 No.49, September (2007),pp. 17-26.
- [2] Andrea Goldsmith, *Wireless Communications*, Cambridge University Press, (2005).
- [3] Farid Dowla, *Handbook of RF and Wireless Technologies*, Elsevier, Inc,(2004).
- [4] Vijaya Chandran Ramasami, KUID 698659, *Orthogonal Frequency Division Multiplexing*.
- [5] All N. Akansu and Richard A. Haddad, *Multiresolution Signal Decomposition Transforms, Subbands, and Wavelets*, Academic Press,(2001)
- [6] Robi Polikar, *The Wavelet Tutorial*, November,(2006).
- [7] Chun-Lin, Liu, *A Tutorial of the Wavelet Transform*, February 23, 2010.
- [8] Fuqin Xiong, *Digital Modulation Techniques*, Artech House, Inc,(2006).
- [9] Yesuf Shiferaw, *Comparative Performance Study on Wavelet Based Orthogonal Frequency Division Multiplexing (OFDM) Using Different Wavelets*, Addis Ababa University, March (2007).
- [10] Barbara Burke Hubbard, *The World According to Wavelets*, A K Peters, Ltd, (1996).
- [11] Tim Edwards, *Discrete Wavelet Transforms: Theory and Implementation*, Stanford University, June 4, (1992).
- [12] Seong Taek Chung and Andrea Goldsmith, *Adaptive Multicarrier Modulation for Wireless Systems*, IEEE, Vol. 2, (2000), pp. 1603-1607.
- [13] Kok-Wui Cheong, John M. Cioffi, *Discrete wavelet transforms in multi-carrier modulation*, IEEE, Vol.5, (1998), pp. 2794-2799.
- [14] Rishabh Kasliwal, Nachiket Kale, and Piyush Nahar, *EE678 WAVELETS APPLICATION ASSIGNMENT WAVELET OFDM*.
- [15] Gao Xingxin, Lu Mingquan, and Feng Zhenming, *Optimal Wavelet Packet Based Optimal Wavelet Packet based Multicarrier Modulation Over Multipath Wireless Channels*, IEEE (2002) International Conference on *Communications, Circuits and Systems*.
- [16] Deepak Gupta, Vipin B Vats, and Kamal K. Garg, *Performance Analysis of DFT-OFDM, DCT-OFDM, and DWT-OFDM Systems in AWGN Channel*, The Fourth International Conference on *Wireless and Mobile Communications*, IEEE, August 2008, pp. 214 – 216.

- [17] Khaizuran Abdullah and Zahir M. Hussain, *Performance of Fourier-Based and Wavelet-Based OFDM for DVB-T Systems*, Australasian Telecommunication Networks and Applications Conference, (2007).
- [18] Prema.G, Amrutha.E, *A New MIMO-OFDM Transmit Preprocessing Using Pilot Symbol Assisted Rateless Codes to Mitigate Fading and Wavelet Based OFDM for PAPR Reduction*, International Conference on Signal Processing, Communication, Computing and Networking Technologies, IEEE, (2011), pp. 679 - 684.
- [19] M. Yasir, M.J. Mughal, N.D. Gohar, S.A. Moiz, *Performance comparison of Wavelet based OFDM (WOFDM) V-BLAST MIMO system with different detection algorithms*, fourth International Conference on Emerging Technologies, IEEE (2008), pp.110 -115.
- [20] David Tse, Pramod Viswanath, *capacity of wireless channels, fundamentals of wireless communication*, Cambridge University Press, (2005), pp. 166-227.
- [21] Branka Vucetic, Jinhong Yuan, *Space Time Coding*, John Wiley & Sons Ltd, (2003).
- [22] Jeffrey G. Andrews, Arunabha Ghosh, and Rias Muhamed, *Multiple Antenna Techniques, Fundamentals of WiMAX Understanding Broadband Wireless Networking*, Pearson Education, Inc (2007), pp. 149-197.
- [23] Hamid Jafarkhani, *Space-Time Coding Theory and Practice*, Cambridge University Press, (2005).
- [24] K. Fazel, and S. Kaiser, *Multi-Carrier and Spread Spectrum Systems*, John Wiley & Sons Ltd, (2003).
- [25] Stuart D. Sandberg, and Michael A. Tzannes, *Overlapped Discrete Multitone Modulation for High Speed Copper Wire Communications*, IEEE Journal On Selected Areas In Communications, Vol. 13, No. 9, December, (1995).
- [26] Kok-Wui Cheong, John M. Cioffi, *Discrete wavelet transforms in multi-carrier modulation*, IEEE, Vol.5, (1998), pp. 2794-2799.
- [27] M. K. Lakshmanan, and H. Nikookar, *a Review of Wavelets for Digital Wireless Communication*, Wireless Personal Communications, Vol.37, (2006), pp. 387-420.
- [28] R. Prasad, S. Dixit, R. Van Nee, T. Ojanpera, *Wavelet Radio: A future Vision for wireless communication, Globalization of Mobile and Wireless Communications today and in 2020, Signals and Communication Technology Series*, Springer Science + Business Media B.V. (2011), pp. 223-236.

[29] Khaizuran Abdullah, *Interference Mitigation Techniques for Wireless OFDM*, Degree of Doctor of Philosophy, RMIT University, August (2009).

[30] Markku Renfors, Pierre Siohan, Behrouz Farhang-Boroujeny, and Faouzi Bader, *Filter Banks for Next Generation Multicarrier Wireless Communications*, EURASIP Journal on Advances in Signal Processing, Markku Renfors et al., (2010).

[31] Marius Oltean, a *Study of the Multi-Scale W-OFDM Transmission in Time Variant Channels*, International Journal of Communications, Vol.2, (2008), pp.96-105.

[32] Fritz J., and Dolores H. Russ, *M-Ary Orthogonal Modulation Using Wavelet Basis Functions*, Degree Master of Science, Ohio University, November (2000).

# **Appendices**

# Appendix A

## MATLAB code

### A.1: SISO DWT based multicarrier and conventional OFDM using BPSK

```
% %%%%%%%%%%%%%%%%%%%%%%%%%%%%%%%%%%%%%%%%%%%%%%%%%%%%%%%%%%
%%% Bit Error Rate probability of DWT based multicarrier modulation
%%% and conventional OFDM based FFT using BPSK under AWGN channel
%%% OFDM symbol with guard
%%%%%%%%%%%%%%%%%%%%%%%%%%%%%%%%%%%%%%%%%%%%%%%%%%%%%%%%%
clc ; close all ; clear all

N = 64 ; % number of subcarriers
nfft = 52; % number of data subcarriers for OFDM
iteration = 5; % number of iterations ( increase the number of bits)
nbit= iteration*N*nfft; % number of bits for data
nSymFFT=ceil(nbit/nfft);% number of symbols for OFDM system
nSymDWT=ceil(nbit/N);% number of symbols for DWT system
EbNo = [0:15]; % bit to noise ratio in dB
% power normlization of the OFDM symbol, since there
% is 16 subcarrier for cyclic prefix then the power of
% OFDM symbol is extended over a length of 80 subcarrier

EbNofft =EbNo + 10*log10(N/80);

%%% generate random data with nbit size, i.e, random 1's and 0's
DATA1=rand(1,nbit)>0.5;

%%% BPSK modulation 0 --> -1, 1 --> +1
DATA=2*DATA1 -1 ;

%%% serial to parallel( grouping into multiple symbols)
DATAFFT = reshape(DATA,nfft,nSymFFT).'; % for OFDM
DATADWT = reshape(DATA,N,nSymDWT).'; % for dwt

%%% Add the guard band ( 12- null subcarriers), such that the
%%% data assigning to the subcarriers 1-->26 , 27-->59
DATAFFT=[zeros(nSymFFT,6) DATAFFT(:, [1:nfft/2]) zeros(nSymFFT,1) ...
        DATAFFT(:, [nfft/2+1:nfft]) zeros(nSymFFT,5)] ;

%%% loop over the bit to noise ratio (Eb/No)
h = waitbar(0, 'Percentage Completed');
set(h, 'name', 'Please wait...');

for i= 1:length(EbNo)
    %%% intilization matrix
    RXDWT=[]; RXFFT=[]; TXDWT=[]; TXFFT=[];
```

```

%%% multicarrier modulation process
%%% first:inverse discrete Wavelet transform (IDWT)
%%% with Haar mother wavelet

for uu=1:nSymDWT

    AC = DATADWT(uu,1:N/2); %% approximation coefficients
    DC = DATADWT(uu,N/2+1:N);%% detailed (wavelet) coefficients
    IDWT=idwt(AC,DC,'haar');% IDWT process
    TXDWT(uu ,:)= IDWT;% transmitted data for DWT
end

%%% second: OFDM with inverse discrete Fourier transform (IFFT)

TXFFT=(N/sqrt(nfft))*ifft(fftshift(DATAFFT.')).'; %% IFFT

%%% Add cyclic prefix with 0.25 of the OFDM symbol length
TXFFT = [TXFFT(:, [49:64]) TXFFT];

%%% parallel to serial =====> to the channel
TXDWT = reshape(TXDWT.',1,[]);% for DWT
TXFFT = reshape(TXFFT.',1,[]);% for OFDM

%%% create Gaussian noise with unit variance and zero mean
ntDWT = 1/sqrt(2)*[randn(1,nSymDWT*N) + ...
                  j*randn(1,nSymDWT*N)];%noise for DWT multicarrier
ntFFT = 1/sqrt(2)*[randn(1,nSymFFT*(N+16)) + ...
                  j*randn(1,nSymFFT*(N+16))];%noise for OFDM

%%% the transmitted signal is corrupted with additive noise
ytDWT = TXDWT + 10^(-EbNo(i)/20)*ntDWT; %%receive signal DWT
ytFFT = TXFFT + 10^(-EbNofft(i)/20)*ntFFT; %%receive signal OFDM

%%%Receiver=====
%%% serial to parallel (formatting the received vector into symbols)

ytDWT=reshape(ytDWT,N,nSymDWT).'; %% for DWT
ytFFT=reshape(ytFFT,(N+16),nSymFFT).'; %% for OFDM

%%% remove the Cyclic prefix from OFDM symbol
ytFFT= ytFFT(:, [17:80]);

%%% multicarrier demodulation process
%%% first: discrete Wavelet transform (DWT) with Haar mother wavelet
for zz=1:nSymDWT

    [DWT,cd]=dwt(ytDWT(zz,:), 'haar');%% DWT
    RXDWT(zz,:)= [DWT cd];% recieved data for DWT
end

```

```

end

%%% second: OFDM with discrete Fourier transform (FFT)

RXFFT=(sqrt(nfft)/N)*fftshift(fft(ytFFT.')).';%% FFT

%%% remove the guard band (12- null subcarrier)from OFDM symbol
RXFFT= RXFFT(:, [6+[1:nfft/2] 7+[nfft/2+1:nfft] ]);

%%% parallel to serial
RXDWT = reshape(RXDWT.',1,[]);% at DWT
RXFFT = reshape(RXFFT.',1,[]);% at OFDM

%%% BPSK demodulation for DWT system where
%%% negative value --> -1, positive value--> +1
BPSKmodDWT = 2*floor(real(RXDWT/2)) + 1;
BPSKmodDWT(find(BPSKmodDWT>1)) = +1;
BPSKmodDWT(find(BPSKmodDWT<-1)) = -1;
% converting modulated values into bits
DATARXDWT = (BPSKmodDWT+1)/2;

%%% BPSK demodulation for OFDM system where
%%% negative value --> -1, positive value--> +1
BPSKmodFFT = 2*floor(real(RXFFT/2)) + 1;
BPSKmodFFT(find(BPSKmodFFT>1)) = +1;
BPSKmodFFT(find(BPSKmodFFT<-1)) = -1;
%%% converting modulated values into bits 0's and 1's
DATARXFFT = (BPSKmodFFT+1)/2;

% counting the errors and ratio
[nDWT,rDWT]=biterr(DATA1,DATARXDWT); simBerDWT(i)=rDWT;%% DWT system
[nFFT,rFFT]=biterr(DATA1,DATARXFFT); simBerFFT(i)=rFFT;%% OFDM system

end

%%% theoretical bit error rate of BPSK modulation

theory_Pb_BPSK = (1/2)*erfc(sqrt(10.^(EbNo/10)));

%%% plot the BER for DWT based multicarrier, OFDM and the theoretical BPSK
close all; figure;
semilogy(EbNo,theory_Pb_BPSK,'bs-','LineWidth',2);
hold on
semilogy(EbNo,simBerDWT,'mx-','LineWidth',2);
semilogy(EbNo,simBerFFT,'ro-','LineWidth',2);
axis([0 16 10^-6 1]); grid on
legend('theory', 'simulation for DWT(Haar)', 'simulation for FFT');
xlabel('SNR, dB') ; ylabel('Bit Error Rate')
title('BER for BPSK using DWT multicarrier and OFDM (based FFT) "AWGN"')

```

## A.2: SISO DWT based multicarrier and conventional OFDM using QAM

```

% %%%%%%%%%%%%%%%%%%%%%%%%%%%%%%%%%%%%%%%%%%%%%%%%%%%%%%%%%%
%% Bit Error Rate probability of DWT based multicarrier modulation
%% and conventional OFDM based FFT using QAM under AWGN channel
%% OFDM symbol with guard
% %%%%%%%%%%%%%%%%%%%%%%%%%%%%%%%%%%%%%%%%%%%%%%%%%%%%%%%%%%
clc ; close all ; clear all

N = 64 ; % number of subcarriers
nFFT = 52; % number of data subcarriers for OFDM
iteration = 100; % number of iterations ( increase the number of bits)
nbit = iteration*N*nFFT; % number of bits for data
nSymFFT=ceil(nbit/nFFT);% number of symbols for OFDM system
nSymDWT=ceil(nbit/N);% number of symbols for DWT system
M = 4; k=log2(M); %% 4- QAM
EbNo = [0:16]; %(dB) bit to noise ratio + 10*log10(k);

% power normlization of the OFDM symbol, since there
% is 16 subcarrier for cyclic prefix then the power of
% OFDM symbol is extended over a length of 80 subcarrier
EsN0FFT=EbNo+10*log10(N/80);

%% generate random data with nbit size, then QAM modulation
DATA = (2*(rand(1,nbit)>0.5)-1) + j*(2*(rand(1,nbit)>0.5)-1);
DATA1 = (1/sqrt(2))*DATA ;

%% serial to parallel( grouping into multiple symbols)
DATAFFT=reshape(DATA1,nFFT,nSymFFT).'; %% for OFDM
DATADWT=reshape(DATA1,N,nSymDWT).'; %% for dwt

%% Add the guard band ( 12- null subcarriers), such that the
%% data assigning to the subcarriers 1-->26 , 27-->59
DATAFFT=[zeros(nSymFFT,6) DATAFFT(:, [1:nFFT/2]) zeros(nSymFFT,1) ...
        DATAFFT(:, [nFFT/2+1:nFFT]) zeros(nSymFFT,5) ] ;

%% loop over the bit to noise ratio (Eb/No)

for i= 1:length(EbNo)
    %% initialization matrix
    RXDWT=[]; RXFFT=[]; TXDWT=[]; TXFFT=[];

    %% multicarrier modulation process
    %% first:inverse discrete Wavelet transform (IDWT)
    %% with Haar mother wavelet

    for uu=1:nSymDWT

        AC = DATADWT(uu,1:N/2); %% approximation coefficients
    end
end

```

```

        DC = DATADWT(uu,N/2+1:N); %% detailed (wavelet) coefficients
        IDWT=idwt(AC,DC,'haar');%% IDWT
        TXDWT(uu ,:)= IDWT; %% transmitted data for DWT
end

%%% second: OFDM with inverse discrete Fourier transform (IFFT)
TXFFT =(N/sqrt(nFFT))*ifft(fftshift(DATAFFT.')).';%IFFT

%%% Add cyclic prefix with 0.25 of the OFDM symbol length
TXFFT = [TXFFT(:, [49:64]) TXFFT];%transmitted data for OFDM

%%% parallel to serial =====> to the channel
TXDWT = reshape(TXDWT.',1,[]);% reshape for transmitted data for DWT
TXFFT = reshape(TXFFT.',1,[]);% reshape for transmitted data for OFDM

%%% create Gaussian noise with unit variance and zero mean
ntDWT = 1/sqrt(2)*[randn(1,nSymDWT*N) + ...
                 j*randn(1,nSymDWT*N)];%noise for DWT
ntFFT = 1/sqrt(2)*[randn(1,nSymFFT*(N+16)) + ...
                 j*randn(1,nSymFFT*(N+16))];%noise for OFDM

%%% the transmitted signal is corrupted with additive noise
ytDWT =TXDWT+ 10^(-EsNo(i)/20)*ntDWT; %receive signal DWT
ytFFT =TXFFT+ 10^(-EsNoFFT(i)/20)*ntFFT; %receive signal OFDM

%
Receiver=====

%%% serial to parallel (formatting the received vector into symbols)

ytDWT=reshape(ytDWT,N,nSymDWT).'; % for DWT
ytFFT=reshape(ytFFT,(N+16),nSymFFT).'; % for OFDM

%%% remove the Cyclic prefix from OFDM symbol
ytFFT= ytFFT(:, [17:80]);

%%% multicarrier demodulation process
%%% first: discrete Wavelet transform (DWT)
%%% with Haar mother wavelet
for zz=1:nSymDWT

    [DWT,cd]=dwt(ytDWT(zz,:), 'haar');% DWT
    RXDWT(zz,:)= [DWT cd];% recieved data for DWT
end

%%% second: OFDM with discrete Fourier transform (FFT)

RXFFT =(sqrt(nFFT)/64)*fftshift(fft(ytFFT.')).';% FFT

```

```

%%% remove the guard band (12- null subcarrier)from OFDM symbol
RXFFT= RXFFT(:, [6+[1:nFFT/2] 7+[nFFT/2+1:nFFT] ]);

%%% parallel to serial
RXDWT = reshape(RXDWT',1,[]);% at DWT
RXFFT = reshape(RXFFT.',1,[]);% at OFDM

%%% QAM demodulation for DWT multicarrier process
RXDWT_re = real(RXDWT); % real part
RXDWT_im = imag(RXDWT); % imaginary part

RXDWTThat(find(RXDWT_re < 0 & RXDWT_im < 0)) = -1-j;
RXDWTThat(find(RXDWT_re >= 0 & RXDWT_im > 0)) = 1+j;
RXDWTThat(find(RXDWT_re < 0 & RXDWT_im >= 0)) = -1+j;
RXDWTThat(find(RXDWT_re >= 0 & RXDWT_im < 0)) = 1-j;

%%% QAM demodulation for OFDM (FFT) process
RXFFT_re = real(RXFFT); % real part
RXFFT_im = imag(RXFFT); % imaginary part

RXFFTHat(find(RXFFT_re < 0 & RXFFT_im < 0)) = -1-j;
RXFFTHat(find(RXFFT_re >= 0 & RXFFT_im > 0)) = 1+j;
RXFFTHat(find(RXFFT_re < 0 & RXFFT_im >= 0)) = -1+j;
RXFFTHat(find(RXFFT_re >= 0 & RXFFT_im < 0)) = 1-j;

% counting the errors and ratio
nErrDWT(i) = size(find([DATA - RXDWTThat]),2);
nErrFFT(i) = size(find([DATA- RXFFTHat]),2);

end

simBerDWT = nErrDWT/nbit; simBerFFT = nErrFFT/nbit;

%%% theoritical bit error rate of BPSK modulation
theoryBerqam = erfc(sqrt(0.5*(10.^(EbNo/10))));

%%% plot the BER for DWT based multicarrier, OFDM and the theoritical QAM
close all; figure
semilogy(EbNo,theoryBerqam,'cs-','LineWidth',2);
hold on
semilogy(EbNo,simBerDWT,'mx-','LineWidth',2);
semilogy(EbNo,simBerFFT,'ro-','LineWidth',2);
axis([0 16 10^-6 1])
grid on
legend('theory QAM', 'simulation for DWT(Haar)', 'simulation for FFT');
xlabel('SNR, dB'); ylabel('Bit Error Rate')
title('BER for QAM using DWT multicarrier and OFDM (based FFT) "AWGN"')

```

### A.3: Alamouti using BPSK in Rayleigh channel

```
% %%%%%%%%%%%%%%%%%%%%%%%%%%%%%%%%%%%%%%%%%%%%%%%%%%%%%%%%%%%%%%%%%%%%%%%%%%
%% Bit Error Rate probability of Alamouti using BPSK in Rayleigh channel
%% OFDM symbol with guard
%%%%%%%%%%%%%%%%%%%%%%%%%%%%%%%%%%%%%%%%%%%%%%%%%%%%%%%%%%%%%%%%%%%%%%%%%
clc; clear all; close all

nbit = 10^6; % number of bits
Eb_N0_dB = [0:15]; % bit to noise in dB

%% In Alamouti scheme the number of transmitting antenna is two
%% the number of receiving antenna is varying

nTX = 2; % number of tran. antenna
nRX = input(' what is the # of receive antenna '); % number of receive
antenna

%% generate random data with nbit size, i.e, random 1's and 0's
ip = rand(1,nbit)>0.5;

%% BPSK modulation 0 --> -1, 1 --> +1
s = 2*ip-1; % BPSK modulation 0 -> -2; 1 -> 0

% Alamouti STBC Encoder
% first time slot : s0 and s1 are transmitted simultaneously from
% antenna one and antenna two, respectively
% second time slot : -s1* and s0* are transmitted simultaneously from
% antenna one and antenna two, respectively

sCode = zeros(2,nbit);
sCode(:,1:2:end) = (1/(sqrt(2)))*reshape(s,2,nbit/2); % [s1 s2 ...]
sCode(:,2:2:end) = (1/(sqrt(2)))*(kron(ones(1,nbit/2),[-1;1]).* ...
    flipud(reshape(conj(s),2,nbit/2))); % [-s2* s1* ....]

%% create Gaussian noise with unit variance and zero mean
nt = 1/sqrt(2)*[randn(nRX,nbit) + j*randn(nRX,nbit)];

%% create Rayleigh flat fading channel
ht = 1/sqrt(2*sqrt(nRX))*[randn(nRX,nbit) + j*randn(nRX,nbit)];

%% loop over the bit to noise ratio (Eb/No)
h = waitbar(0, 'Percentage Completed');
set(h, 'name', 'Please wait...');

for ii = 1:length(Eb_N0_dB)

    hEq = zeros(2*nRX,nbit); hMod = zeros(2*nRX,nbit);

    %%% Received signal for each nRx antenna
```

```

for kk=1:nRX
    h=ht(kk,:);    n=nt(kk,:);

    %% repeating the same channel for two symbols
    hMod = kron(reshape(h,2,nbit/2),ones(1,2));

    %% Convolution between transmitted signal and Rayleigh flat fading
    %% channel, then add the AWGN

    y = sum(hMod.*sCode,1)+ 10^(-Eb_NO_dB(ii)/20)*n ;

    % Receiver
    %% forming the equalization matrix , Maximal Ratio Combiner
    yMod([2*kk-1:2*kk],:) = kron(reshape(y,2,nbit/2),ones(1,2));
    yMod(2*kk,:) = conj(yMod(2*kk,:));

    hEq([2*kk-1:2*kk],[1:2:end]) = reshape(h,2,nbit/2);
    hEq([2*kk-1:2*kk],[2:2:end]) = kron(ones(1,nbit/2),[1;-1]).*...
        flipud(reshape(h,2,nbit/2));
    hEq(2*kk-1,:) = conj(hEq(2*kk-1,:));
end

%% Maximal Likelihood (ML) ==> estimated transmitted signal
hEqPower = sum(hEq.*conj(hEq),1);
yHat = sum(hEq.*yMod,1)./hEqPower; % [h1*y1 + h2y2*, h2*y1 -h1y2*,
... ]
yHat(2:2:end) = conj(yHat(2:2:end));

%% BPSK demodulation for OFDM system where
%% negative value --> -1, positive value--> +1
ipHat = real(yHat)>0;
% counting the errors
nErr(ii) = size(find([ip- ipHat]),2);

end

%% plot the BER for Alamouti with under BPSK

simBer = nErr/nbit;% simulated ber
semilogy(Eb_NO_dB,simBer,'mo-','LineWidth',2);
axis([0 15 10^-5 0.5])
grid on
legend('sim (nTx=2, nRx=1, Alamouti)');
xlabel('Eb/No, dB');
ylabel('Bit Error Rate');
title('BER for BPSK modulation with Alamouti STBC (Rayleigh channel)');

```

## A.4: SIMO DWT based multicarrier and conventional OFDM using BPSK

```

% %%%%%%%%%%%%%%%%%%%%%%%%%%%%%%%%%%%%%%%%%%%%%%%%%%%%%%%%%%
%%% Bit Error Rate probability of Alamouti with DWT based multicarrier
%%% modulation and conventional OFDM based FFT using BPSK
%%% OFDM symbol with guard
% %%%%%%%%%%%%%%%%%%%%%%%%%%%%%%%%%%%%%%%%%%%%%%%%%%%%%%%%%%
clc; close all; clear all

N = 64 ; % number of subcarriers
nFFT = 52; % number of data subcarriers
iteration = 5; % number of iterations ( increase the number of bits)
nbit= iteration*N*nFFT; % number of bits for data
nSymFFT=ceil(nbit/nFFT);% number of symbols for OFDM system
nSymDWT=ceil(nbit/N);% number of symbols for DWT system
EbNo = [0:15]; % bit to noise ratio in dB

% power normlization of the OFDM symbol, since there
% is 16 subcarrier for cyclic prefix then the power of
% OFDM symbol is extended over a length of 80 subcarrier
EbNofft = EbNo+10*log10(N/80);

%%% generate random data with nbit size, i.e, random 1's and 0's
DATA1=rand(1,nbit)>0.5;

%%% BPSK modulation 0 --> -1, 1 --> +1
DATA=2*DATA1 -1 ;

%%% serial to parallel( grouping into multiple symbols)
DATAFFT=reshape(DATA,nFFT,nSymFFT)'; % for OFDM
DATADWT=reshape(DATA,N,nSymDWT)'; % for DWT

%%% Add the guard band ( 12- null subcarriers), such that the
%%% data assigning to the subcarriers 1-->26 , 27-->59
DATAFFT=[zeros(nSymFFT,6) DATAFFT(:, [1:nFFT/2]) zeros(nSymFFT,1) ...
        DATAFFT(:, [nFFT/2+1:nFFT]) zeros(nSymFFT,5) ] ;

%%% input the number of receive antenna
nRx=input(' what is the No. of recievers ? ');

%%% loop over the bit to noise ratio (Eb/No)
h = waitbar(0, 'Percentage Completed');
set(h, 'name', 'Please wait...');
for i= 1:length(EbNo)

    %%% intilization matrix
    TXDWT=[]; TXFFT=[]; RXDWT1=[]; RXFFT1=[];

    %%% multicarrier modulation process

```

```

%%% first:inverse discrete Wavelet transform (IDWT)
%%% with Haar mother wavelet

for uu=1:nSymDWT

    IDWT=idwt(DATADWT(uu,1:N/2),DATADWT(uu,N/2+1:N),'haar');% IDWT
    TXDWT(uu,:) = IDWT;% transmitted data for DWT
end

%%% second: OFDM with inverse discrete Fourier transform (IFFT)
TXFFT = (N/sqrt(nFFT))*ifft(fftshift(DATAFFT.')).';% IFFT

%%% Add cyclic prefix with 0.25 of the OFDM symbol length
TXFFT = [TXFFT(:, [49:64]) TXFFT];

%%% parallel to serial =====> to the channel
TXDWT = reshape(TXDWT.',1,[]);% reshape for transmitted data for DWT
TXFFT=reshape(TXFFT.',1,[]); % reshape for transmitted data for OFDM

%%% create Gaussian noise with unit variance and zero mean
ntDWT = 1/sqrt(2)*[randn(nRx,nSymDWT*N) + ...
    j*randn(nRx,nSymDWT*N)];%noise for DWT
ntFFT = 1/sqrt(2)*[randn(nRx,nSymFFT*(N+16)) + ...
    j*randn(nRx,nSymFFT*(N+16))];%noise for OFDM

%%% create Rayleigh flat fading channel
hDWT = 1/sqrt(2)*[randn(nRx,nSymDWT*N) + ...
    j*randn(nRx,nSymDWT*N)];% for DWT
hFFT= 1/sqrt(2)*[randn(nRx,nSymFFT*nFFT) + ...
    j*randn(nRx,nSymFFT*nFFT)];% for OFDM

%%% the transmitted signal is corrupted with additive noise
TXDWT = kron(ones(nRx,1),TXDWT);
TXFFT = kron(ones(nRx,1),TXFFT);
ytDWT1 = TXDWT+ 10^(-EbNo(i)/20)*ntDWT;%receive signal DWT
ytFFT1 = TXFFT+ 10^(-EbNofft(i)/20)*ntFFT;%receive signal OFDM

%%% Received signal for each nRx antenna
for nr=1:nRx
    RXDWT=[]; RXFFT=[];
    ytFFT= ytFFT1(nr,:); ytDWT= ytDWT1(nr,:);

%%% serial to parallel( grouping into multiple symbols)

ytDWT=reshape(ytDWT,N,nSymDWT).'; % for DWT
ytFFT=reshape(ytFFT,(N+16),nSymFFT).'; % for OFDM

%%% remove the Cyclic prefix from OFDM symbol
ytFFT= ytFFT(:, [17:80]);

```

```

%%% multicarrier demodulation process
%%% first: discrete Wavelet transform (DWT)
%%% with Haar mother wavelet
for zz=1:nSymDWT
    [DWT,cd]=dwt(ytDWT(zz,:), 'haar');% DWT
    RXDWT(zz,:)= [DWT cd];% recived data for DWT
end

%%% second: OFDM with discrete Fourier transform (FFT)
RXFFT=(sqrt(nFFT)/64)*fftshift(fft(ytFFT.')).';% FFT

%%% remove the gaurd band (12- null subcarrier)from OFDM symbol
RXFFT= RXFFT(:, [6+[1:nFFT/2] 7+[nFFT/2+1:nFFT]]);

%%% parallel to serial
RXDWT1(nr,:) = reshape(RXDWT.',1,[]);% at DWT
RXFFT1(nr,:)= reshape(RXFFT.',1,[]);% at OFDM
end

%%% Convolution between transmitted signal and Rayleigh flat fading
%%% channel

ytDWTRX =hDWT.*RXDWT1;%at DWT
ytFFTRX =hFFT.*RXFFT1;%at OFDM

%%% Maximal ratio Combiner (MRC), Maximal Liklehood (ML)
ytDWTRX = sum(conj(hDWT).*ytDWTRX,1)./sum(hDWT.*conj(hDWT),1);% at
DWT
ytFFTRX= sum(conj(hFFT).*ytFFTRX,1)./sum(hFFT.*conj(hFFT),1);% at
OFDM

%%% BPSK demodulation for DWT system where
%%% negative value --> -1, positive value--> +1
BPSKmodDWT = 2*floor(real(ytDWTRX/2)) + 1;
BPSKmodDWT(find(BPSKmodDWT>1)) = +1;
BPSKmodDWT(find(BPSKmodDWT<-1)) = -1;

%%% converting modulated values into bits 0's and 1's
DATARXDWT = (BPSKmodDWT+1)/2;

%%% BPSK demodulation for OFDM system where
%%% negative value --> -1, positive value--> +1
BPSKmodFFT = 2*floor(real(ytFFTRX/2)) + 1;
BPSKmodFFT(find(BPSKmodFFT>1)) = +1;
BPSKmodFFT(find(BPSKmodFFT<-1)) = -1;

%%% converting modulated values into bits 0's and 1's

```

```

DATARXFFT = (BPSKmodFFT+1)/2;

%%% counting the errors and ratio
[nfft,rFFT]=biterr(DATA1,DATARXFFT); simBerFFT(i)=rFFT;% at OFDM
[nDWT,rDWT]=biterr(DATA1,DATARXDWT); simBerDWT(i)=rDWT;% at DWT

end

%%% plot the BER for SIMO with DWT based multicarrier
%%% and OFDM under BPSK
close all; figure
semilogy(EbNo,simBerDWT,'mx-','LineWidth',2);
hold on
semilogy(EbNo,simBerFFT,'ro-','LineWidth',2);
axis([0 16 10^-6 1])
grid on
legend( 'simulation for DWT(Haar)', 'simulation for FFT');
xlabel('SNR, dB')
ylabel('Bit Error Rate')
title('BER of SIMO multicarrier using BPSK ')

```

## A.5: Alamouti DWT based multicarrier and conventional OFDM using BPSK

```

% %%%%%%%%%%%%%%%%%%%%%%%%%%%%%%%%%%%%%%%%%%%%%%%%%%%%%%%%%%
%%% Bit Error Rate probability of Alamouti with DWT based multicarrier
%%% modulation and conventional OFDM based FFT using BPSK
%%% OFDM symbol with guard
% %%%%%%%%%%%%%%%%%%%%%%%%%%%%%%%%%%%%%%%%%%%%%%%%%%%%%%%%%%
clc; close all; clear all
%%% initialization the following parameters

N = 64 ; % number of data subcarriers
nfft = 52; % number of data subcarriers for OFDM
iteration = 50; % number of iterations ( increase the number of bits)
nbit= iteration*N*nfft; % number of bits for data
nSymFFT=ceil(nbit/nfft);% number of symbols for OFDM system
nSymDWT=ceil(nbit/N);% number of symbols for DWT system

%%% In Alamouti scheme the number of transmitting antenna is two
%%% the number of receiving antenna is varying

```

```

nt= 2% number of tran. antenna
nr= input(' what is the # of receive antenna')% number of receive antenna

EbNo = [0:15]; % bit to noise ratio in dB

%%% power normalization with respect to the nt
EbNo1=EbNo+10*log10(nt);

% power normlization of the OFDM symbol since there is 16
% subcarrier for cyclic prefix then the power
% of OFDM symbol is extended over a length of 80 subcarrrier

EbNofft = EbNo1 +10*log10(N/80);

%%% generate random data with nbit size, i.e, random 1's and 0's
DATA1=rand(1,nbit)>0.5;
%%% BPSK modulation 0 --> -1, 1 --> +1
DATA=2*DATA1 -1 ;

% Alamouti STBC Encoder
% first time slot : s0 and s1 are transmitted simultaneously from
% antenna one and antenna two, respectively
% second time slot : -s1* and s0* are transmitted simultaneously from
% antenna one and antenna two, respectively

alamouti_Code = zeros(2,nbit);
alamouti_Code(:,1:2:end) =(1/sqrt(2))*reshape(DATA,2,nbit/2);% [s1 s2
...]
alamouti_Code(:,2:2:end) = (1/sqrt(2))*kron(ones(1,nbit/2),[-1;1]).*...
      flipud(reshape(conj(DATA),2,nbit/2)); % [-s2* s1* ....]

%%% serial to parallel( grouping into multiple symbols)
DATADWT=reshape(alamouti_Code',N,nt*nSymDWT)'; % for dwt
DATAFFT=reshape(alamouti_Code',nfft,nt*nSymFFT)'; % for OFDM

%%% Add the guard band ( 12- null subcarriers), such that the
%%% data assigning to the subcarriers 1-->26 , 27-->59
DATAFFT=[zeros(nt*nSymFFT,6) DATAFFT(:,[1:nfft/2]) zeros(nt*nSymFFT,1)...
      DATAFFT(:,[nfft/2+1:nfft]) zeros(nt*nSymFFT,5)] ;

%%% loop over the bit to noise ratio (Eb/No)
h = waitbar(0, 'Percentage Completed');
set(h, 'name', 'Please wait...');

for i= 1:length(EbNo)
    %%% initialization matrix
    TXDWT=[];TXFFT=[]; RXDWT=[]; RXFFT=[];

    %%% multicarrier modulation process

```

```

for uu=1:nSymFFT
    %%% first:inverse discrete Wavelet transform (IDWT)
    %%% with Haar mother wavelet
    for tt=1:nt
        if (uu<=nSymDWT)
            IDWT=idwt(DATADWT((uu+(tt-1)*nSymDWT),1:N/2),...
                DATADWT((uu+(tt-1)*nSymDWT),N/2+1:N),'haar');%%IDWT
            TXDWT((uu+(tt-1)*nSymDWT),:)= IDWT;% transmitted data for DWT
        end

    %%% second: OFDM with inverse discrete Fourier transform (IFFT)
    IFFT=(N/sqrt(nfft))*ifft(fftshift(DATAFFT((uu+(tt-1)*nSymFFT),:)));%IFFT
    TXFFT((uu+(tt-1)*nSymFFT),:)=IFFT;%transmitted data for FFT
    end

end

%% Add cyclic prefix with 0.25 of the OFDM symbol length
TXFFT = [TXFFT(:, [49:64]) TXFFT];

%% parallel to serial =====> to the channel
TXDWT = reshape(TXDWT.', [], 2).';% for DWT
TXFFT=reshape(TXFFT.', [], 2).';% for FFT

%% create Gaussian noise with unit variance and zero mean
ntDWT1 = 1/sqrt(2)*[randn(nr,nSymDWT*N) + ...
    j*randn(nr,nSymDWT*N)];%noise for DWT
ntFFT1 = 1/sqrt(2)*[randn(nr,nSymFFT*(N+16)) + ...
    j*randn(nr,nSymFFT*(N+16))];%noise for OFDM

%% create Rayleigh flat fading channel
hDWT = 1/sqrt(2)*[randn(nr,nSymDWT*N) + ...
    j*randn(nr,nSymDWT*N)];% for DWT
hFFT = 1/sqrt(2)*[randn(nr,nSymFFT*nfft) + ...
    j*randn(nr,nSymFFT*nfft)];% for OFDM

%% Received signal for each nRx antenna
hEqDWT = zeros(2*nr,nbit); hEqFFT = zeros(2*nr,nbit);
hModDWT = zeros(2*nr,nbit); hModFFT = zeros(2*nr,nbit);
for kk=1:nr

    ntDWT = ntDWT1(kk,:) ; ntFFT = ntFFT1(kk,:) ;
    ntDWT = kron(ntDWT,ones(1,2));ntDWT=reshape(ntDWT,nt,nSymDWT*N);
    ntFFT = kron(ntFFT,ones(1,2));ntFFT=reshape(ntFFT,nt,nSymFFT*(N+16));

    %%% Adding the additive noise to the transmitted signal only
    %%% since we assume the effect of the AWGN on the DWT and OFDM
    ytDWT =TXDWT + 10^(-EbNol(i)/20)*ntDWT;%receive signal DWT
    ytFFT =TXFFT + 10^(-EbNofft(i)/20)*ntFFT;%receive signal OFDM

```

```

%
Receiver=====
    %% serial to parallel( grouping into multiple symbols)

    ytDWT=reshape(ytDWT.',N,2*nSymDWT).'; %% for DWT
    ytFFT=reshape(ytFFT.',(N+16),2*nSymFFT).'; % for OFDM

    %% remove the Cyclic prefix from OFDM symbol
    ytFFT= ytFFT(:, [17:80]);

    %% multicarrier demodulation process

    for zz=1:2*nSymFFT
        %% first: discrete Wavelet transform (DWT)
        %% with Haar mother wavelet
        if (zz<=2*nSymDWT)
            [DWT,cd]=dwt(ytDWT(zz,:), 'haar');% DWT
            RXDWT(zz,:)=[DWT cd];% received data for DWT
        end
        %% second: OFDM with discrete Fourier transform (FFT)
        FFT=(sqrt(nfft)/64)*fftshift(fft(ytFFT(zz,:)));% FFT
        RXFFT(zz,:)=FFT;%received data for FFT

    end

    %% remove the gaurd band (12- null subcarrier)from OFDM symbol
    RXFFT= RXFFT(:, [6+[1:nfft/2] 7+[nfft/2+1:nfft] ]);

    %% parallel to serial
    RXDWT = reshape(RXDWT.', [], 2).';% for DWT
    RXFFT = reshape(RXFFT.', [], 2).';% for FFT

    %% repeating the same channel for two symbols (assuming flat fading)
    %% channel

    hModDWT = kron(reshape(hDWT(kk,:), 2, nSymDWT*N/2), ones(1, 2));
    hModFFT = kron(reshape(hFFT(kk,:), 2, nSymFFT*(nfft)/2), ones(1, 2));

    %% Maximal ratio Combiner (MRC)
    RXDWT = sum(hModDWT.*RXDWT, 1);%receive signal DWT;
    RXFFT = sum(hModFFT.*RXFFT, 1);%OFDM

    %% forming the equalization matrix

    %% first: for DWT system

    yModDWT([2*kk-1:2*kk], :) = kron(reshape(RXDWT, 2, nbit/2), ones(1, 2));
    yModDWT(2*kk, :) = conj(yModDWT(2*kk, :));

    hEqDWT([2*kk-1:2*kk], [1:2:end]) = reshape(hDWT(kk,:), 2, nbit/2);

```

```

hEqDWT([2*kk-1:2*kk],[2:2:end]) = kron(ones(1,nbit/2),[1;-1]).* ...
    flipud(reshape(hDWT(kk,:),2,nbit/2));
hEqDWT(2*kk-1,:) = conj(hEqDWT(2*kk-1,:));

%%% second: for OFDM system
yModFFT([2*kk-1:2*kk],:) = kron(reshape(RXFFT,2,nbit/2),ones(1,2));
yModFFT(2*kk,:) = conj(yModFFT(2*kk,:));

hEqFFT([2*kk-1:2*kk],[1:2:end]) =
reshape(hFFT(kk,:),2,nSymFFT*nfft/2);
hEqFFT([2*kk-1:2*kk],[2:2:end]) = kron(ones(1,nSymFFT*nfft/2),...
    [1;-1]).*flipud(reshape(hFFT(kk,:),2,nSymFFT*nfft/2));
hEqFFT(2*kk-1,:) = conj(hEqFFT(2*kk-1,:));

end

%%% Maximal Likelihood (ML) =====> estimated transmitted signal

%%% first: for DWT system

hEqPowerDWT = sum(hEqDWT.*conj(hEqDWT),1);
yHatDWT = sum(hEqDWT.*yModDWT,1)./hEqPowerDWT;
yHatDWT(2:2:end) = conj(yHatDWT(2:2:end));

%%% second: for OFDM system

hEqPowerFFT = sum(hEqFFT.*conj(hEqFFT),1);
yHatFFT = sum(hEqFFT.*yModFFT,1)./hEqPowerFFT;
yHatFFT(2:2:end) = conj(yHatFFT(2:2:end));

%%% BPSK demodulation for DWT system where
%%% negative value --> -1, positive value--> +1
BPSKmodDWT = 2*floor(real(yHatDWT/2)) + 1;
BPSKmodDWT(find(BPSKmodDWT>1)) = +1;
BPSKmodDWT(find(BPSKmodDWT<-1)) = -1;

% converting modulated values into bits
DATARXDWT = (BPSKmodDWT+1)/2;

%%% BPSK demodulation for OFDM system where
%%% negative value --> -1, positive value--> +1
BPSKmodFFT = 2*floor(real(yHatFFT/2)) + 1;
BPSKmodFFT(find(BPSKmodFFT>1)) = +1;
BPSKmodFFT(find(BPSKmodFFT<-1)) = -1;

% converting modulated values into bits
DATARXFFT= (BPSKmodFFT+1)/2;

% counting the errors and ratio

```

```
[nDWT,rDWT]=biterr(DATA1,DATARXDWT); simBerDWT(i)=rDWT;  
[nFFT,rFFT]=biterr(DATA1,DATARXFFT); simBerFFT(i)=rFFT;
```

```
end
```

```
%%% plot the BER for Alamouti with DWT based multicarrier  
%%% and OFDM under BPSK  
close all; figure  
semilogy(EbNo,simBerDWT,'gx-','LineWidth',2);  
hold on  
semilogy(EbNo,simBerFFT,'ro-','LineWidth',2);  
axis([0 16 10^-5 1])  
grid on  
legend('simulation for DWT(Haar)','simulation for FFT');  
xlabel('SNR dB'); ylabel('Bit Error Rate')  
title('BER of Alamouti using multicarrier (DWT and OFDM ) using BPSK')
```

# Appendix B

## Orthogonal Matrix Design

The theory of orthogonal designs is an arcane branch of mathematics which was studied by several great number theorists including Radon and Hurwitz. Radon's results are only concerned with real square orthogonal designs. In this work, we extend the results of Radon to both non-square and complex orthogonal designs and introduce a theory of generalized orthogonal designs. Using this theory, we construct space-time block codes for any number of transmit antennas.

In this part, we define a Hurwitz-Radon family of matrices. These matrices encode the interactions between variables in an orthogonal design.

**Definition 1:** A set of  $N \times N$  real matrices  $\{B_1, B_2, \dots, B_k\}$  is a size  $k$  Hurwitz-Radon family of matrices if the matrices  $B_i$  are orthogonal, that is,  $B_i^T B_i = I$  the identity matrix, for all  $i = 1, \dots, k$ , and the products  $B_i^T B_j$  are skew-symmetric, that is  $B_i^T B_j = -B_j^T B_i$  for all  $i, j = 1, \dots, k$ .  $i \neq j$ .

**Theorem 1:** Any positive integer number  $N$  can be written as  $N = 2^a b$ , where  $a = 4c + d$ ,  $c \geq 0$ ,  $0 \leq d < 4$  and  $b$  is odd number. Any  $N \times N$  Hurwitz-Radon family contains less than  $\rho(N) = 8c + 2d \leq N$  matrices. A Hurwitz-Radon family containing  $N - 1$  matrices exists if and only if  $N = 2, 4$ , or  $8$ .

**Definition 2:** Let  $A = [a_{ij}]$  be an  $p \times q$  matrix and let  $B$  be an arbitrary matrix. Then the tensor product  $A \otimes B$  is the matrix given by

$$A \otimes B = \begin{pmatrix} a_{11}B & a_{12}B & \cdots & a_{1q}B \\ a_{21}B & a_{22}B & \cdots & a_{2q}B \\ \vdots & \vdots & \ddots & \vdots \\ a_{p1}B & a_{p2}B & \cdots & a_{pq}B \end{pmatrix}$$

**Definition 3:** A matrix is called an integer matrix if all of its entries are in the set  $\{-1, 0, 1\}$ .

Hurwitz-Radon integer matrixes are:

$$P = \begin{pmatrix} 0 & 1 \\ 1 & 0 \end{pmatrix}, \quad Q = \begin{pmatrix} 1 & 0 \\ 0 & -1 \end{pmatrix}$$

$$R = \begin{pmatrix} 0 & 1 \\ -1 & 0 \end{pmatrix}, \quad S = \begin{pmatrix} 1 & 0 \\ 0 & 1 \end{pmatrix}$$

Maximum possible size of a Hurwitz-Radon matrix family is  $\rho(N) - 1$ .

Table B.1: values of  $\rho(N)$

$N = 2^a b$	$a = 4c + d$	$b$ Must be odd	$c$ $c \geq 0$	$d$ $0 \leq d < 4$	$\rho(N)$ $= 8c + 2d$ $\leq N$
2	1	1	0	1	2
4	2	1	0	2	4
8	3	1	0	3	8
16	4	1	1	0	9
32	5	1	1	1	10
64	6	1	1	2	12
128	7	1	1	3	16
256	8	1	2	0	17

Table B.1 gives an idea about how we can choose  $N$  from  $a, b, c$  and  $d$ . Hurwitz-Radon word system or family from table B.1 :

1. For  $a = 1, N = 2, c = 0, d = 1$  and  $\rho(2) = 2$ . Therefore, a Hurwitz-Radon family of size  $\rho(2) - 1 = 1$  has only one member. For example:

$$R = \begin{pmatrix} 0 & 1 \\ -1 & 0 \end{pmatrix}$$

2. For  $a = 2, N = 4, c = 0, d = 2$  and  $\rho(4) = 4$ . Therefore, a Hurwitz-Radon family of size  $\rho(4) - 1 = 3$  has only one member. And they are:

$$\{(Q \otimes R), (R \otimes S), (P \otimes R)\}$$

3. For  $a = 3, N = 8, c = 0, d = 3$  and  $\rho(8) = 8$ . Therefore, a Hurwitz-Radon family of size  $\rho(8) - 1 = 7$  has only one member. And they are:

$$\{(Q \otimes Q \otimes R), (S \otimes R \otimes S), (S \otimes P \otimes R), (R \otimes Q \otimes S), (P \otimes Q \otimes R), (R \otimes P \otimes Q), (R \otimes P \otimes P)\}$$

From the table it is seen that a Hurwitz-Radon family of size  $N - 1$  exists if and only if  $N = 2, 4, 8$ . Because  $\rho(N) = N$  if and only if  $N = 2, 4, 8$ .

## Encoding Algorithm of OSTBC

In this part we will show some terminology design for the real orthogonal design and complex orthogonal design with  $N = 2, 4$  and  $8$ .

### 1. Real Orthogonal Design :

- An  $2 \times 2$  orthogonal design is :

$$G_2 = s_0 S + s_1 R = s_0 \begin{pmatrix} 1 & 0 \\ 0 & 1 \end{pmatrix} + s_1 \begin{pmatrix} 0 & 1 \\ -1 & 0 \end{pmatrix} = \begin{pmatrix} s_0 & s_1 \\ -s_1 & s_0 \end{pmatrix}$$

- An  $8 \times 8$  orthogonal design is :

$$G_8 = s_0 B_1 + s_1 B_2 + s_2 B_3 + s_3 B_4 + s_4 B_5 + s_5 B_6 + s_6 B_7 + s_7 B_8$$

$$B_1 = I_8, \quad B_2 = Q \otimes Q \otimes R, \quad B_3 = S \otimes R \otimes S, \quad B_4 = S \otimes P \otimes R, \quad B_5 = R \otimes Q \otimes S$$

$$B_6 = P \otimes Q \otimes R, \quad B_7 = R \otimes P \otimes Q, \quad B_8 = R \otimes P \otimes P$$

$$G_8 = \begin{pmatrix} s_0 & s_1 & s_2 & s_3 & s_4 & s_5 & s_6 & s_7 \\ -s_1 & s_0 & s_3 & -s_2 & s_5 & -s_4 & -s_7 & -s_6 \\ -s_2 & -s_3 & s_0 & s_1 & s_6 & s_7 & -s_4 & -s_5 \\ -s_3 & s_2 & -s_1 & s_0 & s_7 & -s_6 & s_5 & -s_4 \\ -s_4 & -s_5 & -s_6 & -s_7 & s_0 & s_1 & s_2 & s_3 \\ -s_5 & s_4 & -s_7 & s_6 & -s_1 & s_0 & -s_3 & s_2 \\ -s_6 & s_7 & s_4 & -s_5 & -s_2 & s_3 & s_0 & s_1 \\ -s_7 & -s_6 & s_5 & s_4 & -s_3 & -s_2 & s_1 & s_0 \end{pmatrix}$$

### 2. Complex Orthogonal Design:

- The Alamouti code  $2 \times 2$  is,

$$G_2 = \begin{pmatrix} s_0 & s_1 \\ -s_1^* & s_0^* \end{pmatrix}$$

- 16×8 complex design is,

$$G_{16 \times 8} = \begin{pmatrix} G_8 \\ G_8^* \end{pmatrix} = \begin{pmatrix} s_0 & s_1 & s_2 & s_3 & s_4 & s_5 & s_6 & s_7 \\ -s_1 & s_0 & s_3 & -s_2 & s_5 & -s_4 & -s_7 & -s_6 \\ -s_2 & -s_3 & s_0 & s_1 & s_6 & s_7 & -s_4 & -s_5 \\ -s_3 & s_2 & -s_1 & s_0 & s_7 & -s_6 & s_5 & -s_4 \\ -s_4 & -s_5 & -s_6 & -s_7 & s_0 & s_1 & s_2 & s_3 \\ -s_5 & s_4 & -s_7 & s_6 & -s_1 & s_0 & -s_3 & s_2 \\ -s_6 & s_7 & s_4 & -s_5 & -s_2 & s_3 & s_0 & s_1 \\ -s_7 & -s_6 & s_5 & s_4 & -s_3 & -s_2 & s_1 & s_0 \\ s_0^* & s_1^* & s_2^* & s_3^* & s_4^* & s_5^* & s_6^* & -s_7^* \\ -s_1^* & s_0^* & s_3^* & -s_2^* & s_5^* & -s_4^* & -s_7^* & -s_6^* \\ -s_2^* & -s_3^* & s_0^* & s_1^* & s_6^* & s_7^* & -s_4^* & -s_5^* \\ -s_3^* & s_2^* & -s_1^* & s_0^* & s_7^* & -s_6^* & s_5^* & -s_4^* \\ -s_4^* & -s_5^* & -s_6^* & -s_7^* & s_0^* & s_1^* & s_2^* & s_3^* \\ -s_5^* & s_4^* & -s_7^* & s_6^* & -s_1^* & s_0^* & -s_3^* & s_2^* \\ -s_6^* & s_7^* & s_4^* & -s_5^* & -s_2^* & s_3^* & s_0^* & s_1^* \\ -s_7^* & -s_6^* & s_5^* & s_4^* & -s_3^* & -s_2^* & s_1^* & s_0^* \end{pmatrix}$$

- the rate of the code is defined as the number of the transmitted symbol,  $K$ , over the number of time periods for transmission of one block of coded symbol  $T$ .  $R = \frac{K}{T}$ .
- The code rate in real design is 1, whereas in complex design it is  $\frac{1}{2}$  except in Alamouti it is 1.

A generalized orthogonal design is a  $T \times N$  orthogonal matrix  $G_{T \times N}$  with real entries. For constructing a full code rate for any number of transmit antennas the minimum value of the transmission periods be  $T = \min(2^{4c+d})$  and the minimization is taken over the set  $c \geq 0$ ,  $d \geq 0$  and  $8c + 2^d \geq N$ .

For example, if the number of transmit antenna  $N = 5$ . From table B.1, If  $c = 0$ ,  $d = 3$  then  $8 * (0) + 2^3 = 8 \geq 5$ . And,  $T = \min(2^{4*0+3}) = 8$ , this is the minimum value of  $T$ .

This is a full rate code. So,  $K = T = 8$  and the message points are  $S = (s_1, s_2, s_3, s_4, \dots, s_8)$  and the code be  $G_{8 \times 5}$ . The  $8 \times 8$  family of Hurwitz-Radon contains  $N - 1 = 5 - 1 = 4$  members and they are:

$$B_1 = I_8, \quad B_2 = Q \otimes Q \otimes R, \quad B_3 = S \otimes R \otimes S, \quad B_4 = S \otimes P \otimes R, \quad B_5 = R \otimes Q \otimes S.$$

Using five  $8 \times 8$  matrices  $B_1, B_2, B_3, B_4$  and  $B_5$  a real  $8 \times 5$  real orthogonal design  $G_{8 \times 5}$  is created. The  $n^{th}$  column of  $G_{8 \times 5}$  is  $B_n S^T$  for  $n = 1, 2, \dots, 5$ .

$$B_1 S^T = \begin{bmatrix} 1 & 0 & 0 & 0 & 0 & 0 & 0 & 0 \\ 0 & 1 & 0 & 0 & 0 & 0 & 0 & 0 \\ 0 & 0 & 1 & 0 & 0 & 0 & 0 & 0 \\ 0 & 0 & 0 & 1 & 0 & 0 & 0 & 0 \\ 0 & 0 & 0 & 0 & 1 & 0 & 0 & 0 \\ 0 & 0 & 0 & 0 & 0 & 1 & 0 & 0 \\ 0 & 0 & 0 & 0 & 0 & 0 & 1 & 0 \\ 0 & 0 & 0 & 0 & 0 & 0 & 0 & 1 \end{bmatrix} \times \begin{bmatrix} s_1 \\ s_2 \\ s_3 \\ s_4 \\ s_5 \\ s_6 \\ s_7 \\ s_8 \end{bmatrix} = \begin{bmatrix} s_1 \\ s_2 \\ s_3 \\ s_4 \\ s_5 \\ s_6 \\ s_7 \\ s_8 \end{bmatrix}, \dots, B_2 S^T = \begin{bmatrix} 0 & 1 & 0 & 0 & 0 & 0 & 0 & 0 \\ -1 & 0 & 0 & 0 & 0 & 0 & 0 & 0 \\ 0 & 0 & 0 & -1 & 0 & 0 & 0 & 0 \\ 0 & 0 & 1 & 0 & 0 & 0 & 0 & 0 \\ 0 & 0 & 0 & 0 & 0 & -1 & 0 & 0 \\ 0 & 0 & 0 & 0 & 1 & 0 & 0 & 0 \\ 0 & 0 & 0 & 0 & 0 & 0 & 0 & 1 \\ 0 & 0 & 0 & 0 & 0 & 0 & -1 & 0 \end{bmatrix} \times \begin{bmatrix} s_1 \\ s_2 \\ s_3 \\ s_4 \\ s_5 \\ s_6 \\ s_7 \\ s_8 \end{bmatrix} = \begin{bmatrix} s_2 \\ -s_1 \\ -s_4 \\ s_3 \\ -s_6 \\ s_5 \\ s_8 \\ -s_7 \end{bmatrix}$$

$$B_3 S^T = \begin{bmatrix} 0 & 0 & 1 & 0 & 0 & 0 & 0 & 0 \\ 0 & 0 & 0 & 1 & 0 & 0 & 0 & 0 \\ -1 & 0 & 0 & 0 & 0 & 0 & 0 & 0 \\ 0 & -1 & 0 & 0 & 0 & 0 & 0 & 0 \\ 0 & 0 & 0 & 0 & 0 & 0 & 1 & 0 \\ 0 & 0 & 0 & 0 & 0 & 0 & 0 & 1 \\ 0 & 0 & 0 & 0 & -1 & 0 & 0 & 0 \\ 0 & 0 & 0 & 0 & 0 & -1 & 0 & 0 \end{bmatrix} \times \begin{bmatrix} s_1 \\ s_2 \\ s_3 \\ s_4 \\ s_5 \\ s_6 \\ s_7 \\ s_8 \end{bmatrix} = \begin{bmatrix} s_3 \\ s_4 \\ -s_1 \\ -s_2 \\ s_7 \\ s_8 \\ -s_5 \\ -s_6 \end{bmatrix}, \dots, B_4 S^T = \begin{bmatrix} 0 & 0 & 0 & 1 & 0 & 0 & 0 & 0 \\ 0 & 0 & -1 & 0 & 0 & 0 & 0 & 0 \\ 0 & 1 & 0 & 0 & 0 & 0 & 0 & 0 \\ -1 & 0 & 0 & 0 & 0 & 0 & 0 & 0 \\ 0 & 0 & 0 & 0 & 0 & 0 & 0 & 1 \\ 0 & 0 & 0 & 0 & 0 & 0 & -1 & 0 \\ 0 & 0 & 0 & 0 & 0 & 1 & 0 & 0 \\ 0 & 0 & 0 & 0 & -1 & 0 & 0 & 0 \end{bmatrix} \times \begin{bmatrix} s_1 \\ s_2 \\ s_3 \\ s_4 \\ s_5 \\ s_6 \\ s_7 \\ s_8 \end{bmatrix} = \begin{bmatrix} s_4 \\ -s_3 \\ s_2 \\ -s_1 \\ s_8 \\ -s_7 \\ s_6 \\ -s_5 \end{bmatrix}$$

$$B_5 S^T = \begin{bmatrix} 0 & 0 & 0 & 0 & 1 & 0 & 0 & 0 \\ 0 & 0 & 0 & 0 & 0 & 1 & 0 & 0 \\ 0 & 0 & 0 & 0 & 0 & 0 & -1 & 0 \\ 0 & 0 & 0 & 0 & 0 & 0 & 0 & -1 \\ -1 & 0 & 0 & 0 & 0 & 0 & 0 & 0 \\ 0 & -1 & 0 & 0 & 0 & 0 & 0 & 0 \\ 0 & 0 & 1 & 0 & 0 & 0 & 0 & 0 \\ 0 & 0 & 0 & 1 & 0 & 0 & 0 & 0 \end{bmatrix} \times \begin{bmatrix} s_1 \\ s_2 \\ s_3 \\ s_4 \\ s_5 \\ s_6 \\ s_7 \\ s_8 \end{bmatrix} = \begin{bmatrix} s_5 \\ s_6 \\ -s_7 \\ -s_8 \\ -s_1 \\ -s_2 \\ s_3 \\ s_4 \end{bmatrix}$$

$$G_{8 \times 5} = \begin{bmatrix} s_1 & s_2 & s_3 & s_4 & s_5 \\ s_2 & -s_1 & s_4 & -s_3 & s_6 \\ s_3 & -s_4 & -s_1 & s_2 & -s_7 \\ s_4 & s_3 & -s_2 & -s_1 & -s_8 \\ s_5 & -s_6 & s_7 & s_8 & -s_1 \\ s_6 & s_5 & s_8 & -s_7 & -s_2 \\ s_7 & s_8 & -s_5 & s_6 & s_3 \\ s_8 & -s_7 & -s_6 & -s_5 & s_4 \end{bmatrix}$$

A generalized orthogonal design for complex design is as real design with take the conjugate of the real design, i.e, if  $G_{T \times N}$  is a  $T \times N$  orthogonal matrix with real entries, then  $G_{2T \times N}$  orthogonal matrix with complex entries such that:

$$G_{2T \times N} = \begin{bmatrix} G_{T \times N} \\ G_{T \times N}^* \end{bmatrix}$$